Influence of the geminal-dialkyl-effect on the reactivity of 3-chloropiperidines

---

JUSTUS-LIEBIG-UNIVERSITÄT GIESSEN

Masterthesis

For the award of the degree of

Master of Science (M. Sc.)

Institute of Organic Chemistry

Justus-Liebig-Universität Giessen

Under the guidance of

Prof. Dr Richard Göttlich

Dr Alice Sosic

Period of elaboration: 04/2022 – 10/2022

Submitted by:

Maximilian Alexander Haumann

born in Giessen

Selbstständigkeitserklärung

Hiermit versichere ich, die vorgelegte Thesis selbstständig und ohne unerlaubte fremde Hilfe und nur mit den Hilfen angefertigt zu haben, die ich in der Thesis angegeben habe. Alle Textstellen, die wörtlich oder sinngemäß aus veröffentlichten Schriften entnommen sind, und alle Angaben, die auf mündlichen Auskünften beruhen, sind als solche kenntlich gemacht. Bei den von mir durchgeführten und in der Thesis erwähnten Untersuchungen habe ich die Grundsätze gute wissenschaftlicher Praxis, wie sie in der ‚Satzung der Justus-Liebig-Universität zur Sicherung guter wissenschaftlicher Praxis' niedergelegt sind, eingehalten. Entsprechend § 22 Abs. 2 der Allgemeinen Bestimmungen für modularisierte Studiengänge dulde ich eine Überprüfung der Thesis mittels Anti-Plagiatssoftware.

27.10.2022
Datum

Maximilian Alexander Haumann

Acknowledgements

First of all, I would like to thank Prof. Dr Richard Göttlich for the opportunity to work on such an exciting topic and to expand my skills as a chemist.

Furthermore, I would also like to thank Prof. Dr Barbara Gatto and Alice Sosic (Padova, Italy), who agreed to co-supervise this work and warmly welcomed me into their group during my stay in Italy.

Additionally, I would like to express my gratitude to Michael and Mats, who patiently answered all my concerns, provided me with valuable advice, and helped me develop fresh ideas and abilities.

Also, I would like to thank the rest of the Göttlich working group for the friendly and pleasant atmosphere.

I want to thank the analytics department of the Justus-Liebig-University for the provided infrastructure regarding chemical analytics and the HKHLR for the access to their computing cluster.

Finally, I would like to thank my family, my friends and my girlfriend who have supported me during this stressful time.

"The difference between screwing around and science is writing it down."

- Adam Savage -

List of Abbreviations

atm	Atmospheric pressure
Boc	*tert*-Butyloxycarbonyl group
BSSE	Basis Set Superposition Error
Bu	Butylgroup
d	Day
DCM	Dichloromethane
DDC	Dicyclohexylcarbodiimide
dest.	Distilled
DFT	Density functional theory
DHF	Double Hybrid Functional
DIPEA	*N*,*N*-Diisopropylethylamine
DMAP	4-Dimethylaminopyridine
DMP	Dess-Martin periodinane
DNA	Deoxyribonucleic acid
EDC	1-Ethyl-3-(3-dimethylaminopropyl)carbodiimide
equiv	Equivalent
ESI-MS	Electrospray ionisation mass spectrometry
Et_3N	Triethylamine
EtOAc	Ethyl acetate
GC	Gas chromatography
GC-MS	Gas chromatographic-mass spectrometry
gem	geminal
GGA	General Gradient Approximation
GS	Ground state
HF	Hartree Fock
HOBt	Hydroxybenzotriazole
HV	High vacuum

Hz	Hertz
IRC	Intrinsic Reaction Coordinate
LAH	Lithium Aluminium Hydride
LDA	Lithium Diisopropyl Amine
LDA	Local Density Approximation
M	Molar mass
M	Molarity
MP	Møller-Plesset perturbation theory
Ms	Mesyl group
n	normal
NCS	*N*-chlorosuccinimide
NEt_3	Triethylamine
NMR	Nuclear magnetic resonance
OAc	Acetate
Ph	Phenyl group
Quant.	Quantitative
R	General carbon residue
RT	Room temperature
sec	Secondary
sol	Solution
TBAI	Tetrabutylammoniumiodid
TBME	*tert*-Butyl methyl ether
tert	Tertiary
THF	Tetrahydrofuran
TLC	Thin layer chromatography
t_R	Retention time
TsOH	*para*-Toluene sulfonic acid
TST	Transition state

Table of contents

1 Introduction

Cancer treatment relies on three methods: Surgery, radiotherapy, and chemotherapy. Surgery is used to remove more extensive local collections of tumour tissue, while radiotherapy serves to remove regional smaller tumour foci. With chemotherapy, tumour cells distributed in the body, so-called metastases, can be treated.[1] Metastases are daughter cells of the tumour detached from it and spread through the bloodstream. These daughter cells can form new tumour foci in different body parts.[2] However, anti-cancer drugs do not distinguish between healthy body cells and tumour cells. Therefore, rapidly reproducing cells are particularly affected by this. In addition to tumour cells, these include mucous membranes, hair roots and bone marrow. The lack of selectivity explains the frequently occurring side effects such as nausea, hair loss and bone marrow depression. For these reasons, developing novel anti-proliferate substances that act more selectively and have milder side effects is one of the current research goals.[3]

In the past, the *Göttlich* group developed (*bis*-)3-chloropiperidines that can alkylate deoxyribonucleic acid (DNA).[4,5] As a result, it can no longer be read correctly, leading to the disruption of cell division and, ultimately, apoptosis. The double alkylation at position five of the piperidine backbone showed an increased DNA alkylation rate in biological tests[4] and an overall enhanced reaction rate (Scheme 1).[6] However, increased reactivity and alkylation rates are associated with lower activity in cell studies. Because more reactive drugs commonly react with thiol or hydroxyl functionalities of proteins, other nucleophiles, or even water in biological systems, thus the alkylation rate is inhibited.[7] In further investigations of the components, it was observed that sterically demanding substituents in position five, such as phenyl groups, further increased the reactivity. In contrast, a decrease in reactivity was observable with strained substituents such as cyclopropane rings. The Thorpe-Ingold effect and the resulting angular expansions and contractions are responsible for this.[8]

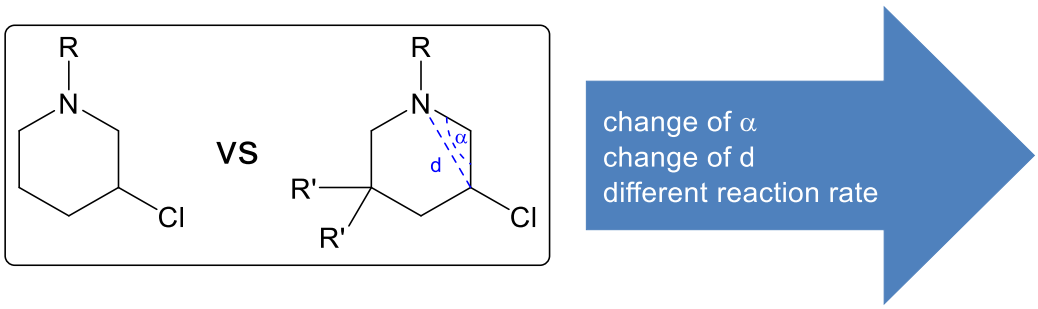

SCHEME 1: INVESTIGATIONS DONE IN PREVIOUS WORK.

In 1956, *Brown et al*. investigated to what extent the substitution pattern and the substitution type influence the cyclisation rate of bromobutylamines.[9] This thesis will examine how the alkylation pattern and alkylation type impact the reactivity of 3-chloropiperidines based on the work of *Brown et al.* and *Göttlich et al.* (Scheme 2). For this purpose, the structures and the resulting activation energies are first calculated using DFT. Then the structures are synthesised, and the compounds are investigated in kinetic studies. Lastly, the measured rate constants are compared with the calculated activation energies.

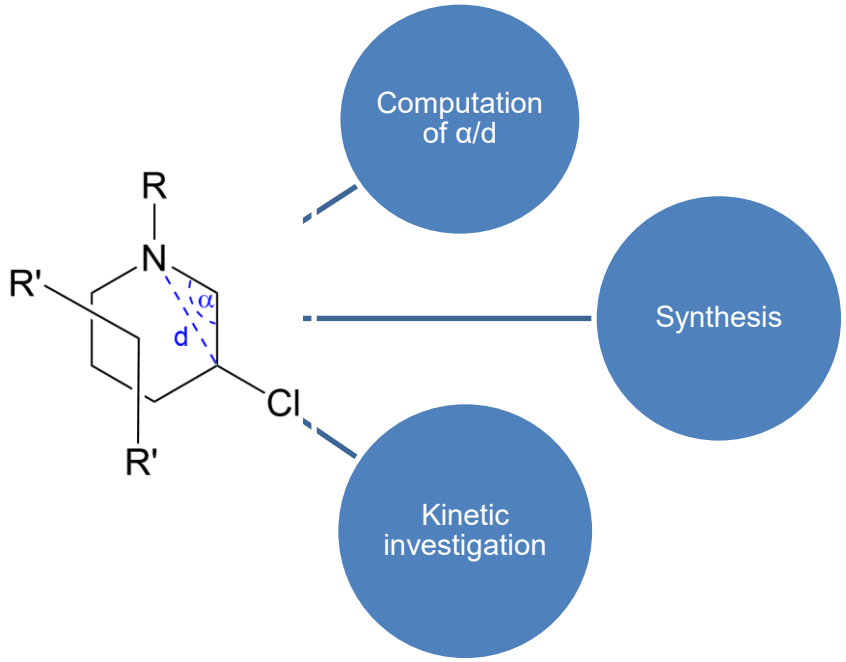

SCHEME 2: EVALUATION OF THE EFFECT OF THE 3-CHLOROPIPERIDINES' ALKYLATION PATTERN AT DIFFERENT POSITIONS ON THE REACTION RATE.

In the following section, the theoretical background of this work is discussed (chapter 2). At the end of the chapter, known synthesis routes (chapter 2.6) and the used calculation methods are presented (chapter 2.7). Afterwards, the calculations on the reactivity of the *N*-butyl-3-chloropiperidine derivatives are discussed (chapter 3.1). Then the applied synthesis routes are highlighted (chapter 3.2), and the previously predicted reactivities are compared with kinetic measurements (chapter 3.3). In the end, a short outlook is given in chapter 4.

2 Theoretical Background

2.1 Development of Chemotherapy

The origin of chemotherapy lies in the warfare of the first and second World Wars. In September 1917, mustard gas had its first deployment as a combat agent. In the Second World War, the antineoplastic effect was established. Bombs were dropped on a ship carrying 100 tonnes of mustard gas grenades that was docked in the Italian port city of Bari. The antineoplastic capabilities of mustard gas were discovered during the treatment of those exposed to the mustard gas. In the patients, there was a noticeable decrease in the number of white blood cells.[3] This discovery resulted in the exploitation of the cytotoxic properties of mustards and the employment to fight tumour cells. Because those mustards were too reactive to be helpful in a clinical application, the less reactive *N*-Losts were developed for tumour control. Mechlorethamine (Figure 1Figure 1) was synthesised as early as 1935 by K. Ward[10] and became the first clinically used nitrogen mustard in 1942. It is still used and is now known under the brand name Mustargen®.[7] A. Gilman and F. Philips found that the underlying mechanism is the formation of a reactive aziridinium ion, which leads to the alkylation of proteins and nucleic bases.[11]

FIGURE 1: *S*-LOST (LEFT) AND *N*-LOST MECHLORETHAMINE (RIGHT).

As mechlorethamine was still too reactive, too much peripheral cytotoxicity posed a severe problem, as well as storing due to its sensitivity to hydrolysis.[3] Therefore, the electron density of the nitrogen was lowered, which aimed to slow the formation of the reactive aziridinium ion. For this purpose, the methyl group was replaced by an electron-withdrawing aryl substituent. This substitution made intravenous administration more difficult because the water solubility was reduced. Therefore, a carboxyl group was placed at the para position of the aromatic molecule to increase its solubility. As a result, the electron-withdrawing action increased, and the reactivity decreased, making it hard to observe any activity. The activity was raised again by introducing an alkyl group as a spacer. These steps led to the development of the drug chlorambucil in 1950[12], which is still used today as a standard cytostatic drug for treating chronic lymphocytic leukaemia.[3,12] Several approaches for *N*-Lost-based antineoplastic drugs were explored in the following years. (Figure 2)

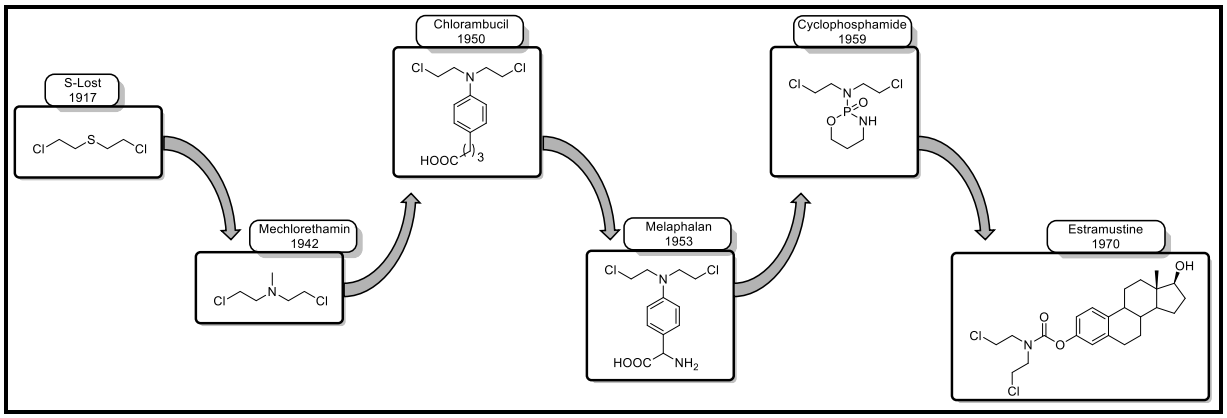

FIGURE 2: EARLY DEVELOPMENT OF *N*-LOSTS.

In 1953, the drug Melphalan® was developed to improve cellular uptake. Melphalan® was created as an amino acid derivative that could utilise the phenylalanine transport mechanism for this purpose.[13] The 1959-developed drug cyclophosphamide displays no activity in vitro and only shows in vivo activity. As a result, it was discovered that it functions as a prodrug and must be metabolised to have any impact. Through oxidative degradation with the enzyme CYP450, cyclophosphamide is converted to 4-hydroxy-cyclophosphamide, and via tautomerism, aldolphosphamide is formed. Lastly, acrolein is cleaved off by β-elimination and the alkylating species phosphoramide-Lost is formed (Scheme 3).[3] As a new approach, hormone-based alkylating agents were developed in 1970. Here hormones were coupled to *N*-Lost to combat hormone-dependent tumour cells more selectively.[3,14]

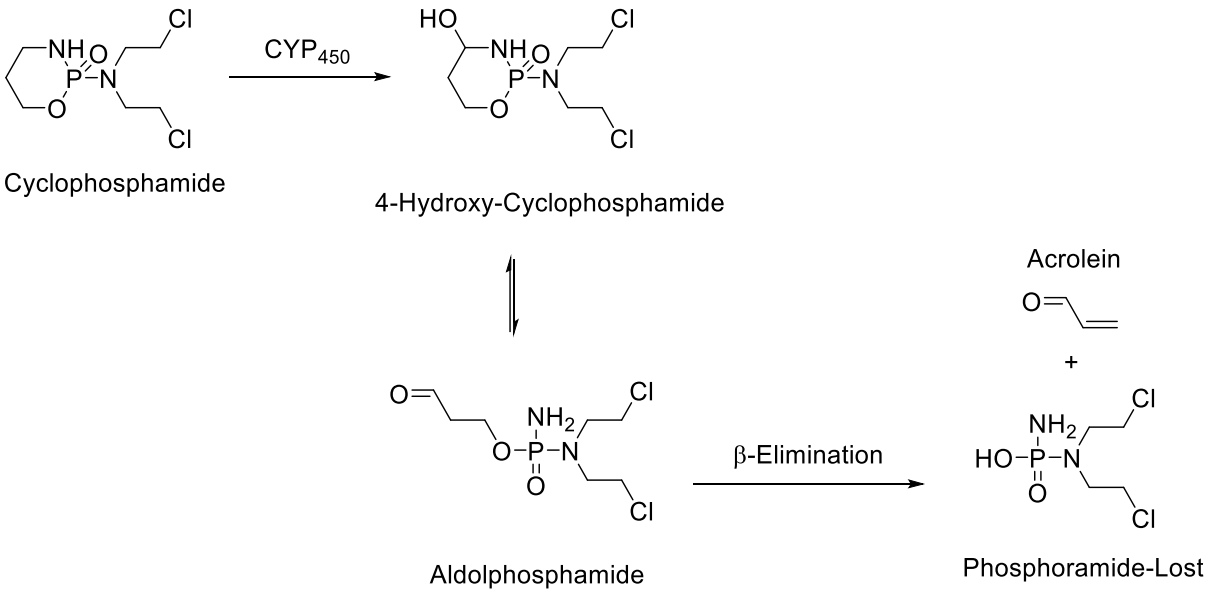

SCHEME 3: METABOLIZATION OF CYCLOPHOSPHAMIDE.[3]

Alkylating compounds inhibit cell growth and division by creating covalent adducts with DNA. If too much of such DNA damage accumulates, cell division is prevented, and controlled cell death (apoptosis) is initiated. Several cytostatic drugs are usually used to circumvent any resistance during chemotherapeutic treatment. Combination treatment is typically used to increase the effectiveness of the therapy. The interplay between a local therapeutic strategy, such as radiation or surgery, and a systemic treatment using cytostatics is described with this term.[2] What kind of covalent adducts alkylating agents can form with DNA and how these come about will be discussed in more detail in the next chapter.

2.2 Alkylating Agents

Alkylating agents are substances that bind covalently to the DNA, whereby it can no longer be transcribed correctly. In this way, cell growth is inhibited, and apoptosis is initiated in the case of particularly severe damage to the DNA.[15] Since tumour cells have uncontrolled growth and division phases, they are particularly susceptible to alkylating agents.[16] Due to this fact, alkylating substances are potent chemotherapeutic agents. On the other hand, alkylating agents lack the necessary selectivity towards tumour cells, so this treatment impacts the entire body.[17]

Different alkylation patterns can be achieved depending on the structure of the alkylating agents. Monofunctional alkylating agents lead to a simple alkylation of the DNA, which can usually be more easily repaired. On the other hand, bifunctional alkylating agents can crosslink two nucleic bases, making the repair process more difficult. These crosslinks can occur in two ways (Figure 3). Links can occur between the two DNA strands (interstrand) or between two nucleic bases of the same strand (intrastrand). An interstrand crosslink proves particularly effective, as the induced double-strand breaks and crosslinks can only be repaired with great difficulty due to the lack of an intact complementary strand.[15]

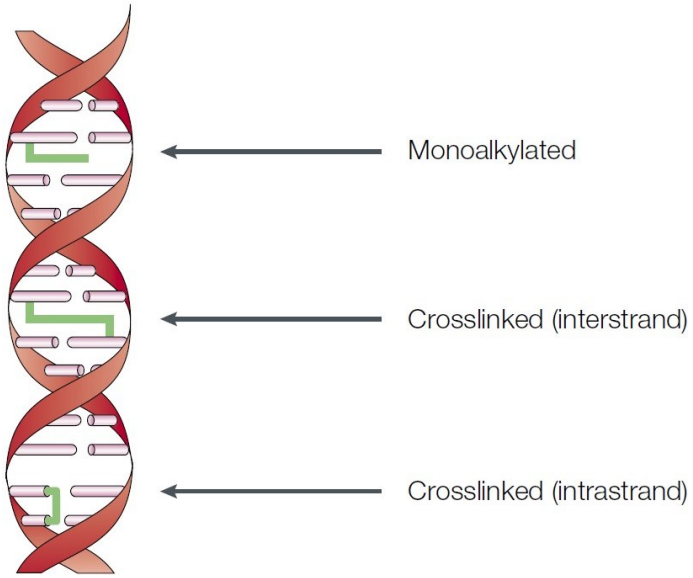

FIGURE 3: ALKYLATION POSSIBILITIES OF THE DNA.[17]

Alkylating agents based on *N*-Lost all function according to the exact mechanism. Here, the chloride acts as an excellent leaving group, facilitating the intramolecular attack of the free electron pair on the nitrogen (Scheme 4). As a result of the attack, a highly strained aziridinium ion is formed. The aziridinium ion gets opened through a nucleophile attack of N^7-nitrogen of guanine, forming a DNA adduct.[18,19] This procedure can be performed again in the presence of a second reactive group. Two DNA bases may get crosslinked because of this. The alkylation takes place preferentially at the N^7-nitrogen of the guanine, as this is the most nucleophilic site of the DNA.[18,20] The next chapter will discuss how and what DNA damage can occur.

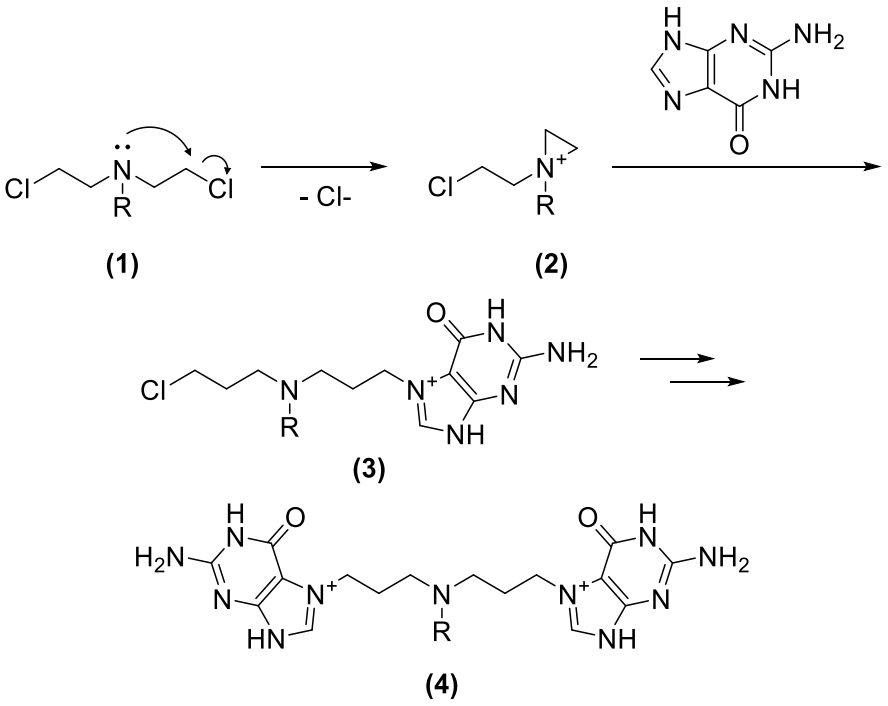

SCHEME 4: ALKYLATING MECHANISM OF THE DNA.

2.3 Development of DNA Damage

During replication, the DNA double helix is split into its respective single strands, with a complementary strand each. Under normal conditions, this semi-conservative replication yields two identical DNA double strands. However, errors can occur during this process due to various endo and exogenous causes. Endogenous causes include depurination, in which the purine bases adenine or guanine can be cleaved off, or point mutations, which can occur due to products of cell metabolism. During depurination, the nucleic base guanine detaches from the sugar-phosphate backbone, creating an apurinic site (Scheme 5). This process can occur spontaneously under acidic conditions or by the alkylation of the guanine. A new false nucleic base can then be incorporated at the resulting apurinic site, or a single-strand break can occur through β-elimination.[4,21,22]

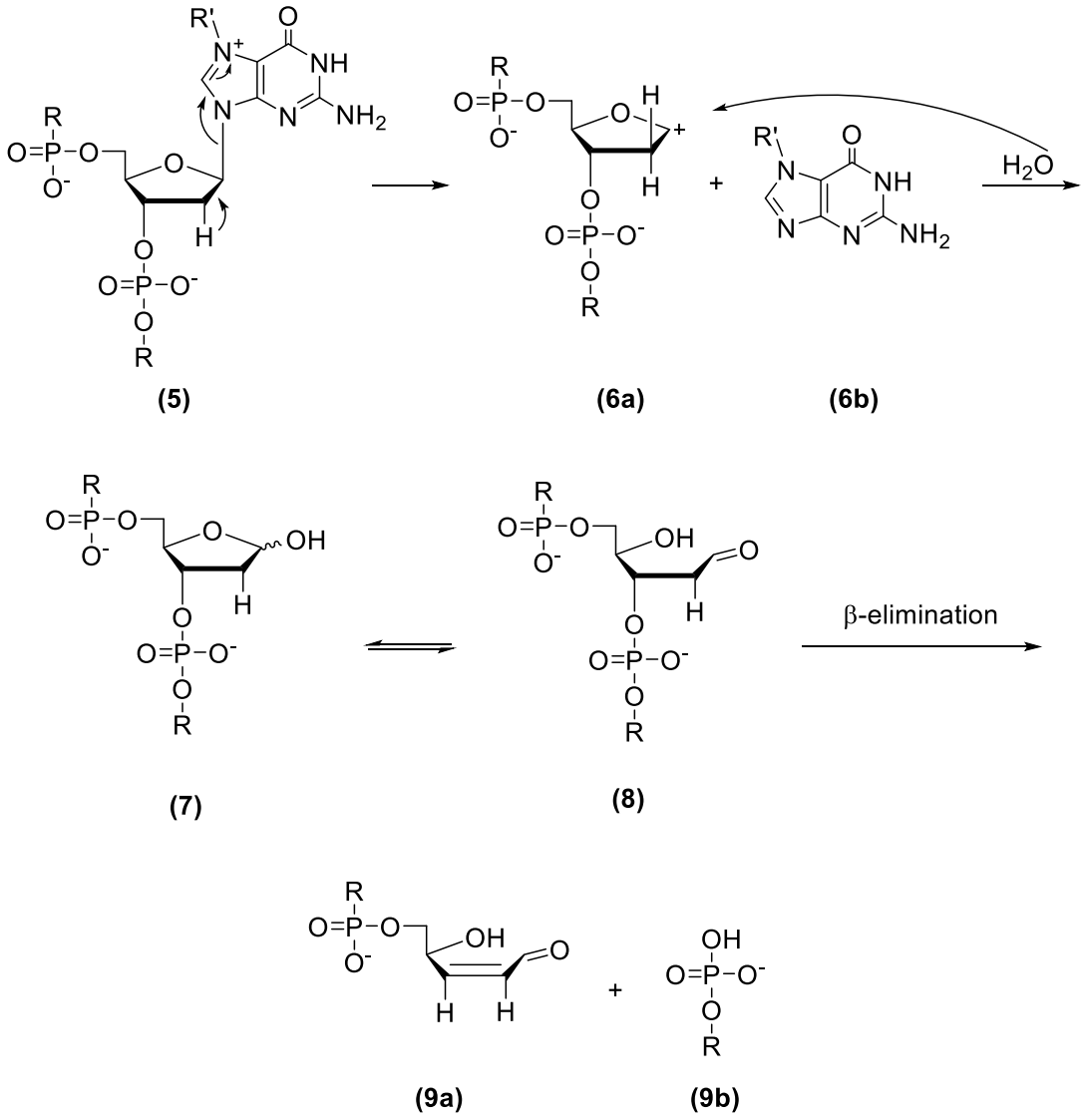

SCHEME 5: DEPURINATION WITH A DOUBLE-STRAND BREAK.[4,21,22]

Point mutations include the reaction of guanine with hydroxyl radicals and subsequent oxidation to 8-oxoguanine.[23] This modification results in an incorrect base pairing with adenine and no longer with cytosine.[24] In addition to the endogenous causes mentioned, exogenous influences can also lead to DNA damage. These include environmental influences such as ionising radiation (UV and X-rays) or chemical mutagens such as *N*-Lost. UV radiation can covalently link the pyridine bases cytosine and thymine so that the DNA strands can no longer be separated from each other during replication.[25] X-rays can cause excess reactive oxygen species (ROS), leading to single and double-strand breaks.[26] As previously mentioned, Lost derivatives can alkylate nucleic bases, leading to single or double-strand breaks.[17]

2.4 Antibiotics 593A

The antibiotic 593A (Figure 4) was first isolated from the bacterium "*Streptomyces griseoluteus*" in 1970 and showed good antineoplastic properties. These can be traced back to the two chloropiperidine systems as active components.[27] Those can, analogous to *N*-Lost compounds, form intermediate aziridinium ions (Figure 4), which can alkylate DNA.

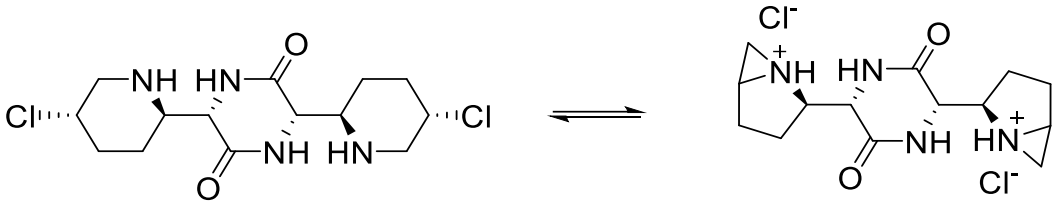

FIGURE 4: FORMATION OF THE AZIRIDINIUM-ION OF ANTIBIOTIC 593A.

Another property of antibiotic 593A is that it also affects tumours that have developed resistance.[27] Despite the promising properties, no clinical use was considered because extraction of the active ingredient is not possible in large quantities, and total synthesis proved difficult.[28]

Based on the structure of the antibiotic 593A, various mono- and bifunctional alkylating agents were produced by the *Göttlich* group and investigated concerning their biological activity. Bifunctional alkylating agents were connected via a linker, while monofunctional alkylating agents had a non-linking residue. (Figure 5).[4,5] The β-chlorinated amine, derived from antibiotic 593A, always serves as the reactive scaffold.

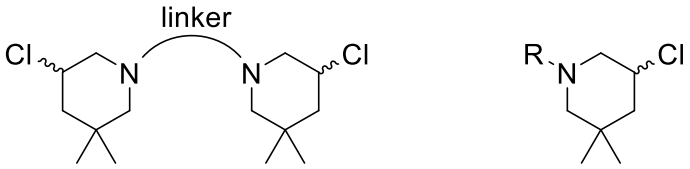

FIGURE 5: *BIS*-3-CHLORPIPERIDINE (LEFT) AND MONO-FUNCTIONAL (RIGHT).

The reactivity of mono-functionalised 3-chloropiperidines can be split up into two steps. First, the nitrogen attacks the β-carbon, forming the aziridinium ion by expelling chloride, and second, a nucleophile attacks the generated aziridinium ion. Three modes are available for adjusting the reactivity (Figure 6). The nitrogen nucleophile's quality can change due to *N*-functionalization, consequently changing the nitrogen's electron density. Increasing the electron density leads to increased reactivity, while decreasing it leads to a decrease in reactivity.[4] Altering the carbon's electrophilic quality is another option. By replacing the leaving group, this alteration can be done. Mesyl groups, which are good leaving groups, improve reactivity, whereas fluorides, which are inferior leaving groups, reduce reactivity.[29] Finally, modification of the ring system by geometric constraints in the form of geminal-alkyl interactions can alter the activation barrier. Thus, strongly strained cyclopropane substituents can lower the reactivity, while strongly repelling groups, such as phenyls, lead to increased reactivity.[4,29] The theoretical background of this observation is discussed in the next chapter.

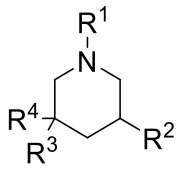

FIGURE 6: POSSIBLE SITES FOR THE MODIFICATION OF 3-CHLOROPIPERIDINES. R^1 = *N*-FUNCTIONALISATION, R^2 = LEAVING GROUP, $R^{3,4}$ = SUBSTITUTION WITH GEM. ALKYL-INTERACTION.

2.5 Geminal-Disubstitution Effect

Replacing hydrogens on a carbon chain connecting two reactive centres with alkyl groups commonly results in enhanced cyclisation processes (Figure 7).[30] This effect is known as the geminal dialkyl-effect (gem. dialkyl-effect) and has been utilised to conduct sophisticated cyclisation reactions.

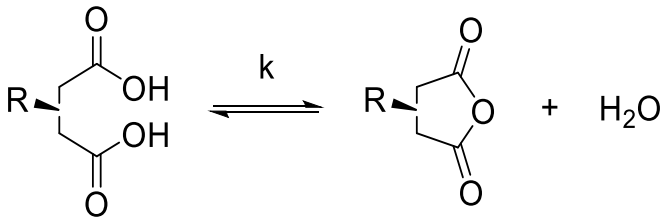

R	k / min^{-1}
Unsubstituted	$9 \cdot 10^{-6}$
Methyl	$5.9 \cdot 10^{-5}$
2,2-dimethyl	$1.1 \cdot 10^{-4}$
tetramethyl	0.018

FIGURE 7: DEPENDENCE OF THE CYCLISATION RATE ON THE SUBSTITUTION.[31]

Thorpe and *Ingold* gave the first explanation for his phenomenon in 1915.[32] They proposed that the introduced alkyl groups reduce the internal chain angle through repulsive interactions. In contrast, the angle can be increased by a strained substituent (Figure 8).[33] Reducing the internal angle brings the two reactive groups closer, favouring cyclisation. When angle *θ* is present in a small ring, the Thorpe-Ingold effect aids ring stabilisation.[30]

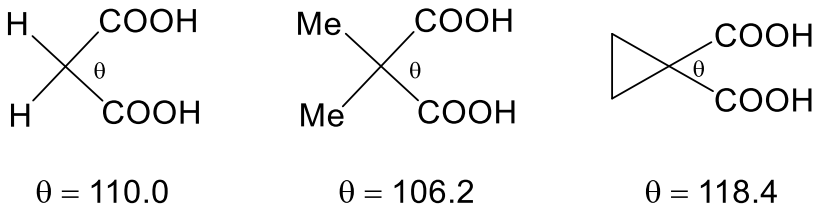

FIGURE 8: ANGLE COMPRESSION AND EXPANSION THROUGH THE THORPE-INGOLD-EFFECT.[33]

In general, for cyclization to occur, the reactive groups of a molecule must approach each other; therefore, a rotation on the C-C bond must occur (Figure 9). *Bruce* and *Pandit* published another theory in 1960 which assumes that the energy of the anti and gauche conformers aligns through the introduction of methyl groups. [34] As a result, the population of the reactive gauche rotamer would increase, and cyclisation would be favoured (Figure 9).

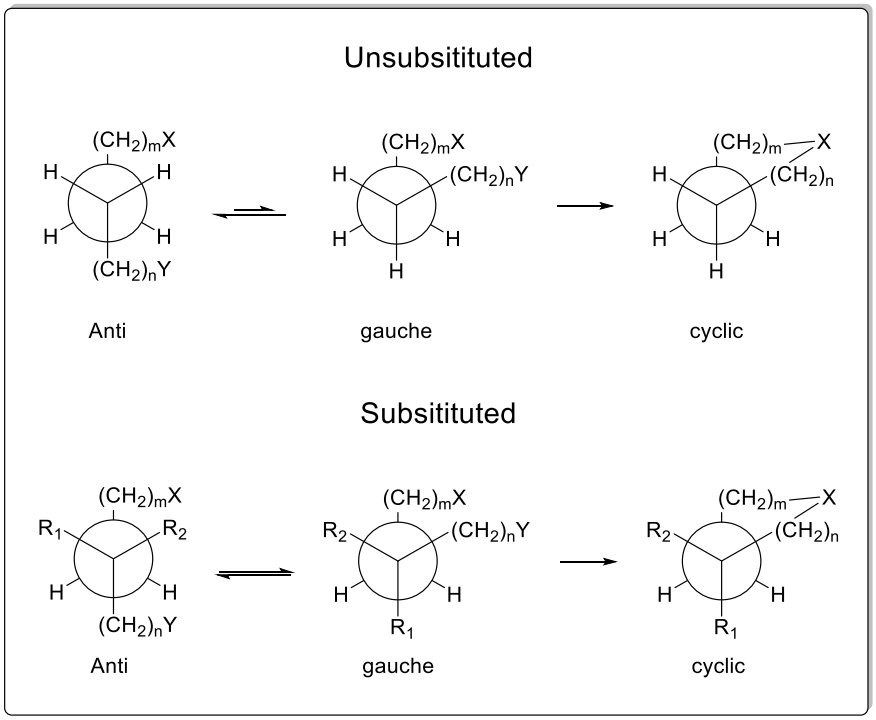

FIGURE 9: REACTIVE ROTAMER EFFECT ON CYCLISATION.[30]

However, this hypothesis contradicts the Curtin-Hammet principle. Which states that an upstream equilibrium does not influence product formation.[35] In the same year (1960), *Zalkow* and *Allinger* published an analysis of the thermodynamic factors of the gem-dialkyl effect.[36] They found that cyclisation is enthalpically preferred through substitution due to fewer gauche interactions in the cyclised product. Furthermore, cyclization is also entropically preferred since branching in open-chain systems restricts rotation more than in a ring system. In 1994, *Dolata* and *Parill* postulated a transition state to facilitate the transition between the reactive rotamer and the cyclisation product.[37] They came up with this assumption while investigating intramolecular Diels-Alder cyclizations. The cyclisation rate and the reactive rotamer's occupancy were not linearly related in their analysis. Therefore, it is unlikely that the gem-dialkyl effect is the primary cause of the rapid reaction. They suggested that the acceleration was due to a general reduction in the activation enthalpy $\Delta H^{\neq}$ through the reduction of the rotational barrier between the ground and transition state due to a dialkyl substitution.

A recent study by the *Göttlich* group investigated the influence of the gem. dialkyl-effect on the reactivity of 3-chloropiperidines.[8] Because of the cyclic nature of those compounds, the orientation of the reactive centres is already fixed; therefore, the population of reactive gauche conformers cannot be the reason for reactivity variation. Consequently, only the change of the internal angle β would contribute to the reaction properties through a classical Thorpe-Ingold effect (Figure 10). Thus, they have separated the two effects of an intramolecular reaction in an already cyclic system.

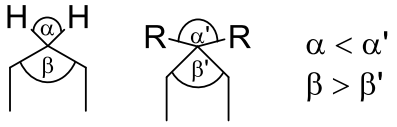

FIGURE 10: COMPRESSION OF THE INTERNAL ANGLE *B* BY INTRODUCING GEMINAL SUBSTITUENTS, WITH R = OTHER SUBSTITUENTS THAN H.[8]

Kinetic measurements were done with various substituted 3-chloropiperidines at position five to examine how the Thorpe-Ingold effect affects the reactivity. Subsequently, it was determined how the substituents influence the angles α and β (Figure 11). Furthermore, these derivatives were investigated computationally utilising DFT calculations, and the assumed angular alterations were confirmed via single-crystal XRD. For this purpose, the derivatives were crystallised as hydrochloride salts. The calculated and measured angles agreed. Furthermore, a correlation was found between the angle β and the relative rate constant. However, there was no connection between α and the rate constant, since the angles do not relate linearly. As

a result, it was possible to conclude that substituents with a small angle α increase angle β and decrease the relative reaction constant. With a large angle α, the opposite effect occurs. These results correspond to the classical Thorpe-Ingold effect. However, the differences in the rate constants are inferior to systems where the reactive Rotamer effect is also present.[30] Additionally, it was discovered that geometric distortion alters the distance (d) between the electrophilic β carbon and the nucleophilic nitrogen, which can be traced back to the altered angles α and β.

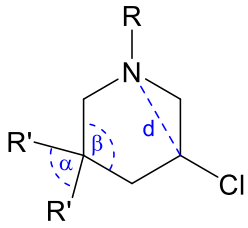

FIGURE 11: INVESTIGATED PARAMETERS OF 3-CHLOROPIPERIDINES UNDER THE INFLUENCE OF THE THORPE-INGOLD-EFFECT.

2.6 Synthesis of 3-Chloropiperidines

The synthesis of 3-chloropiperidine derivatives is mainly done via three routes. The first route uses 2,2-dimethylpent-4-enal (**12**) as its starting material (Scheme 6).[5] The pentenal can be prepared from allyl alcohol (**10**) and isobutyraldehyde (**11**) through a one-pot reaction according to a prescription of *K. C. Brannock*. (Scheme 6).[38]

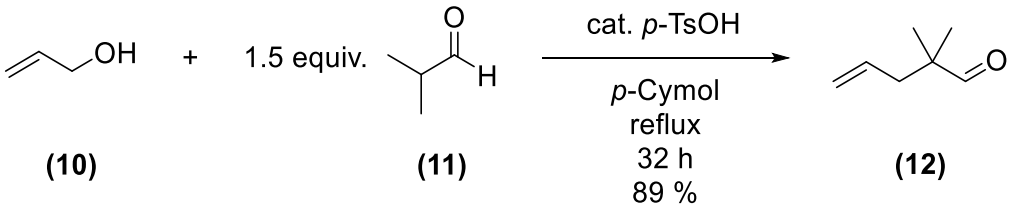

SCHEME 6: SYNTHESIS OF 2,2-DIMETHYLPENT-4-ENAL[38]

A reductive amination reaction with an amine and sodium triacetoxyborohydride can be performed on the produced pentenal (Scheme 7). This reaction produces a secondary amine (**13**) which is chlorinated with *N*-chlorosuccinimide (NCS) in the next step to obtain the *N*-chloramine. According to *Göttlich*, a cyclisation reaction occurs in the last step by catalytic addition of tetrabutylammonium iodide. The reaction yields the desired 3-chloropiperidine (**15**).[5] The last two steps can be substituted by a single reaction using $CuCl_2 \cdot 2\ H_2O$.[39]

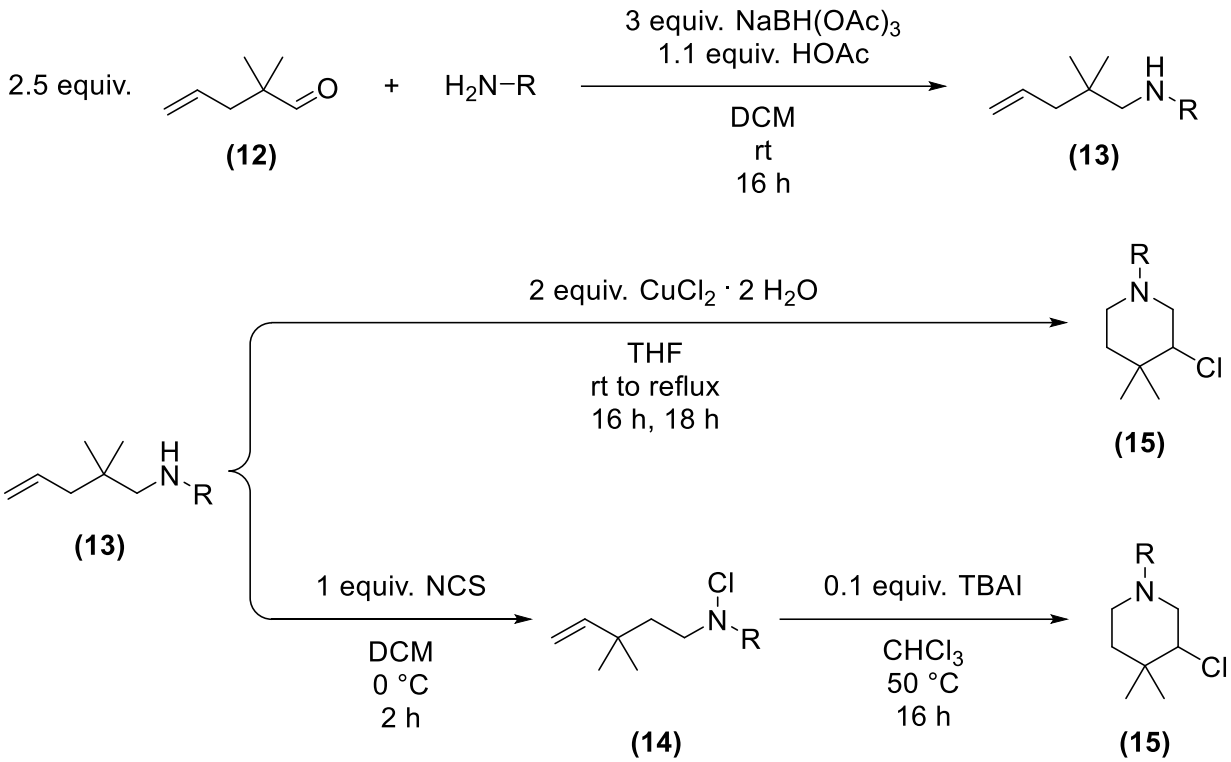

SCHEME 7: SYNTHESIS OF 3-CHLOROPIPERIDINES ACCORDING TO THE CYCLISATION ROUTE[5]

In the second route (Scheme 8), nitrile components (**16**) are used as the starting compound. In the first step, these are deprotonated in α-position and then reacted with allyl bromide to yield (**17**). A subsequent reduction with LAH obtains the primary amine (**18**). The obtained amine can be functionalised again through reductive amination on the nitrogen and then cyclized via the above routes to form the 3-chloropiperidine (**19**).[8]

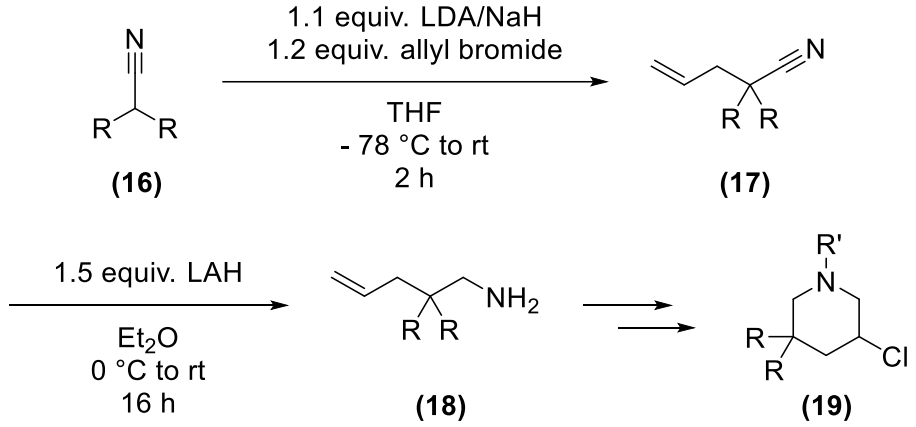

SCHEME 8: SYNTHESIS OF 3-CHLOROPIPERIDINES FROM NITRILES. (R = DIPHENYL, CYCLOPROPYL OR CYCLOBUTYL)

Adding tetrabutylammonium iodide to the *N*-chloramine (**14**) leads to an *N*-iodoamine (**14a**), whereby the nitrogen-iodine species is highly reactive (Scheme 9). The iodine can attach to the double bond, forming an iodonium ion (**14b**). After its rotation (**14c**), an S_N2-like attack of the nitrogen can occur, opening the iodonium ion (**14d**). Due to a renewed nucleophilic attack of nitrogen on the positively polarised carbon, an aziridinium ion is formed (**14e**). Iodide is split off, which is available for the next cyclisation cycle. The aziridinium ion formed is in equilibrium with the desired 3-chloropiperidine (**15**). However, the equilibrium is firmly on the side of the 3-chloropiperidine, as the latter is thermodynamically favoured.[40]

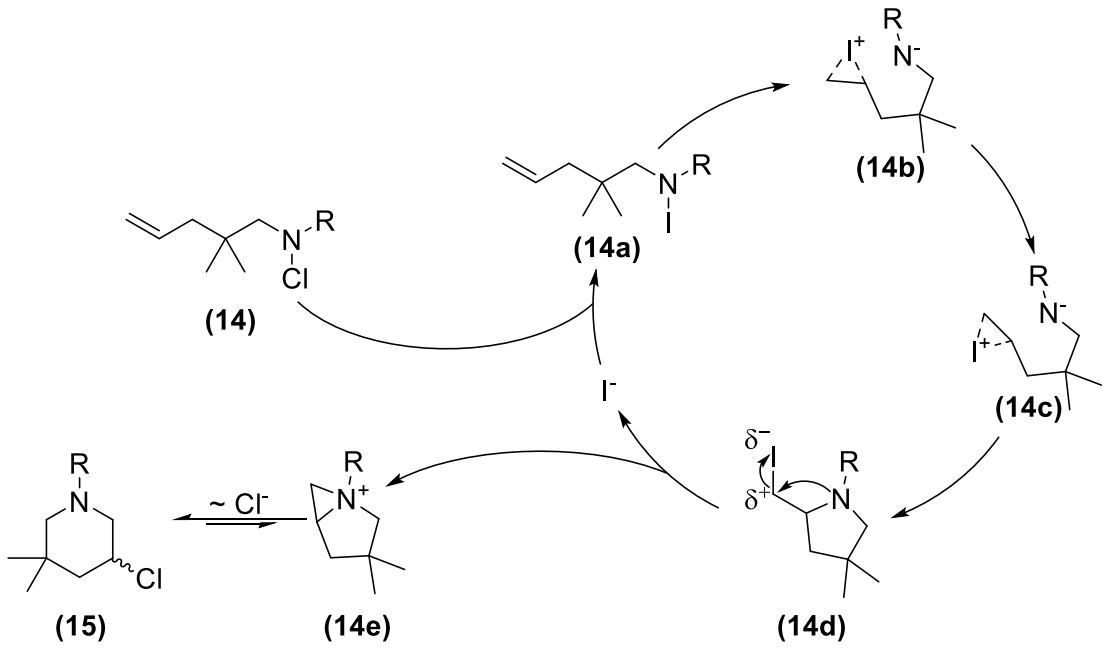

SCHEME 9: IODIDE-CATALYSED CYCLISATION.

However, synthesis according to the described route is not always possible. During chlorination with NCS, for example, nitrogen-containing functional groups can lead to undesired side reactions, as those nitrogen atoms can also be chlorinated.[40] Another problem of this route is the non-adjustable stereochemistry of the product obtained. Therefore, the 3-chloropiperidines are only obtained as a racemic mixture. The mechanism of the last step can explain this since racemisation is possible because of the iodonium ion's ability to be opened from both sides through a nucleophilic attack (Scheme 9).

A synthesis starting from proline can be performed for the formation of enantiomerically pure 3-chloropiperidines (Scheme 10). This route can also be used for non-substituted 3-chloropiperidines since the yield after the previously described route without the gem-dialkyl effect is inferior. In the first step, the starting compound proline (**20**) is reduced with lithium aluminium hydride to prolinol (**21**). The obtained prolinol (**21**) can be *N*-functionalised during an S_N2 reaction utilising *n*-butyl iodide.

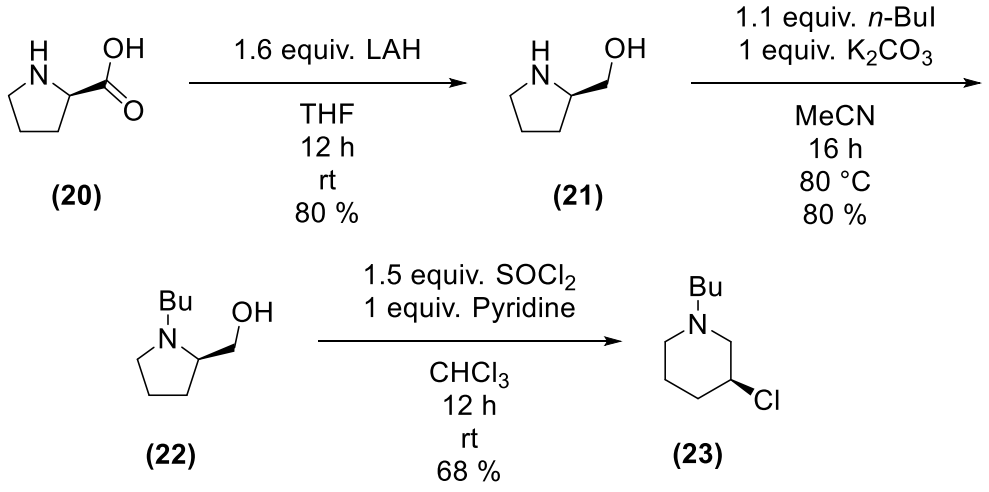

SCHEME 10: SYNTHESIS OF 3-CHLOROPIPERIDINES STARTING FROM PROLINE.[4]

A tertiary amine (**22**) is obtained, which is reacted with thionyl chloride (**22a**), whereby the hydroxyl group gets converted into a chloride (**24**, Scheme 11). After that, a nucleophilic attack of the free electron pair of nitrogen on carbon β occurs. Therefore, a bicyclic aziridinium ion is formed with the exclusion of chloride (**25**). Subsequently, a ring expansion occurs by the chloride anion attacking carbon α, whereby the desired 3-chloropiperidine (**23**) is obtained.[4]

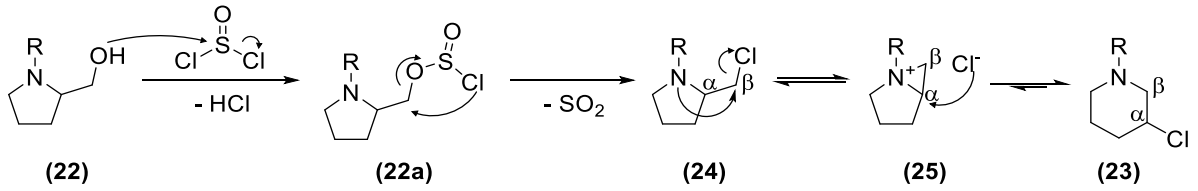

SCHEME 11: CHLORINATION OF PROLINOL WITH SUBSEQUENT RING EXTENSION TO 3-CHLOROPIPERIDINE.

2.7 Computational Methods

The Orca 5.0.3 software suite was used to carry out all density functional theory (DFT) calculations.[41] The Perdew-Burke-Ernzerhoff-hybrid-functional-type composite method PBEh-3c with the modified def2-mSV(P) basis set was used for structure optimisations.[42] Transition states were characterised as a structure with precisely one imaginary frequency with a wavenumber above 100 cm^{-1}. The two connected minima were obtained by calculating the intrinsic reaction coordinate (IRC)[43]. Hence the minima were identified by the absence of any vibrational frequency. The lowest energy conformers were confirmed using the Crest program package.[44] In order to account for solvation, free solvation energies at the PBE0[45]/def2-SVP[46] level of theory were computed using the CPCM-Model[47] for methanol. The standard state correction was applied (1.89 kcal/mol). Accurate electronic energies were calculated using the revDSD-PBEP86-D4[48] double hybrid functional, with the Ahlrichs basis set def2-QZVPP[46] and the corresponding auxiliary basis set. The RIJCOSX approximation with a grid size of three for the coulomb integrals was used.

2.7.1 Density functional theory

Density functional theory (DFT) is based on the Hohenberg-Kohn theorem, which states that a chemical system's physical characteristics can be described by its electron density. Furthermore, the second part of the theorem states that the lowest obtainable energy must be that of the ground state.[49] Thus, this approach is helpful for systems with many electrons since wave function-based calculations provide an exponentially increased effort.[50] In Kohn-Sham's theory, the ground state energy is described by equation (1).[51]

$$E[\rho] = T_s[\rho] + V_{ne}[\rho] + J[\rho] + E_{xc}[\rho] \tag{1}$$

The terms $T_s[\rho]$, $V_{ne}[\rho]$ and $J[\rho]$ are described precisely by equations (2) - (4). The functional $T_s[\rho]$ describes the system's kinetic energy where the subscript s, in equation (1) + (2), indicates that one-electron slater determinants are used. Further $V_{ne}[\rho]$ represents the nuclear electron potential and $J[\rho]$ the electron-electron repulsion. The remaining exchange-correlation functional is thus the decisive term for the quality of the DFT calculation.

$$T_s[\rho] = \sum_i \left\langle \phi_i \middle| -\frac{1}{2}\nabla^2 \middle| \phi_i \right\rangle \tag{2}$$

$$V_{ne}[\rho] = \int \rho(r) v(r)\, dr \tag{3}$$

$$J[\rho] = \frac{1}{2} \iint \frac{\rho(r)\rho(r')}{|r-r'|} dr dr' \tag{4}$$

The first approach was the local density approximation (LDA). Here, the form of Paul Dirac's exchange functional of the uniform electron gas was used (equation (5)).[52] However, the correlation functional was not derived from the exchange functional but determined by limiting case Monte Carlo simulations.[53]

$$E_x^{LDA}[\rho] = -\frac{3}{4}\left(\frac{3}{\pi}\right)^{\frac{1}{3}} \int \rho^{\frac{4}{3}} dr \tag{5}$$

The most commonly used LDA correlation functionals were developed by Vosko et al.[54] and Perdew[55]. Since the uniform electron gas has a fundamentally different electron density than atomic or molecular systems, geometries were determined well, but molecules were bound too firmly, and activation energies were underestimated by several kcal/mol.[56]

A gradually changing electron gas was described to overcome these problems. However, the electron density of atoms and molecules does not change steadily, so a general gradient assumption (GGA) was developed. This assumption can describe strongly localised electron densities as well as electron densities with solid gradients.[56] The most commonly used exchange functionals include B88[57] and PBE.[58] The development of the correlation function proved to be highly challenging too.[56] The most commonly used correlation functionals nowadays are LYP[59] and PBE.[58] However, GGA still underestimates the activation energy by several kcal/mol. The meta-GGA approach, which uses the second derivation of the electron density to define the exchange-correlation-functional, was created as an enhancement to the GGA method.[56]

The next significant advance was the introduction of hybrid functionals that introduce some Hartree Fock exchange (HF) into the functional. The first approach with a linear relationship between LDA and HF exchange was not significantly better than GGA functionals.[60] Due to the influence of experimental data, parameters a, b and c were introduced for the proportions of GGA, LDA and HF influence (equation (6)). Therefore the method is significantly improved.[60] Activation energies can finally be determined to a good approximation, as HF methods tend to overestimate activation energies and thus, the underestimated activation energies of the LDA methods can be compensated.[56]

$$E_{xc}^{B3} = \alpha E_x^{HF} + (1-a)E_x^{LDA} + b\Delta E_x^{B88} + cE_c^{GGA} + (1-c)E_c^{LDA} \tag{6}$$

The last significant step is the development of double hybrid functionals (DHF). While in hybrid functionals, only HF exchange is added to the exchange-correlation functional, in double hybrid functionals, some of the second-order Møller-Plesset perturbation theory (MP2) is added to the functional too. Therefore, unoccupied orbitals are also considered in the calculations. Typically, the admixture consists of 50 – 70%.[61] The first three terms from equation (7) are calculated when carrying out the method, and the obtained values are used to calculate the remaining term. Afterwards, the obtained energies are added together. With this method, ground state energies, excited states and molecular structures can be calculated precisely.[48]

$$E_{xc}^{DHDFT} = (1\text{-}a_x)E_x^{DFT} + a_x E_x^{HF} + (1\text{-}a_c)E_c^{DFT} + a_c E_c^{MP2} \tag{7}$$

2.7.2 PBEh-3c

Grimme et al. published the PBEh-3c method in 2015 to further develop the numerically robust hybrid GGA method Perdew-Burke-Ernzerhoff (PBE). They combined the original method with a triple-corrected Hartree-Fock (HF) method, significantly improving the obtained thermal and electronic structures with comparatively little computational power. The triple correction refers to the correction of the basis set, a dispersion correction for long-range interaction and a correction of the basis set superposition error (BSSE). The corrections are added to the obtained energy of the PBEh method, giving the total energy of PBEh-3c (equation (8)).[42] The correction for long-range interaction E_{Disp} is implemented using the London dispersion energy from the D3-Scheme[62] with *Becke-Johnson* (BJ) damping.[63] Lastly, to account for BSSE, the damped geometrical counterpoise (damped gCP) correction scheme[64] is employed.

$$E_{tot}^{PBEh3c} = E_{tot}^{PBEh} + E_{Disp} + E_{BSSE}^{damped\ gCP} \tag{8}$$

The PBEh exchange-correlation functional is based on the GGA exchange and correlation functional of PBE, to which non-local HF exchange is added through the parameter α_x (equation (9)).[42] The first approach was developed by Adamo and Barone using $\alpha_x = 0.25$.[65] However, this approach was not particularly robust thermochemically. The desired accuracy was achieved with values of $0.3 < \alpha_x < 0.5$. In total, the best results were achieved with $\alpha_x = 0.42$.[42]

$$E_{XC}^{PBEh} = (1\text{-}a_x)E_x^{PBE} + a_x E_x^{HF} + E_C^{PBE} \tag{9}$$

The Ahlrichs-type split valence double-zeta basic set def2 SV(P) was used as the last improvement. Here, the s-function exponents were scaled by a factor of 1.2 to compensate for the missing p-polarisation function of hydrogen. This assumption allowed a better description of bonds involving hydrogens. The modified method was named def2 mSV(P) by *Grimme et al.*, where the m stands for modified.[42]

2.7.3 revDSD-PBEP86-D4

In 2019, *Santra et al*. presented the revDSD-PBEP86-D4 method[48] as a further development of the DSD-PBEP86 method.[66] This new method is minimally empirical, which has very high accuracy and a much lower computational cost than comparable methods. DSD stands for dispersion-corrected scaled spin-component double hybrid method. Furthermore, the P86 method is used for the correlation, while the PBE method is used for the exchange portion. Thus, both methods are based on the GGA approach.[66] The exchange-correlation term of the revDSD-PBEP86-D4 method is described in equation (10) and consists of DFT, HF, MP2 components and a dispersion addition.[48]

$$E_{xc} = c_x E_x^{DFT} + (1\text{-}c_x) E_x^{HF} + c_c E_c^{DFT} + c_o E_o^{MP2} + c_s E_s^{MP2} + s_6 E_D \tag{10}$$

Here, c_x and c_c correspond to the DFT exchange and correlation part, c_o to the opposite spin MP2, c_s to the same spin MP2 and s_6 to the dispersion correction. The dispersion correction is used for a better description of the long-range interactions. Instead of using D3(BJ) as in the original method, the modern D4 method performs the correction in this developed method. Therefore, an improvement is made by determining conformers, harmonic frequencies, and intermolecular interactions. The method achieves the best results with the parameters $c_x^{HF} = 0.69$, $c_c^{DFT} = 0.42$, $c_o = 0.59$, $c_s = 0.06$ and $s_6 = 0.51$. With these parameters, the method reaches the level of empirical methods with only a fraction of the required computation time.[48]

3 Results and discussion

3.1 Computational Investigations of 3-Chloropiperidine Derivatives

Computations were done to estimate how the substitution position impacts the reactivity of 3-chloropiperidines. The structure was pre-optimised in Avogadro using the Merck Molecular Force Field (MMFF94)[67], and then the structure's local minima energy (E^{GS}) was determined using DFT calculations. For the transition state search, the distance between the nitrogen and the chlorocarbon was reduced by 0.25 Å steps down to 1.5 Å. The structure of the local maximum along the investigated mode was augmented with a PBEh-3c TST optimisation (E^{TST}). Afterwards, the zero-point energy (E_{SP}) was calculated from this structure using the revDSD-PBEP86-D4-method. A thermal correction term (E_{tc}) was taken from the PBEh-3c calculations, which was added to the zero-point energies. From these values, the activation energy of the respective 3-chloropiperidine derivatives was calculated according to equation (11).

$$\Delta G = (E_{SP}^{TST} + E_{tc}^{TST}) - (E_{SP}^{GS} + E_{tc}^{GS}) \tag{11}$$

The computational calculations determined the angle θ, the distance d (Figure 12) and the resulting activation energy of the *N*-butyl-3-chloropiperidines. The obtained angles, distances and activation energies of the different compounds are listed in Table 1.

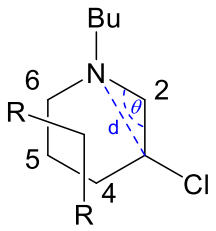

FIGURE 12: INVESTIGATED VALUES OF 3-CHLOROPIPERIDINES.

TABLE 1: ANGLE θ, DISTANCE d AND ACTIVATION ENERGY OF THE 3-CHLOROPIPERIDINE DERIVATIVES CALCULATED SO FAR.

Substance	Angle θ / °	Distance / Å	Activation energy / kcal · mol^{-1}
BuHH	108.76	2.412	20.31
Bu-2-MeMe	103.28	2.367	14.95
Bu-4-MeMe	109.00	2.416	21.50
Bu-5-MeMe	108.36	2.404	18.74
Bu-6-MeMe	109.03	2.414	19.09
Bu-4-PhPh	108.23	2.401	22.37
Bu-5-PhPh	108.05	2.396	19.22
Bu-6-PhPh	110.16	2.427	18.97

The calculated activation energies are shown graphically in Figure 13. The value for the unsubstituted *N*-butyl-3-chloropiperidine (BuHH) is shown in red. It is evident that introducing two methyl groups at position six only leads to a minimal increase in the activation energy. This increase is not significant, as it is still within the mean absolute deviation of the calculation method. By introducing two methyl groups at position two, on the other hand, it can be observed that the activation energy decreases significantly, which increases the reactivity of the compound. Lastly, it is evident that introducing two methyl groups at position four increases the activation energy and thus lowers the reactivity. This increase is outside the mean absolute deviation of the computational methods and is, therefore, significantly relevant.

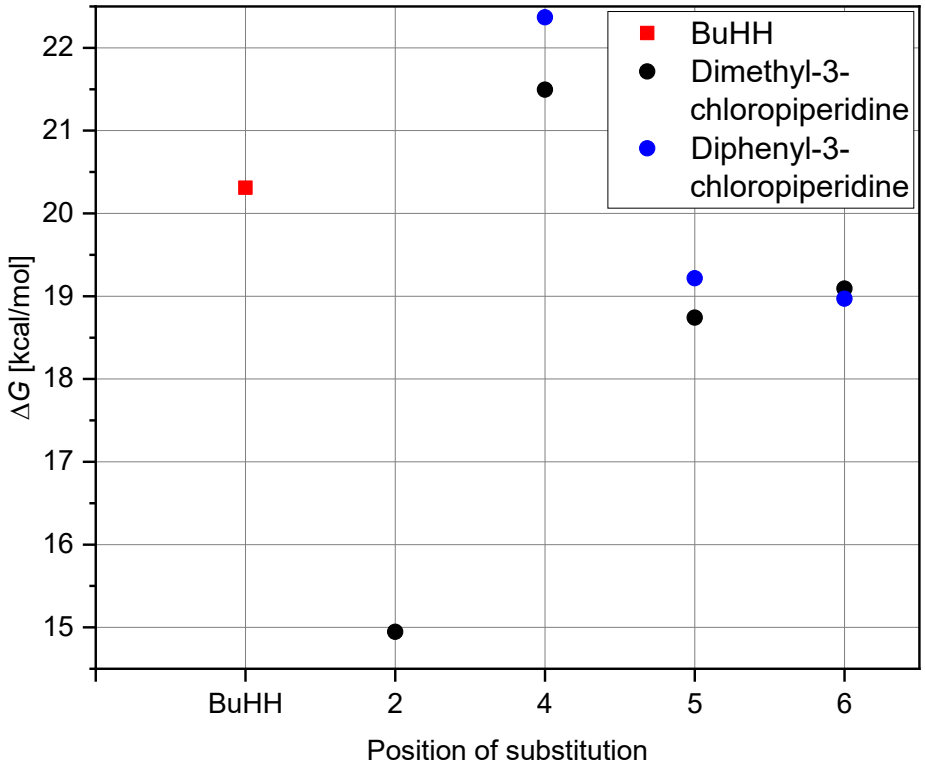

FIGURE 13: ACTIVATION BARRIERS FOR DIFFERENT SUBSTITUTION POSITIONS OF *N*-BUTYL-3-CHLOROPIPERIDINES.

After identifying that a substitution at positions four and six leads to an increase in the activation energy, derivatives were calculated, which have a higher A-value than methyl groups.[68] For this, phenyl groups were chosen. The calculated activation energies are also shown graphically in Figure 13. The *N*-butyl-3-chloro-2-diphenyl derivative was not calculated because the activation energy was already strongly reduced in the dimethyl configuration; therefore, it was suspected that a diphenyl substitution could further intensify this effect. When examining the calculated structures, it becomes apparent that a diphenyl substitution at position six appears to lower the activation energy. However, this change is minimal and lies

within the mean absolute deviation of the method used. Thus, this change is not significant again. On the other hand, a diphenyl substitution at position four significantly increases the activation energy compared to the dimethyl substitution. The next step was to investigate to what extent the activation energy is influenced by the angle *θ*, which is enclosed by the N-C-C(Cl) functionality. For this purpose, the activation energies obtained were plotted against *θ*. (Figure 14). It can be observed that the derivative with the smallest angle also has the lowest activation energy. Furthermore, there is a partial linear relationship between *θ* and the activation energy for the derivatives with dimethyl substitution. Such a trend cannot be seen with the diphenyl derivatives, so other factors may also influence the activation energy. In addition, two values stand out clearly because they have the highest activation energies in their respective series of values while not having the biggest angles. These values are the derivatives with a substitution at position four, as seen in Table 1. Therefore, additional factors must be present in these derivatives for the activation energy to increase.

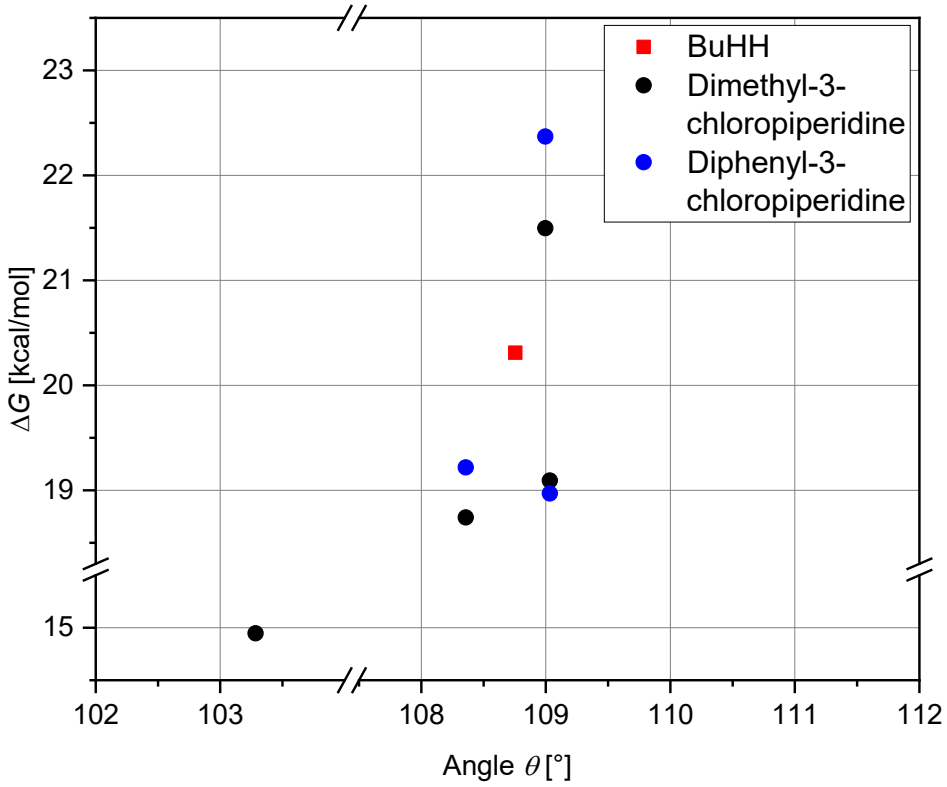

FIGURE 14: DEPENDENCE OF THE ACTIVATION ENERGY OF THE ANGLE *θ*.

A summary of the influence of the substitution position on the activation energy of *N*-butyl-3-chloropiperidines is given in Figure 15. The only derivative that exhibits an increase in activation energies is the one with a twofold substitution at position four, whereas the activation energies for all other derivatives drop.

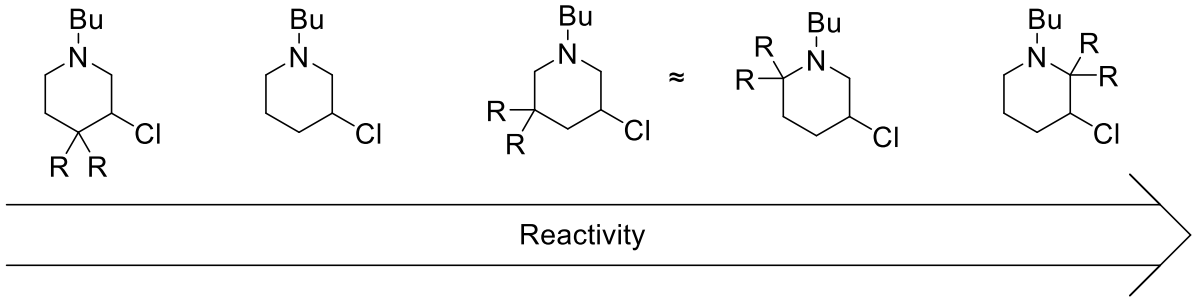

FIGURE 15: REVIEW OF THE IMPACT OF THE SUBSTITUTION POSITION ON THE REACTIVITY OF 3-CHLOROPIPERIDINES WITH R = ME, PH.

As a comparison, derivatives were calculated, which are monomethylated at different positions. Because methyl groups have an A-value of 1.7, they were placed equatorially, while the chloride was placed axially. With the help of these calculations, it can be estimated how strong the influence of the Thorpe-Ingold effect is on the reactivity of the different disubstituted derivatives. The obtained angles, distances and activation energies of the different compounds are listed in Table 2. Furthermore, the obtained activation energies are shown graphically in Figure 16. The value for BuHH is displayed again in red for comparison, while the previously calculated values for the *N*-butyl-3-chlorodimethylpiperidines are displayed in black.

TABLE 2: ANGLE *θ*, DISTANCE d AND ACTIVATION ENERGY OF THE CALCULATED *N*-BUTYL-3-Chloromonomethylpiperidine derivatives

Substance	**Angle *θ* / °**	**Distance / Å**	**Activation energy / kcal · mol^{-1}**
BuHH	108.76	2.412	20.31
2-BuMeH	110.40	2.443	39.35
4-BuMeH	111.46	2.446	41.10
5-BuMeH	111.23	2.441	40.66
6-BuMeH	112.15	2.456	41.33

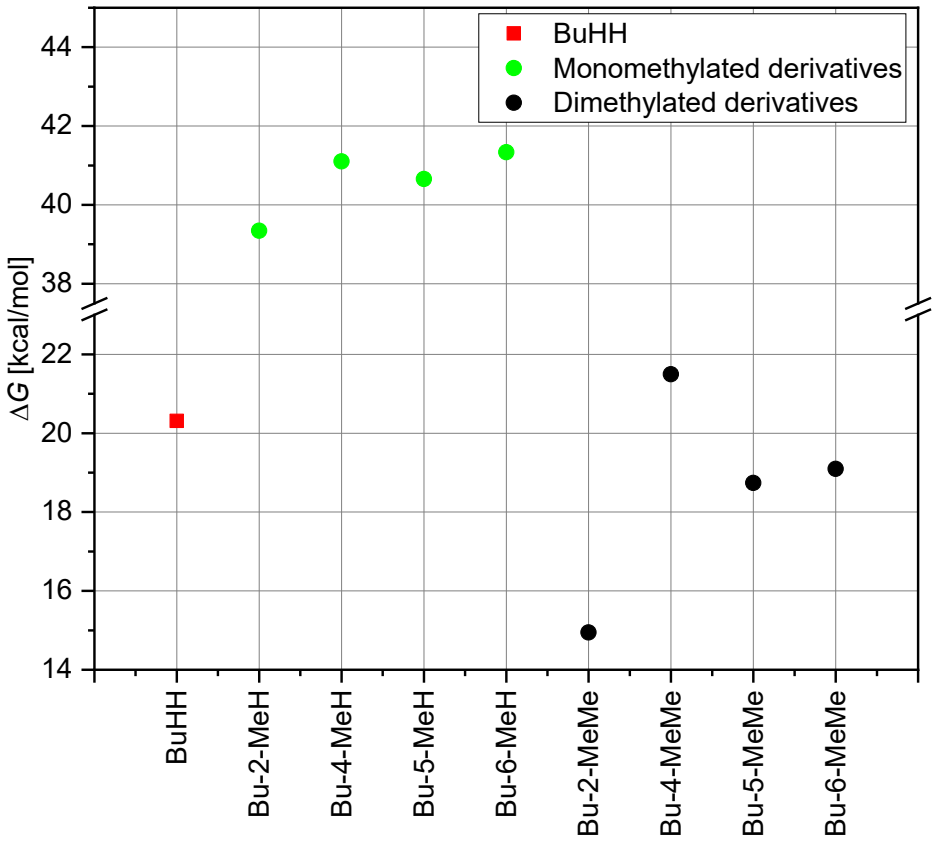

FIGURE 16: ACTIVATION BARRIERS FOR DIFFERENT SUBSTITUTION POSITIONS OF *N*-BUTYL-3-MONOMETHYLCHLOROPIPERIDINES.

Predictably, the monomethylated derivatives should have an activation energy like the unsubstituted counterpart. However, the computationally obtained energies are significantly higher, which is quite peculiar, as, at room temperature, no reactivity should be detected with such high activation energies. Therefore, the calculations should be repeated in the future. However, it could again be determined that substitution at position four leads to an out-of-trend increase in the activation energy. However, this peculiarity is much less pronounced in the monomethylated derivatives since the derivatives with mono substituents at positions four and six have similar activation energy. The extent to which the activation energy depends on the angle θ is also investigated. For this purpose, the activation energy is plotted against the angle (Figure 17). Again, a trend can be seen that the activation energy rises with increasing angle. Additionally, there is a linear relationship between θ and the activation energy. Once more, a value jumps out due to its deviation from this trend. According to Table 2, this is the derivative's value with the substitution at position four. The earlier hypothesis is strengthened through this data that extra factors must exist for the activation energy to rise in these derivatives.

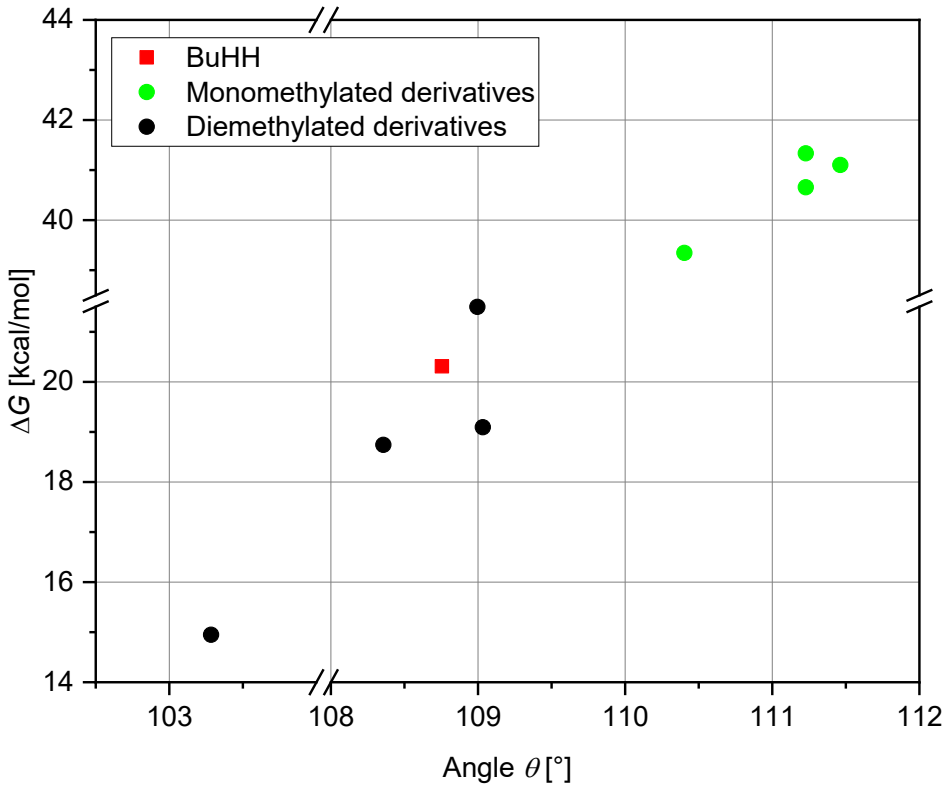

FIGURE 17: DEPENDENCE OF THE ACTIVATION ENERGY OF THE ANGLE θ.

All calculated structures are present as reactants in the chair conformation, while all transition states are present in the half-chair conformation.

The energy values for the calculated structures deviate from the literature values[8] by approximately 1-2 kcal/mol, which could be explained by the method since, as mentioned in chapter 16, the proportion of HF methods can overestimate the activation energy.

3.1.1 Calculation of isodesmic reactions

Furthermore, it was investigated whether 1,3-diaxial interactions occur with the *N*-butyl-3-chloropiperidines and whether these can influence the reactivity as a further factor. For this purpose, isodesmic reactions were calculated. In this context, isodesmic reactions represent reactions in which the number and type of bonds are maintained during the reaction. Furthermore, this allows a characterisation of the systematic error of the computational calculations. An example of such a reaction is given in Scheme 12.

SCHEME 12: EXEMPLARY ISODESMIC REACTION.

The calculated energy values for the 1,3-diaxial interactions with the respective reactions are shown in Scheme 13. It is evident that reaction 1 involves repulsive interactions, whereas reaction 4 exhibits interactions within a typical energy range of approximately 1.7 kcal/mol.[69] Additionally, reaction two exhibits minimal repulsive interactions, while reaction three exhibits stabilising effects.

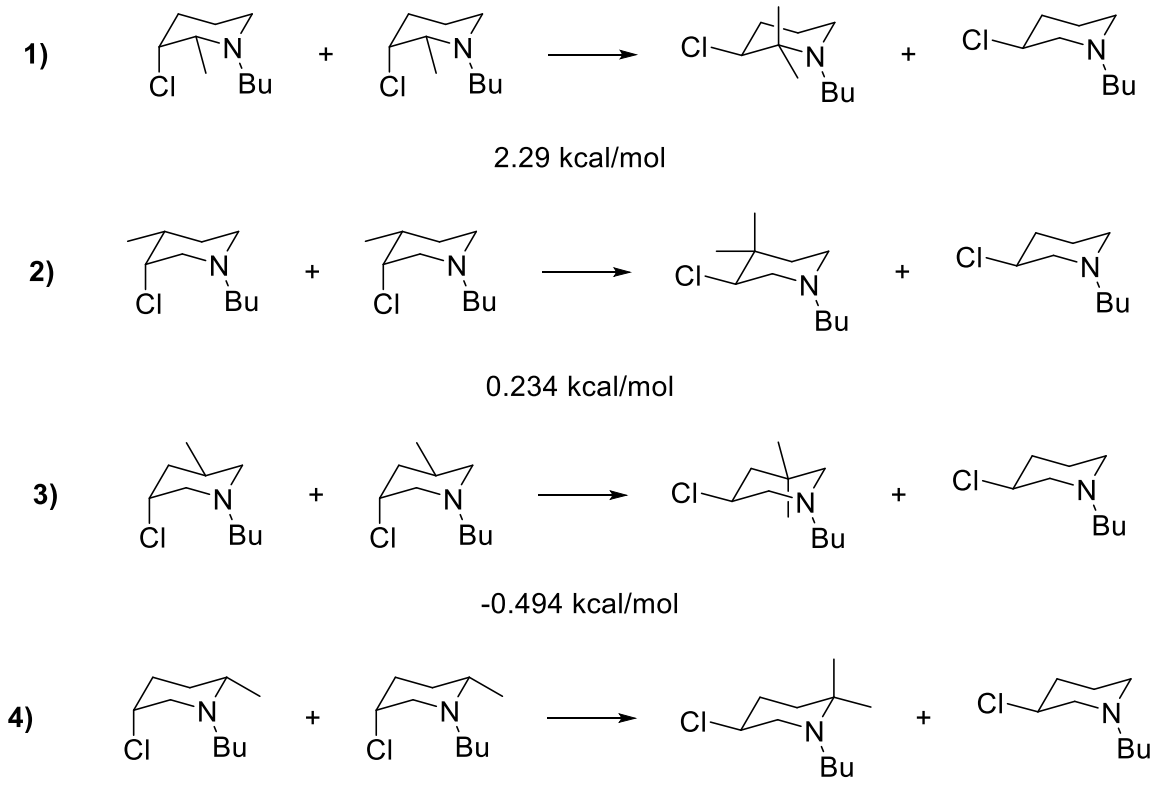

SCHEME 13: ISODESMIC CALCULATION WITH RESULTING 1,3-DIAXIAL INTERACTIONS.

Additionally, the systematic error of the computational calculations can be evaluated through the isodesmic reactions. For this purpose, the energies obtained in Scheme 13 are compared with the typical value of 1.3-diaxial interactions (1.7 kcal/mol[69]). It can be noticed that for reaction **4**) there is only a minimal error, while for reaction **3**) there is the most significant error. Reactions **1**) and **2**) exhibit an error of 0.5 and 1.5 kcal/mol, respectively.

Furthermore, isodesmic reactions were calculated for the transition states. The 1,3-diaxial interactions obtained are listed in Table 3. The energy difference between the axial interactions in the transition and ground states is also calculated. The energy differences obtained are given in column three of Table 3. Solid interactions occur during the transition state. However, the interactions obtained are too firm, so they should be considered cautiously and investigated again in the future. However, a trend can be recognized that significantly lower interactions occur in reaction **2**) than in all other reactions. Furthermore, the highest interactions occur in reaction **3**).

TABLE 3: Obtained 1,3-diaxial interactions in the transition state of the different reactions and energetic difference of the interaction in the ground state to the transition state.

Reaction	**1,3-diaxial interactions / kcal · mol^{-1}**	**ΔE / kcal · mol^{-1}**
1)	-41.1	-43.4
2)	-40.2	-40.4
3)	-42.8	-42.3
4)	-41.7	-43.3

3.2 Synthesis of 3-chloropiperidines

3.2.1 Synthesis of *N*-butyl-3-chloro-2,2-dimethylpiperidine

The synthesis of the first 3-chloropiperidine derivative was analogous to the synthesis of 5,5-dimethyl-3-chloropiperidines known from the literature.[4] First, the natural amino acid L-proline was quantitatively converted to a methyl ester using thionyl chloride in methanol (Scheme 14). Subsequently, nitrogen functionalisation was introduced using *n*-butyl iodide and K_2CO_3 as a base.

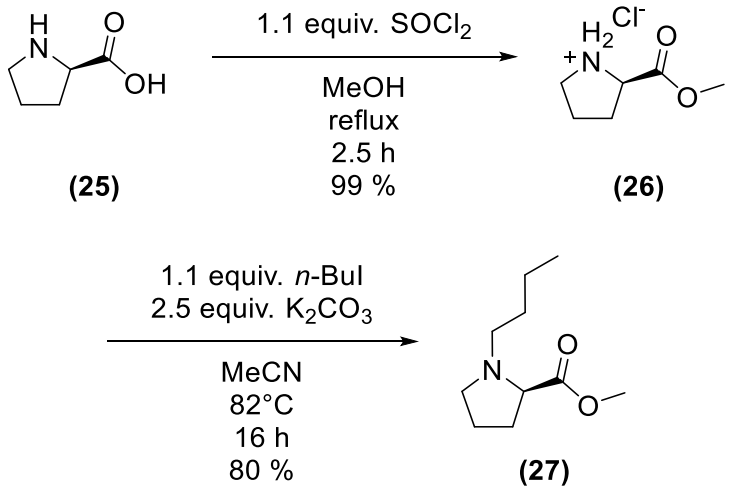

SCHEME 14: FORMATION OF THE FUNCTIONALIZED PROLINE.

In the next step, the two desired methyl groups were introduced employing a Grignard reaction, and lastly, the alcohol was chlorinated using thionyl chloride (Scheme 15). The desired product could be detected by Mass spectrometry, but isolation was impossible. This might be because the reaction mixture was distilled for purification at the HV since a flash chromatographic purification was only achievable with a highly polar eluent of DCM/NH_3 in MeOH. The distillation process may have produced no product because of the product's potential to breakdown at high temperatures. This theory is strengthened through a GC-MS analysis of the reaction mixture, as the product of an HCl elimination could be detected. The product's anticipated high reactivity might be another factor because a methanolysis could happen during the chromatographic purification or hydrolysis during the aqueous treatment.

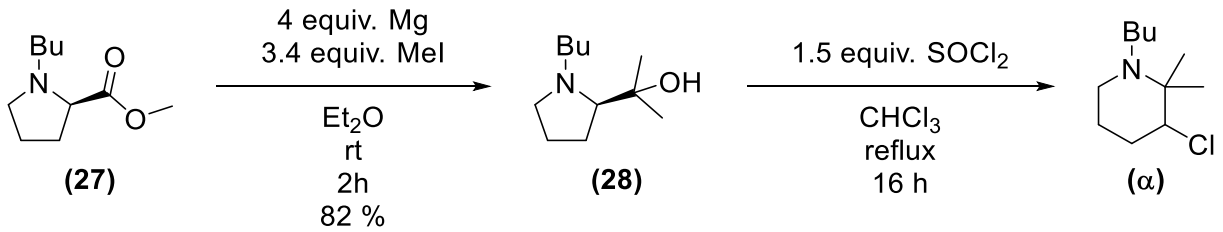

SCHEME 15: ADDITION OF TWO METHYL GROUPS TO THE METHYL ESTER AND UNSUCCESSFUL ISOLATION OF THE 3-CHLOROPIPERIDINE α.

As an alternative, a synthesis route was investigated in which a six-membered ring is first built up, and after that, chlorination takes place (Scheme 16). The alanine derivative 2-methyl alanine was used as the starting material. The amino acid derivative was converted into a methyl ester in the first step using thionyl chloride in methanol (**30**). Subsequently, reductive amination with butanal and triacetoxyborohydride was carried out to obtain a butyl functionalization at the nitrogen (**31**). The ester group was then reduced to the corresponding alcohol using LAH.

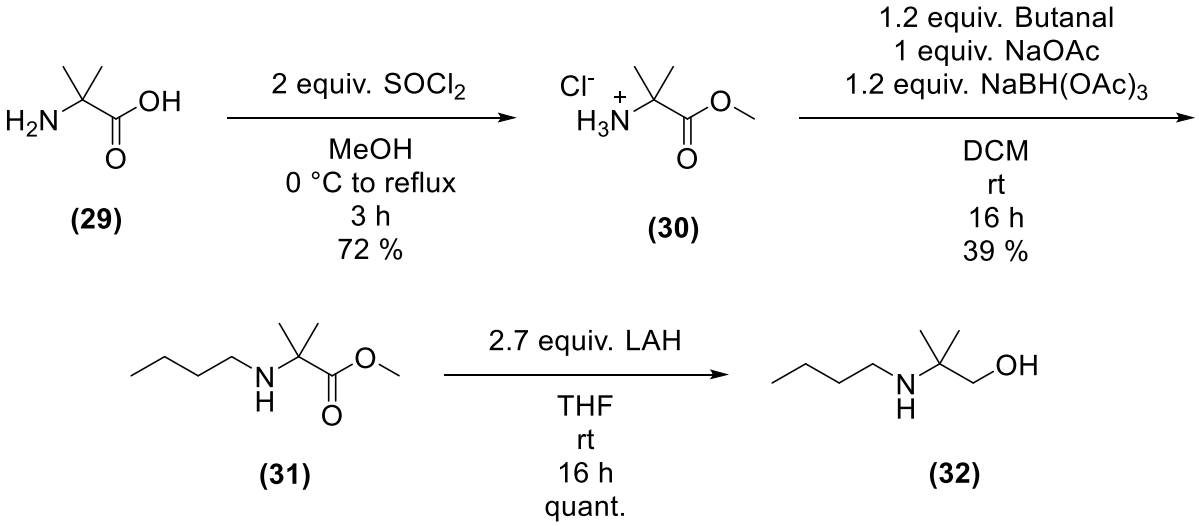

SCHEME 16: ESTERIFICATION OF THE CARBONIC ACID FUNCTION, SUBSEQUENT REDUCTIVE AMINATION, FOR FUNCTIONALISATION OF THE NITROGEN AND REDUCTION OF THE CARBONIC ACID ESTER TO THE CORRESPONDING ALCOHOL.

Subsequently, an endeavour was made to oxidise the obtained alcohol to the corresponding aldehyde (Scheme 17). An Albright-Goldman oxidation was used in the initial attempt.[70] However, it was unable to obtain any aldehyde. As another variant, oxidation was undertaken using PCC under anhydrous conditions. However, in this instance as well, it was impossible to acquire the intended product. Without a protective group on the nitrogen, oxidation to a ketimine could have interfered, so the nitrogen must be protected for a future attempt at oxidation.

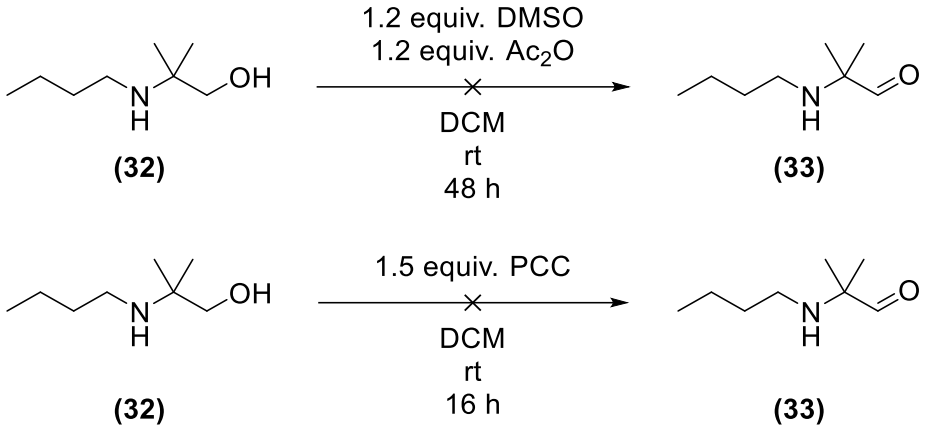

SCHEME 17: UNSUCCESSFUL OXIDATION OF THE ALCOHOL TO THE ALDEHYDE.

An alternative possibility to obtain the aldehyde would be a Swern-oxidation (Scheme 18). However, this tactic could not be tested since the necessary dry DMSO was unavailable. However, the unprotected nitrogen here could potentially be problematic too.

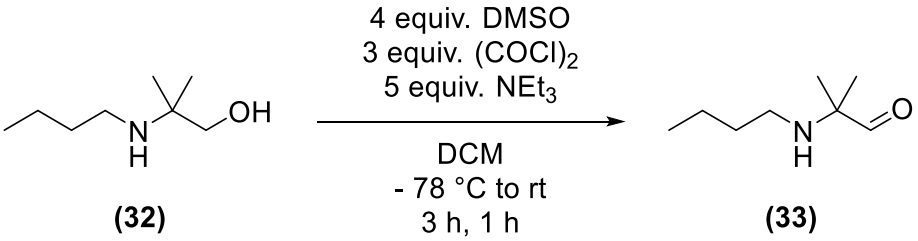

SCHEME 18: POSSIBLE OXIDATION OF THE ALCOHOL THROUGH SWERN-OXIDATION.

An alternative synthesis strategy was explored to overcome this issue (Scheme 19). First, the nitrogen was protected by using a Boc group because the already functionalized nitrogen could lead to problems during the intramolecular formation of the six-membered ring in the form of an ammonium ion.

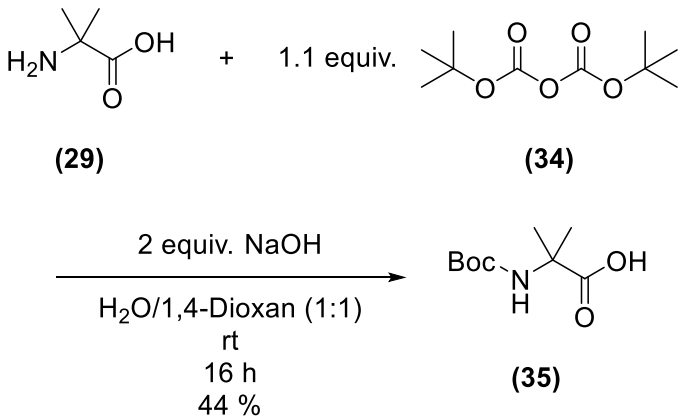

SCHEME 19: BOC PROTECTION OF METHYL ALANINE.

Subsequently, an attempt was made to convert the carboxylic acid into a Weinreb-amide and then reduce it to the desired aldehyde. Various reagents were used in the Weinreb-amide reaction (Scheme 20), but the intended coupling product was never obtained.

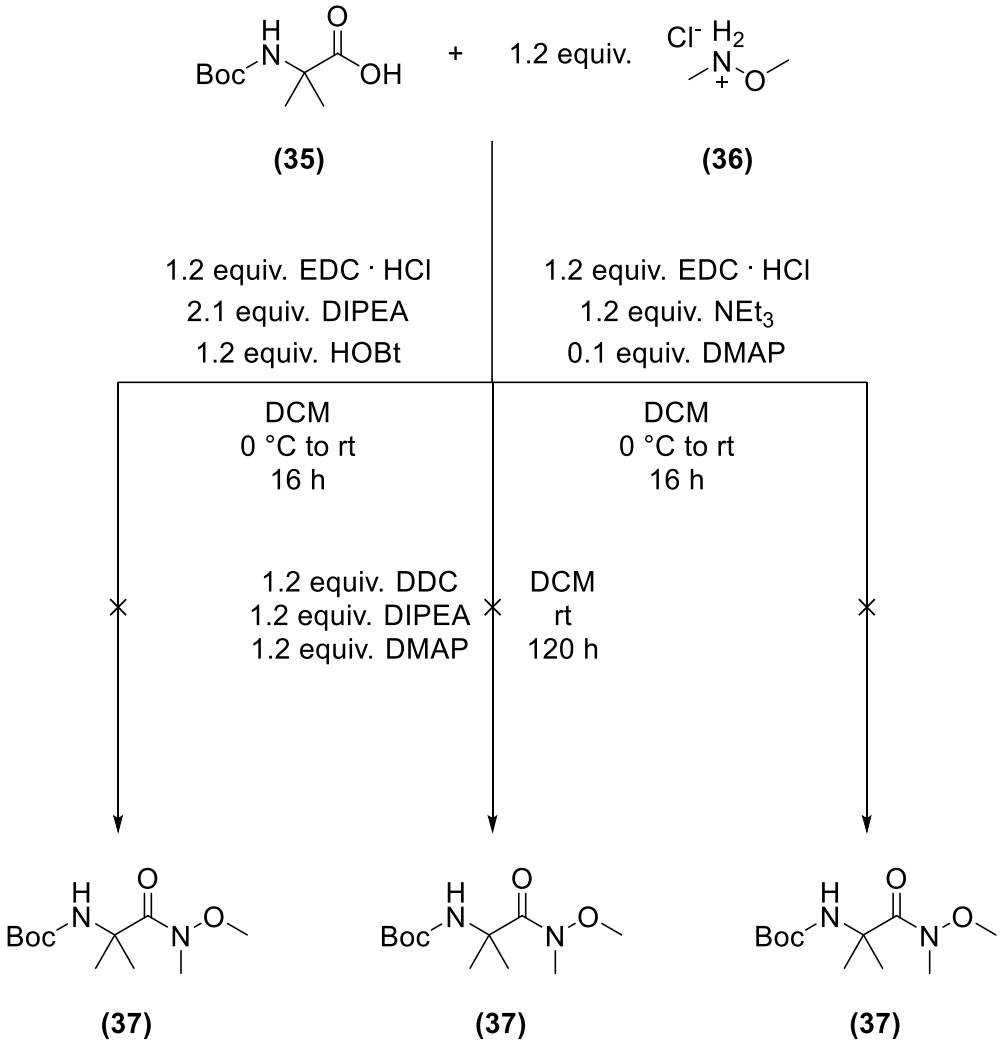

SCHEME 20: FAILED SYNTHESIS OF THE WEINREB-AMIDE.

Should the aldehyde be obtained in the future, e.g. using a Swern-oxidation or successful preparation of a Weinreb-amide with subsequent reduction, it might react with acrolein in a umpolungs reaction and thus represent two carbonyl functions at a 1,4-distance. Triazolium or thiamine salts might be used as a catalyst in a Stetter reaction to carry out the umpolungs process (Scheme 21).[71]

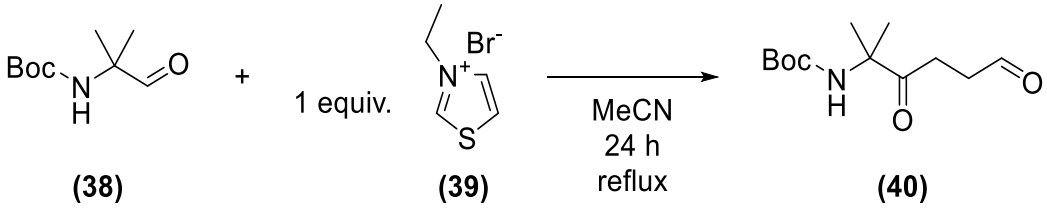

SCHEME 21: STETTER-REACTION FOR THE CHAIN ELONGATION.

Afterwards, the Boc-protecting group can be removed (**41**), and a nucleophilic attack of the nitrogen on the aldehyde can take place, whereby an intramolecular cyclisation is achieved (**42**, Scheme 22). The resulting ketimine and the ketone can be reduced in the same step using sodium cyanoborohydride (**43**). Afterwards, functionalisation of the nitrogen can occur by S_N2 reaction with *n*-butyl iodide (**44**), and, lastly, chlorination by $SOCl_2$ can take place to obtain the product (α).

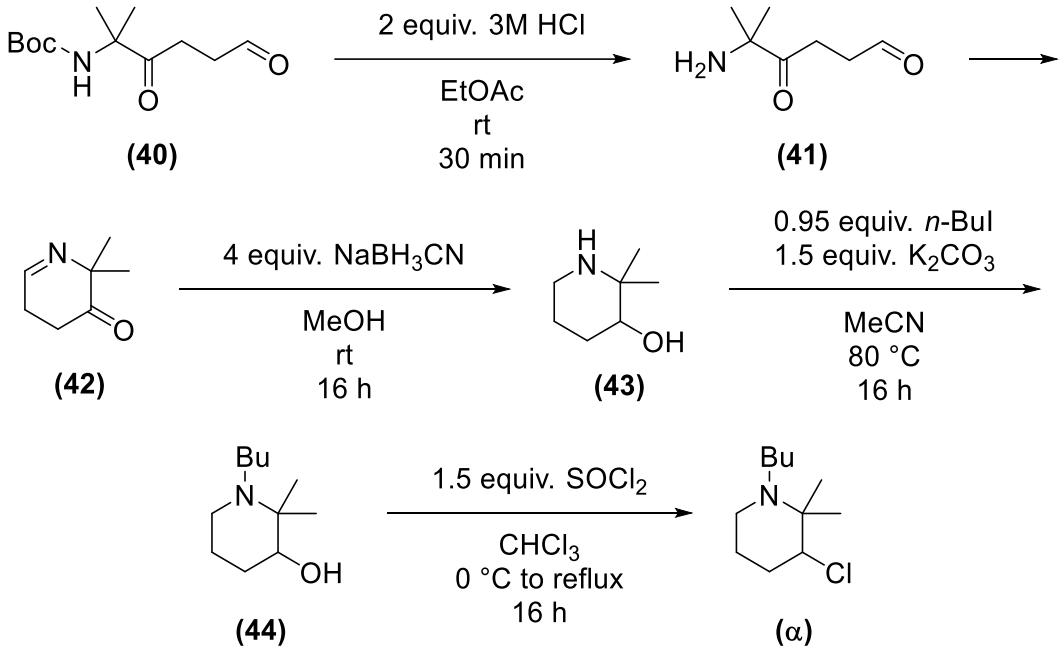

SCHEME 22: ALTERNATIVE SYNTHESIS ROUTE FOR 3-CHLOROPIPERIDIN (α) PRODUCTION.

An alternative route would be to use the methods known so far for cyclisation. This synthesis could start from succinic acid, which is transformed into a single amide utilising 0.95 equiv. *n*-butylamine (**46**). The whole compound would then be reduced with LAH in the following stage (**47**), and the resulting alcohol might then be oxidised to an aldehyde by a Swern-oxidation (**48**, Scheme 23).

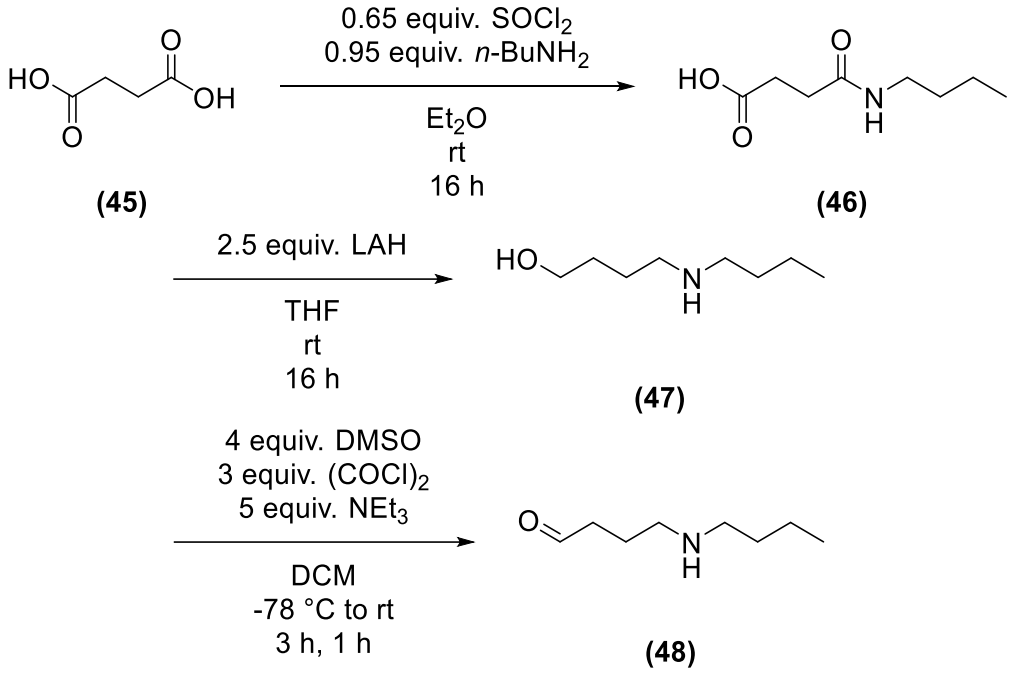

SCHEME 23: CONVERSION OF SUCCINIC ACID TO A SINGLE AMIDE, AFTERWARDS REDUCTION OF THE AMIDE AND SUBSEQUENT OXIDATION OF THE OBTAINED ALCOHOL.

Afterwards, a Wittig reaction can convert the aldehyde into a double bond (**53**, Scheme 24). The necessary phosphorus ylide (**52**) could be created by a reaction of triphenylphosphine and 2-iodopropane and subsequent deprotonation with *n*-BuLi.[72]

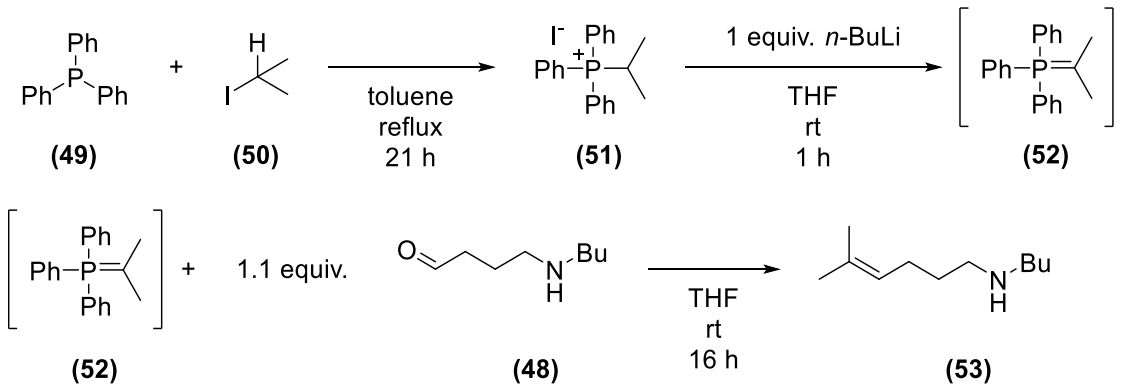

SCHEME 24: PREPARATION OF THE YLIDE AND SUBSEQUENT WITTIG-REACTION TO INTRODUCE THE DOUBLE BOND AND THE TWO METHYL GROUPS.

The resulting compound can be cyclized using established methods to produce the required *N*-butyl-2-dimethyl-3-chloropiperidine (α, Scheme 25).

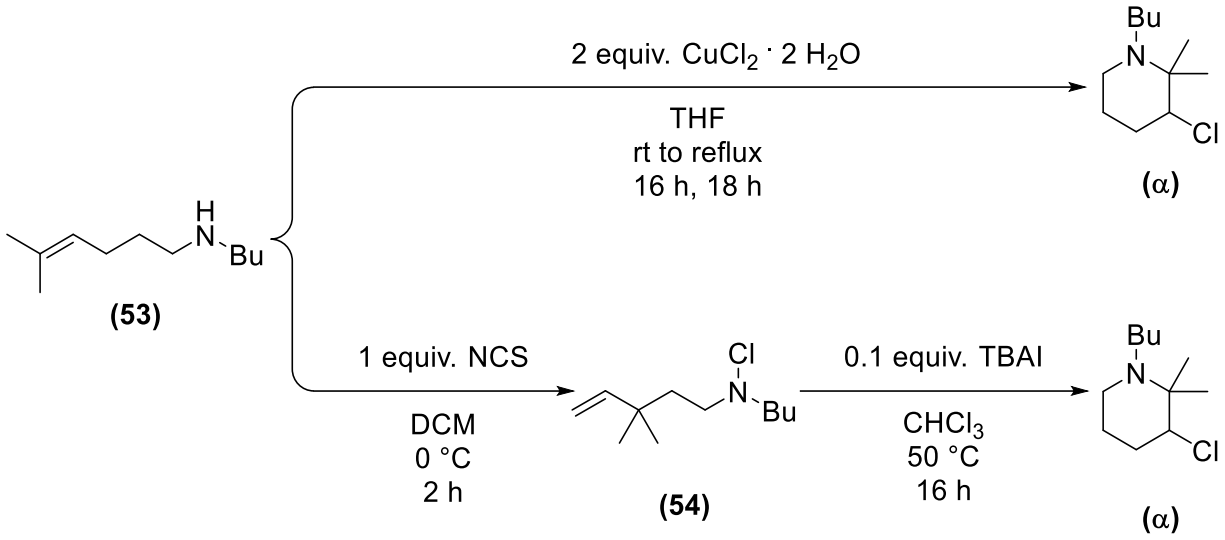

SCHEME 25: CYCLISATION USING THE KNOWN METHODS.

If the production of the ylide or the subsequent Wittig reaction is unachievable, a synthesis utilizing elimination would also be feasible (Scheme 26). Like the previously described synthesis, this might be accomplished with glutaric acid as the starting material. The compound would again be reacted to a single amide (**56**). After that, the remaining carboxylic acid must be converted into a methyl ester (**57**), after which two methyl groups can be introduced to the carboxylic ester using a double Grignard reaction, whereby a tertiary alcohol is obtained (**58**). The acquired alcohol can be converted into a good leaving group (**59**). An E1-reaction could occur at elevated temperatures by adding a non-nucleophilic base, such as triethylamine or pyridine. The desired double bond can be achieved (**60**). After a reduction with LAH, cyclisation can be carried out again using the known methods.

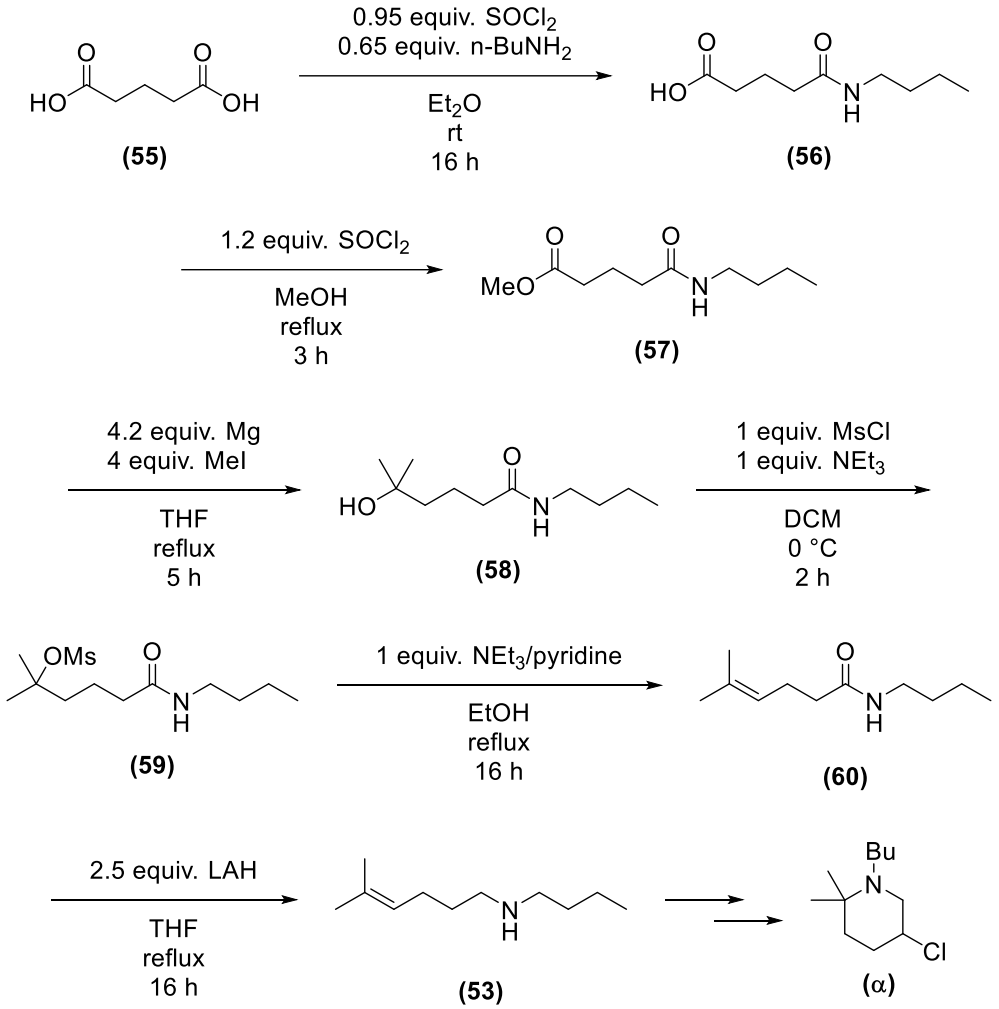

SCHEME 26: PREPARATION OF 3-CHLOROPIPERIDINE α BY ELIMINATION.

3.2.2 Synthesis of *N*-butyl-3-chloro-4,4-dimethylpiperidine

For synthesising the following *N*-butyl-3-chloropiperidine derivative, 3,3-dimethylpent-4-enoic acid methyl ester was used as the starting material (Scheme 27). In the first step, compound **61** was saponified and then reacted with *n*-butylamine to obtain the amide **63**.

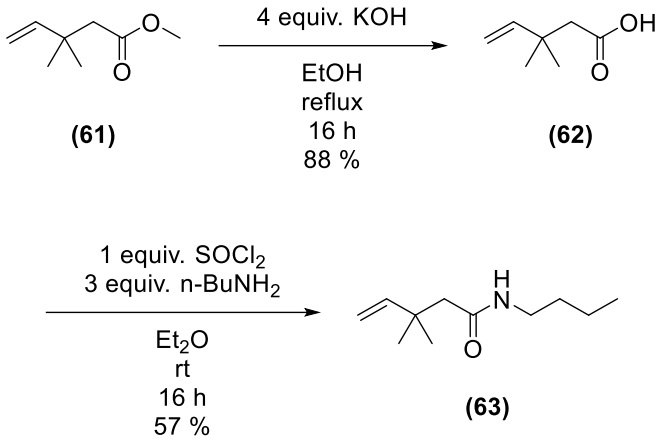

SCHEME 27: FORAMTION OF THE AMIDE (**64**).

The obtained amide was then reduced with LAH to get the corresponding amine (**64**, Scheme 28). For the cyclization of the amine $CuCl_2 \cdot 2\ H_2O$ or NCS/TBAI were used. The *N*-butyl-4-dimethyl-3-chloropiperidine (β) was obtained with NCS/TBAI in a yield of 42 % over two steps and 21 % utilizing $CuCl_2 \cdot 2\ H_2O$.

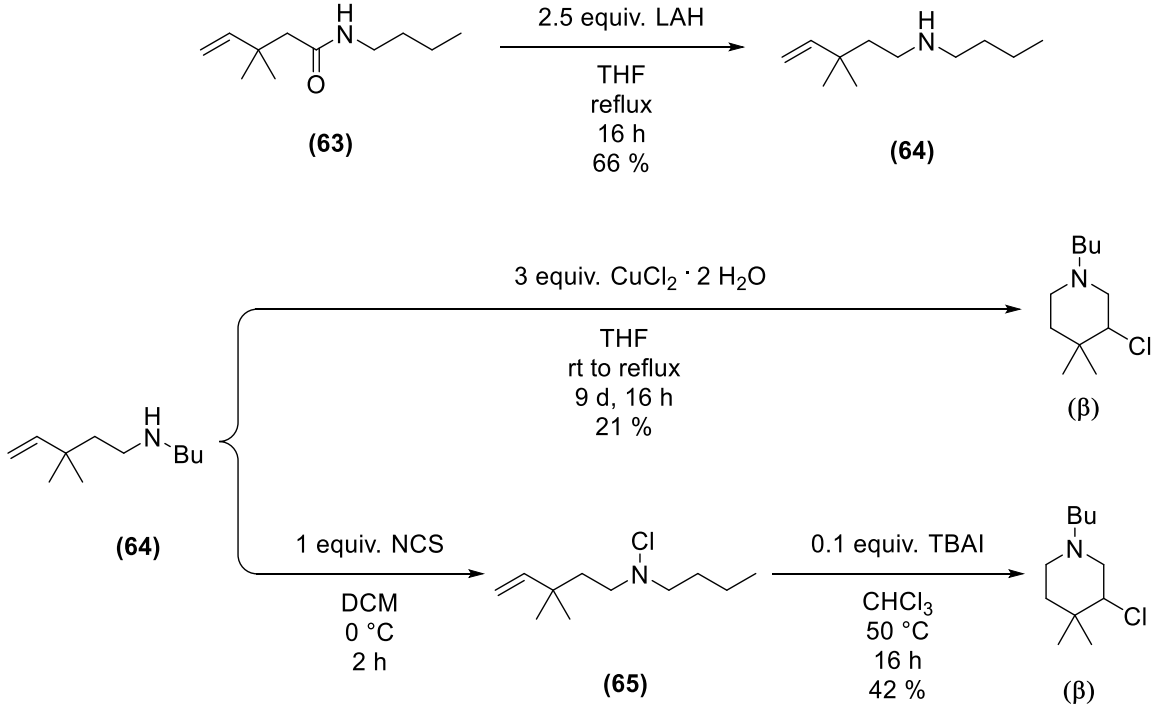

SCHEME 28: REDUCTION OF THE AMIDE AND CYCLISATION OF THE 3-CHLOROPIPERIDINE β.

The obtained compounds were converted to a hydrochloride salt using 2 M HCl in Et_2O. Subsequently, a crystal structure (Figure 18) of compound (β) could be obtained through the method described in chapter 5.1.6.

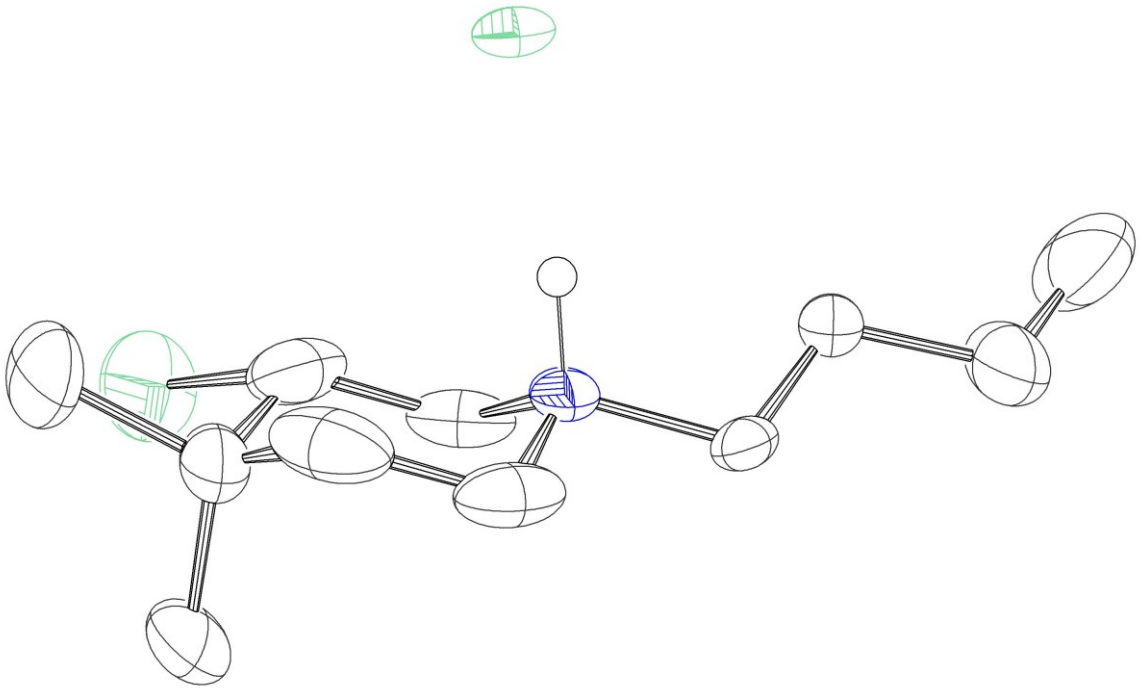

FIGURE 18: CRYSTAL STRUCTURE OF COMPOUND β.

The angle *θ* and the distance d can be measured at this structure, and a determination of how closely these values match the computational computations can be made. The comparison of the two data is listed in Table 4. The calculated and crystallographic values correspond in a reasonable vicinity.

TABLE 4: COMPARISON OF THE CALCULATED AND MEASURED QUANTITIES *θ* AND d USING THE EXAMPLE OF COMPOUND β.

	Computational calculation	**Crystal structure**
Angle *θ* / °	109.0	109.4
Distance d / Å	2.416	2.423

Values known from the literature for the angle *θ* and the distance d for different derivatives are listed in Table 5. It is noticeable that d and *θ* are significantly reduced by a dimethyl substitution at position four. As a result, these parameters are more like the derivative with a cyclopropyl substitution at the position. Compared to the latter, even lower values are obtained.

TABLE 5: ANGLES OF VARIOUS COMPOUNDS FROM THE LITERATURE OBTAINED THROUGH CRYSTAL STRUCTURE ANALYSIS.

Compound	Angle *θ* / °	Distance d / Å
BuHH	108.8	2.449
Bu-5-MeMe	111.4	2.559
Bu-5-Cyclopropyl	110.0	2.474

3.2.3 Synthesis of *N*-butyl-3-chloro-6,6-dimethylpiperidine

Acetylacetone and allyl chloride underwent a malonic ester-type reaction at the start of the synthesis, with a yield of 57 % (Scheme 29, top). The reaction was heated stepwise so that the volatile allyl chloride was not driven out of the reaction solution. In the next step, a ketimine formation was carried out with *p*-TsOH as a catalyst (Scheme 29, bottom). Through this reaction, *N*-functionalisation was introduced.

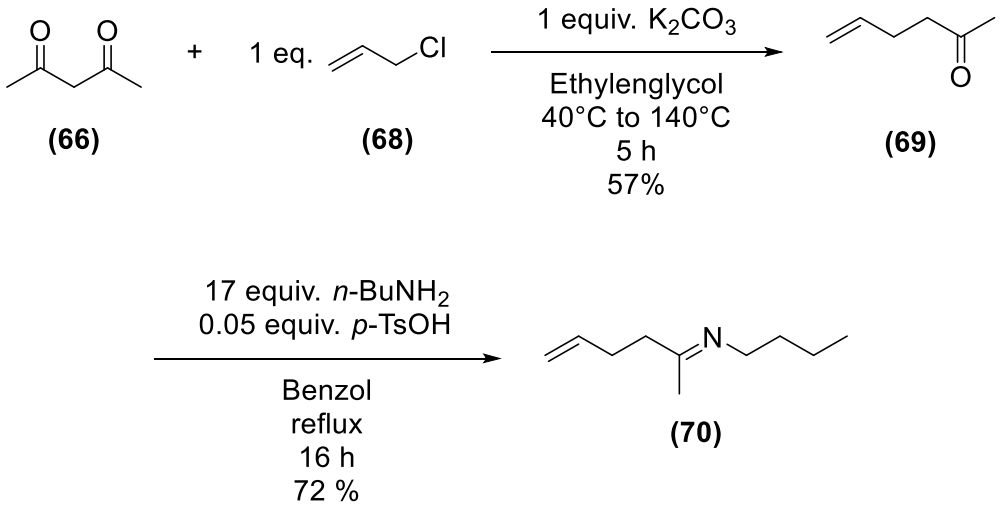

SCHEME 29: SYNTHESIS OF THE UNSATURATED KETONE (**69**) AND SUBSEQUENT FORMATION OF A KETIMINE (**70**).

After the ketimine preparation, an attempt was made to build a quaternary centre by introducing a second methyl group. The process was initially planned as comparable to carbonyl compounds. For this purpose, a Grignard reaction was performed (Scheme 30). In this case, however, no reaction occurred, so only the reactant was regenerated. In the following approach, the more nucleophilic reagent methyllithium was used. However, there was no reaction, and just the reactant was regenerated too. As another approach, the last reaction

was repeated with the Lewis base $AlCl_3$ as an additive to activate the ketimine.[73] Here, too, no reaction took place.

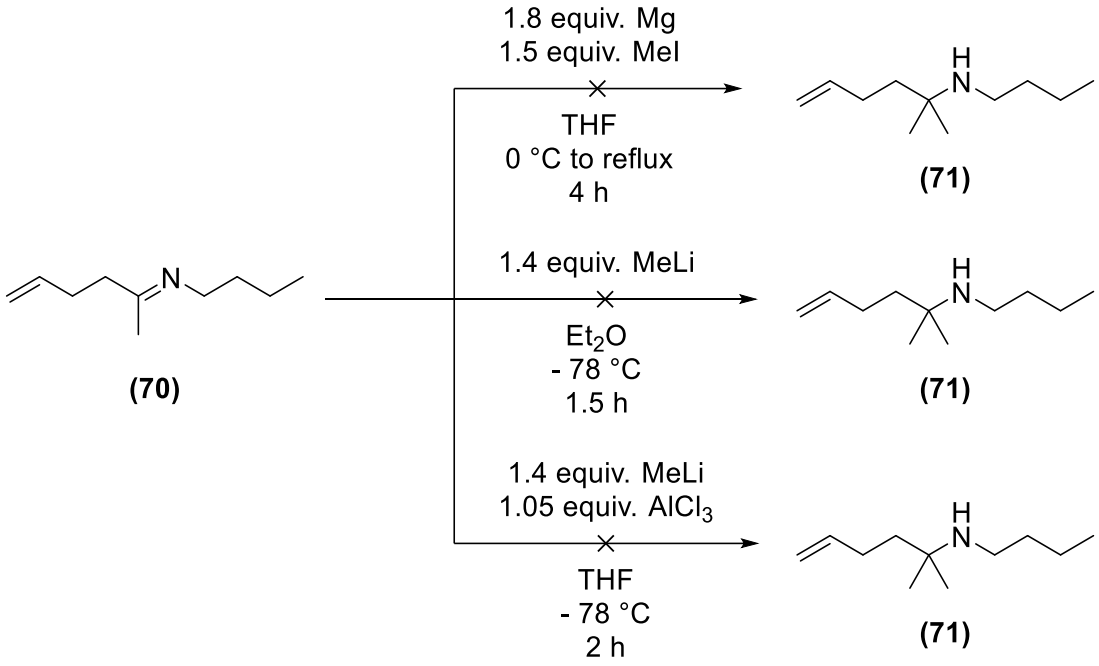

SCHEME 30: UNSUCCESSFUL SYNTHESES OF A QUATERNARY CENTRE.

Lastly, methyllithium and the potent Lewis base $BF_3 \cdot OEt_2$ were employed in the reaction (Scheme 31). Under these circumstances, a conversion was achieved; however, the yield was just 21 %.

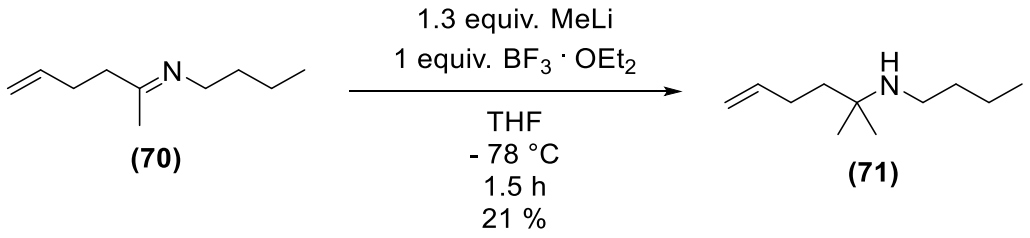

SCHEME 31: SUCCESSFUL SYNTHESES OF A QUATERNARY CENTRE AT THE KETIMINE.

As an alternative synthesis route, an attempt was made to produce amine **71** via nitroalkene **73** (Scheme 32). For this purpose, the bromoalkene was first reacted with $NaNO_2$ and urea, whereby nitroalkene **73** was obtained.

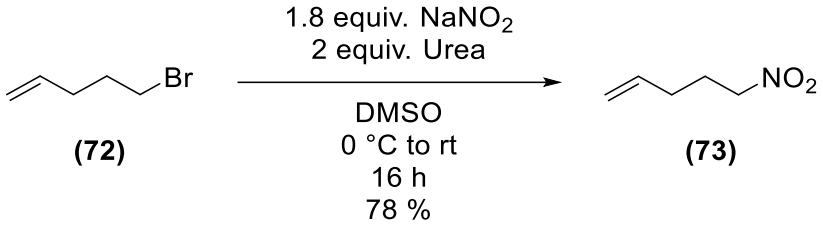

SCHEME 32: SYNTHESIS OF 5-NITRO-1-PENTENE FROM 5-BROMO-1-PENTENE

The nitroalkene was next attempted to be deprotonated in the α position using LDA, and the methyl groups were added using methyl iodide (Scheme 33). However, this did not lead to a mono- or dimethylated species.

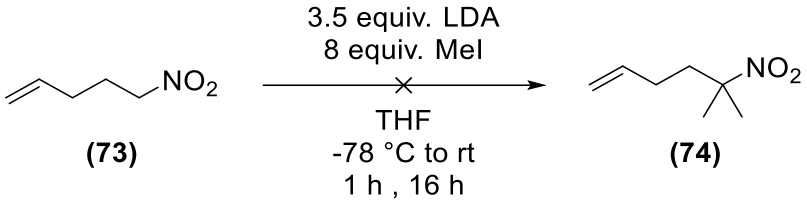

SCHEME 33: UNSUCCESSFUL SYNTHESIS OF 4-DIMETHYL-5-NITRO-1-PENTENE

The reaction might be carried out as an alternative using the corresponding alkene's carboxylic acid ester derivative (**75**) followed by saponification (Scheme 34). The resulting carboxylic acid (**76**) could be transformed into the corresponding amine (**78**) using a Schmidt reaction. Afterwards, amine **71** could be obtained through reductive amination.

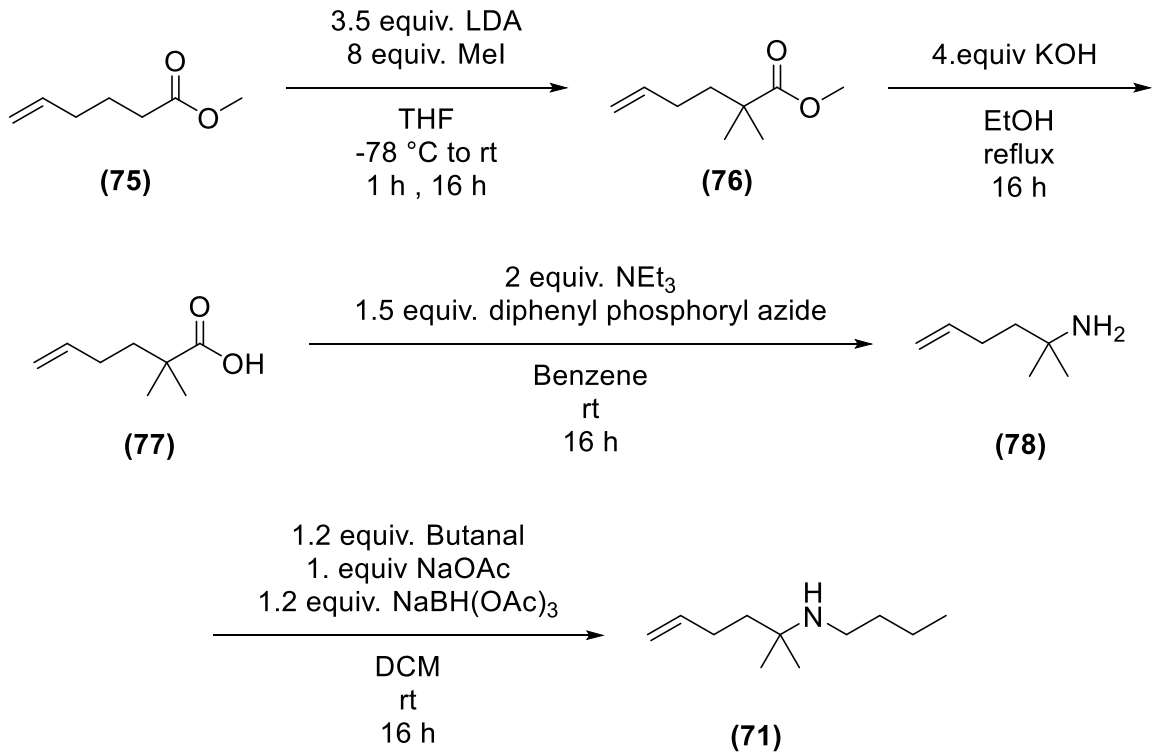

SCHEME 34: ALTERNATIVE SYNTHESIS ROUTE FOR AMINE **71** STARTING FROM A CARBOXYLIC ESTER.

Another possibility would be to use the previously prepared ketone (**69**) and introduce another methyl group using a Grignard reaction (Scheme 35). The resulting tertiary alcohol (**79**) might then be turned into an azide (**80**), and a Staudinger reduction can be used to get the necessary amine (**78**). The desired amine (**72**) can be obtained utilizing a reductive amination.

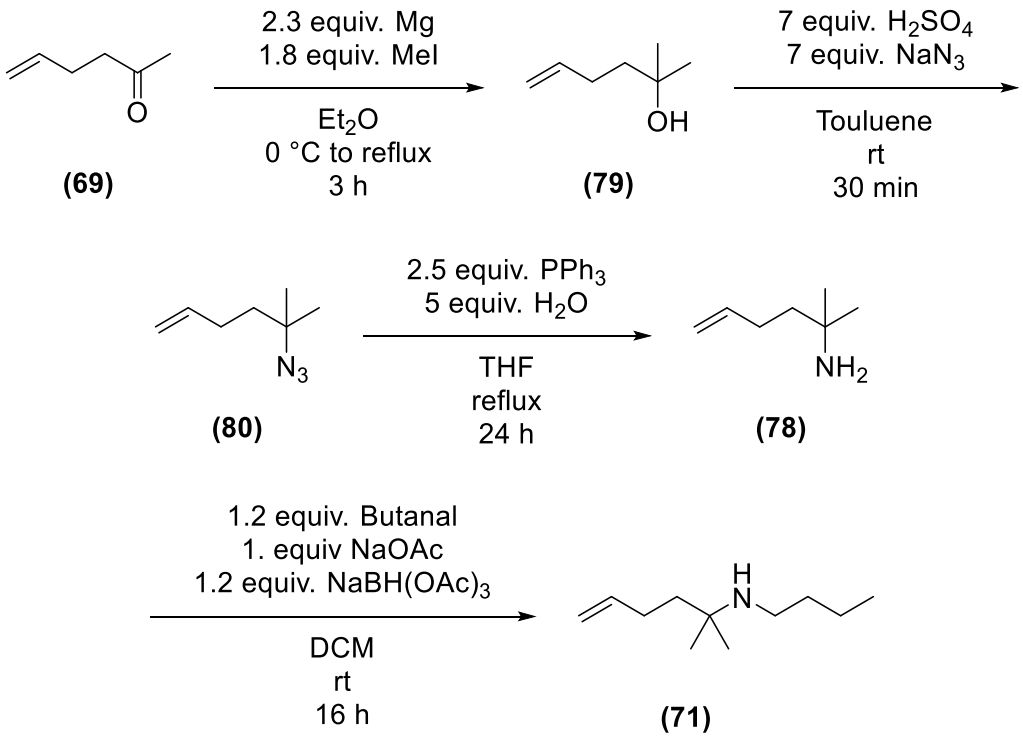

SCHEME 35: ALTERNATIVE SYNTHESIS FOR AMINE **71** VIA STAUDINGER-REDUCTION.

The produced amine (**71,** Scheme 31) was cyclised using $CuCl_2 \cdot 2\ H_2O$ and NCS/TBAI. The cyclisation with NCS/TBAI yielded the *N*-butyl-3-chloro-6-dimethylpiperidine (γ) in 9 % over two steps, whereas cyclisation using $CuCl_2 \cdot 2\ H_2O$ gave a yield of 56 %.

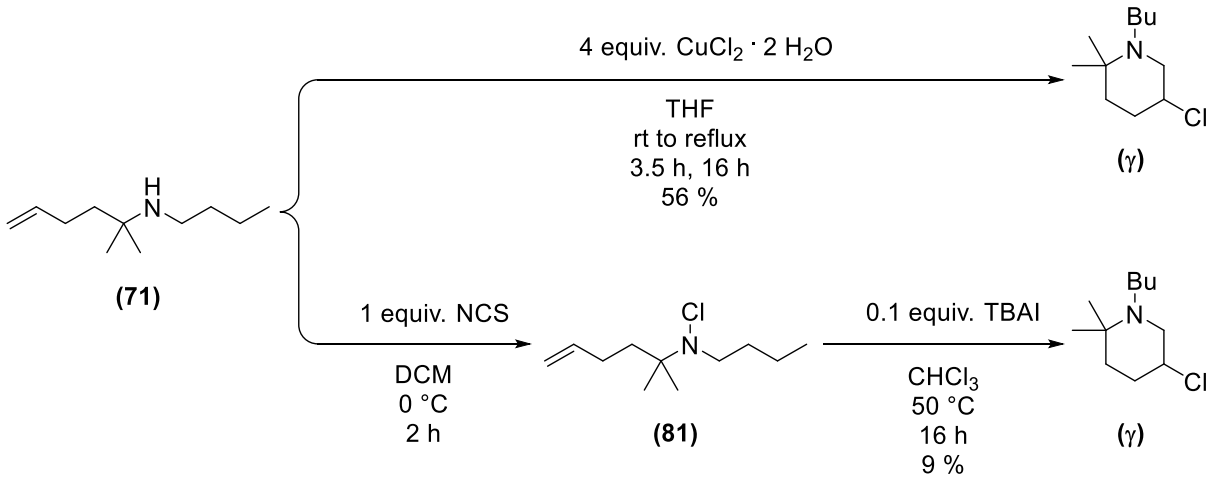

SCHEME 36: CYCLIZATION OF **72** TO OBTAIN THE 3-CHLOROPIPERIDINE γ.

Since the *N*-butyl-3-chloro-6-methyl piperidine (**82**) was easy to obtain through a reduction of the previously prepared ketimine (**70**). A reaction with $NaBH_4$ was done as a stepwise reductive amination, whereby the corresponding amine was obtained (Scheme 37).

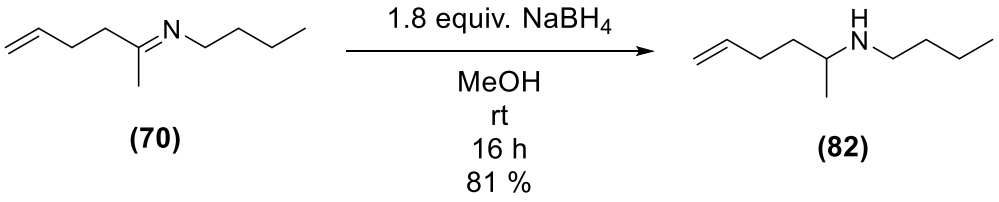

SCHEME 37: REDUCTION OF THE KETIMINE (**70**).

The amine was converted to *N*-butyl-3-chloro-6-methyl piperidine (δ) in the last step through the previously mentioned cyclisation options. The cyclisation with $CuCl_2 \cdot 2\ H_2O$ only gave a yield of 5 %. Cyclisation using NCS/TBAI, on the other hand, worked with 31 % over two steps (Scheme 38).

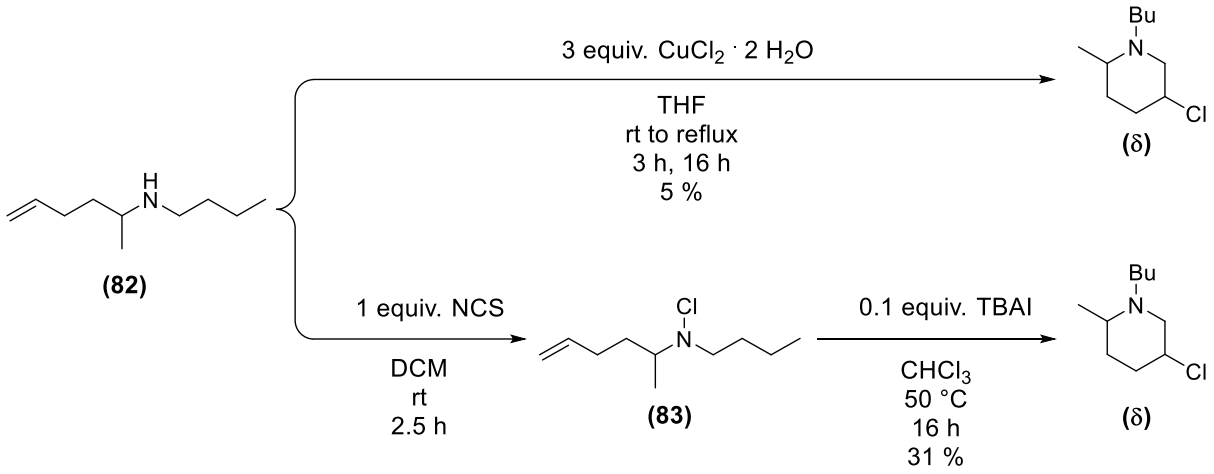

SCHEME 38: PREPARATION OF THE MONO-SUBSTITUTED 3-CHLOROPIPERIDINE (δ).

To check whether several stereoisomers were formed during the reaction, a chiral GC was carried out with the chiral column Hydrodex *β*-PM (Figure 19). Thereby the formation of two stereoisomers was confirmed. However, flash chromatographic purification could not separate both stereoisomers from one another.

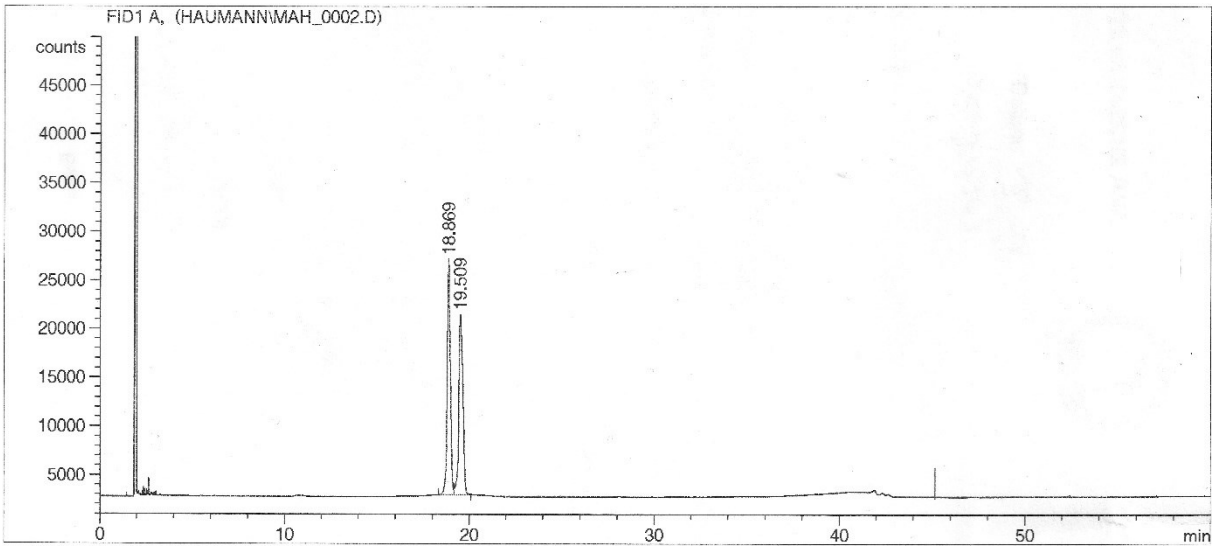

FIGURE 19: CHIRAL GC OF THE MONO-METHYLATED 3-CHLOROPIPERIDINE (δ).

Since the methyl group has a more considerable A-value of 1.7, it will likely be positioned equatorial in the Stereoisomer that forms because the equatorial position is energetically favoured.[68] Therefore, a mixture of the two products is obtained, whereby the chloride is positioned once axially and once equatorially. Consequently, two diastereomers are formed. Based on the integrals obtained (Table 6), it can be concluded that the two diastereomers are energetically very similar. This consideration is supported by computational calculations in which the energy difference does not exceed the mean absolute derivation of the calculation method (see electronic appendix).

TABLE 6: RETENTION TIME AND INTEGRALS OF THE PERFORMED CHIRAL GC.

Peak #	**t_R**	**Area / %**
1	18.869	49.94
2	19.509	50.06

3.2.4 Synthesis of 1-Butyl-3-chloro-4,4-diphenylpiperidine

Since the computational calculations suggested that a substitution at position four of the piperidine scaffold has the most significant slowing effect on the reactivity, an attempt was made to prepare a derivative with a phenyl functionalisation at this position (Scheme 39). The starting material of the synthesis was benzophenone, which was then reacted with KOH in acetonitrile.

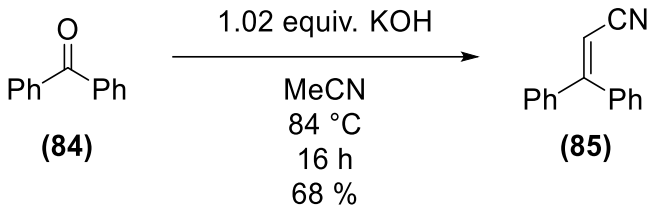

SCHEME 39: CONVERSION OF BENZOPHENONE INTO AN UNSATURATED NITRILE COMPOUND.

Subsequently, an attempt was made to add a vinyl group to the double bond (Scheme 40). Therefore, a Grignard reaction with vinyl magnesium bromide was used. However, the product was not obtained. In the following approach, the reaction was conducted again with the addition of LiCl to activate the Grignard compound.[74] However, detecting the desired product by ESI-MS was once more impossible.

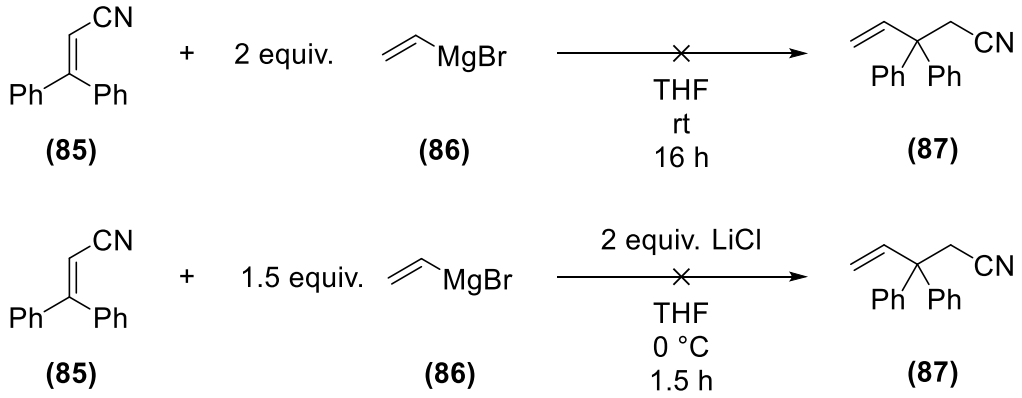

SCHEME 40: UNSUCCESSFUL ADDITION OF THE VINYL GRIGNARD.

Since the desired attack position, according to the HSAB concept[75] is a relatively soft centre, a cuprate was used as a nucleophilic reagent in the following approach (Scheme 41). The Grignard compound and CuI were dissolved in THF, and the conjugated nitrile was added at 0 °C. However, in this instance, the desired outcome was not achievable.

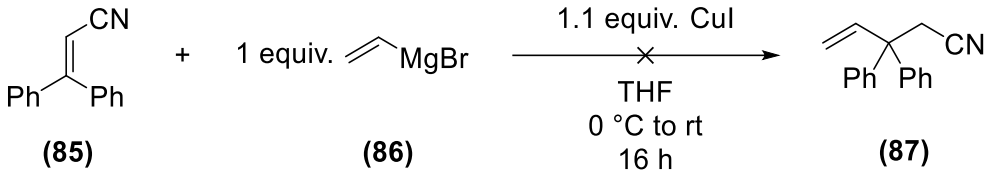

SCHEME 41: UNSUCCESSFUL ADDITION OF THE CUPRATE AT ROOM TEMPERATURE.

Considering that at 0 °C a cuprate might not be stable, another run was repeated at -78 °C (Scheme 42). This time only catalytic amounts of copper salt were used. It can be assumed that this time a cuprate species was formed in this reaction as a colour change occurred. Nevertheless, even under these reaction conditions, no product could be detected via ESI-MS.

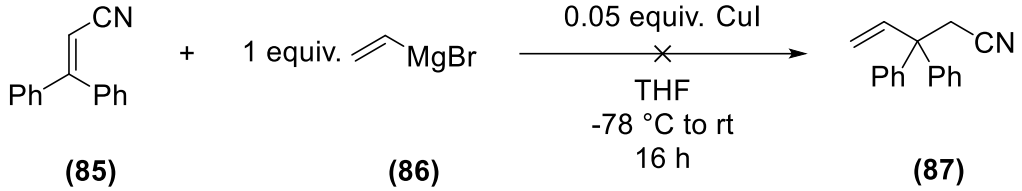

SCHEME 42: UNSUCCESSFUL ADDITION OF THE CUPRATE AT -78 °C.

Since the counterion can strongly influence the outcome of the reaction with cuprates, the reaction was carried out again with CuCN at both temperatures (Scheme 43). Again, a colour change was only observed when the experiment was conducted at -78 °C and not at 0 °C. However, in neither of the two experiments, the intended product was detectable by ESI-MS.

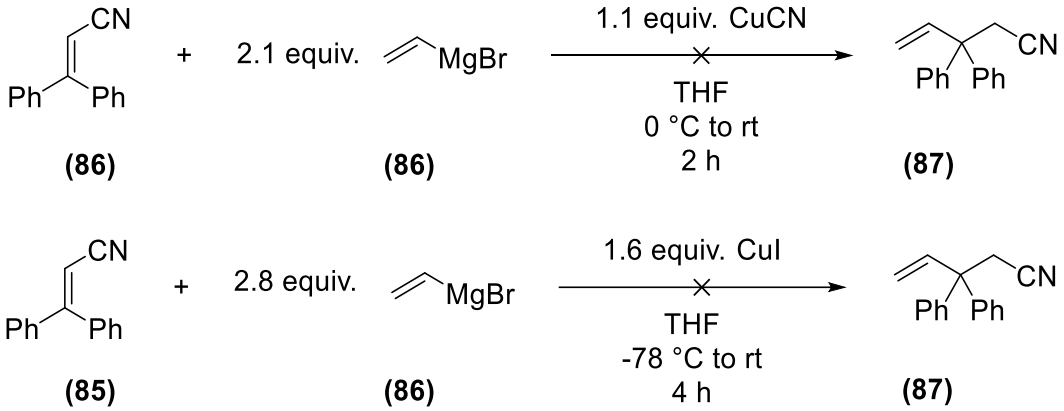

SCHEME 43: REPETITION OF THE EXPERIMENTS FROM SCHEME 41 + SCHEME 42 WITH CUCN AS A COPPER SOURCE.

Since no reaction was observed in any of the experiments, it was assumed that a nitrile group is not electron-withdrawing enough for a reaction to occur. Therefore, a Knoevenagel reaction was used to link benzophenone to malonic acid dimethyl ester to have a more significant electron-withdrawing effect (Scheme 44). $TiCl_4$ was used as a Lewis acid to activate the benzophenone in the reaction.

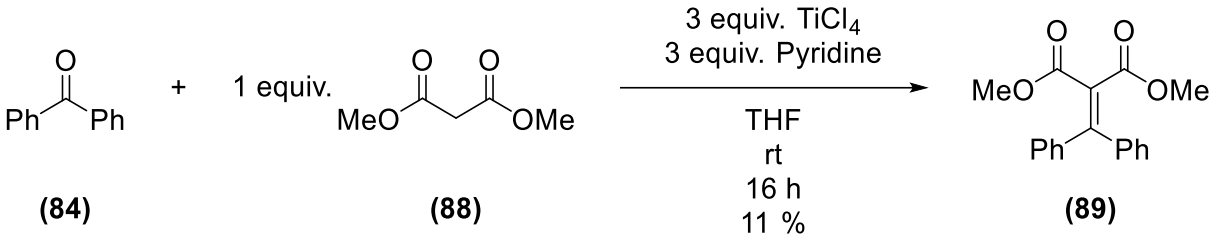

(84) **(88)** **(89)**

SCHEME 44: KNOEVENAGEL-REACTION BETWEEN BENZOPHENONE AND MALONIC ACID DIMETHYL ESTER.

Since the compound now has a group with a more vigorous electron-withdrawing nature, adding vinyl magnesium bromide was attempted again using a cuprate (Scheme 45). The reaction was carried out at -78 °C and with CuI.

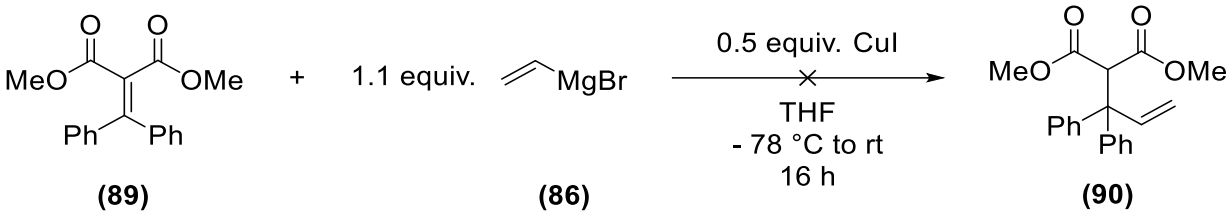

(89) **(86)** **(90)**

SCHEME 45: UNSUCCESSFUL ADDITION OF A VINYL GROUP USING A CUPRATE.

However, no reaction could be accomplished even with this more substantial electron-withdrawing group. Therefore, another assumption was made that the position at which a nucleophilic attack should take place using the cuprate seems to be sterically overloaded. Thus, an attempt was made to reduce steric demand as a new approach (Scheme 46). For this purpose, a new synthesis route was done where the vinyl group was first added to benzaldehyde.

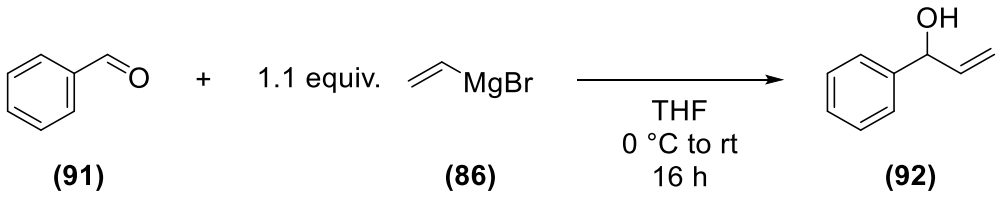

(91) **(86)** **(92)**

SCHEME 46: ADDITION OF A VINYL GROUP TO BENZALDEHYDE.

Subsequently, an attempt was made to oxidise the alcohol to the corresponding ketone (Scheme 47). The reaction was first carried out with DMP as a mild oxidising agent. However, it was impossible to acquire the product. Instead, only benzaldehyde and cinnamaldehyde could be obtained. In a new approach, the reaction was carried out again, but this time with PCC under anhydrous conditions as an oxidation reagent. Once more, just benzaldehyde and cinnamaldehyde were obtained.

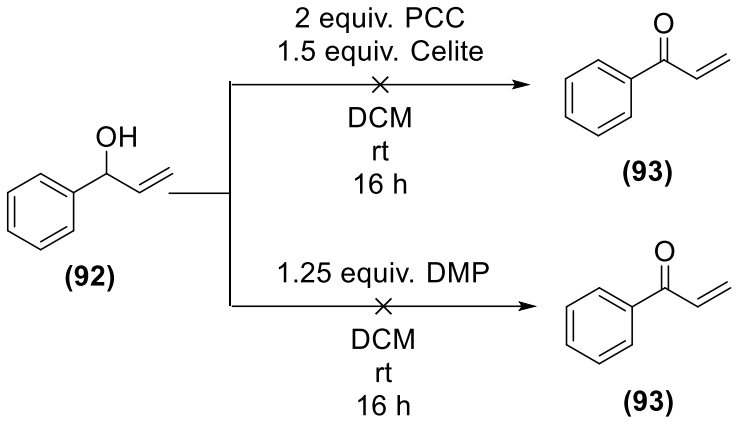

SCHEME 47: UNSUCCESSFUL OXIDATION USING DMP UND PCC.

The reaction was unsuccessful because, with these reagents, a Babler-Dauben reaction occurred.[76] In order to circumvent this problem, oxidation using manganese dioxide was attempted (Scheme 48). However, this was also not successful.

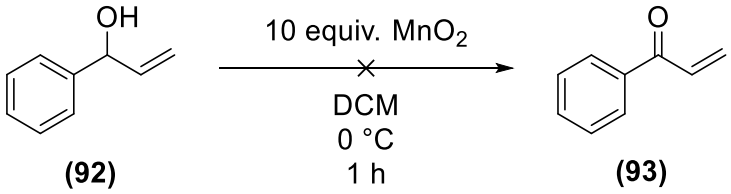

SCHEME 48: UNSUCCESSFUL OXIDATION USING MnO_2.

A novel synthesis was attempted to overcome the oxidation issue, beginning with benzonitrile, as this should result in the required ketone (Scheme 49). However, the intended product could not be detected. As an alternative, a modified Gilman-Cason reaction was used with CuI in place of $CdCl_2$, where the product could be obtained.[77]

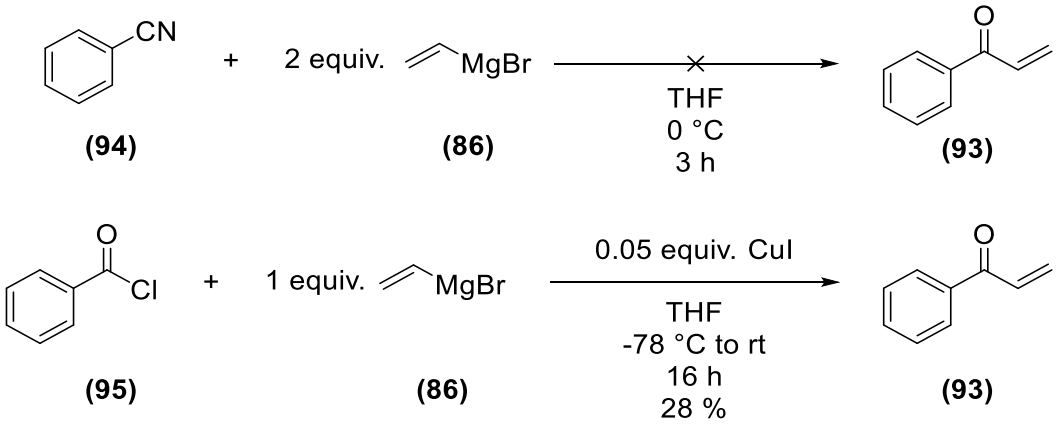

SCHEME 49: UNSUCCESSFUL ADDITION OF THE VINYL GRIGNARD TO BENZONITRILE (TOP).
SUCCESSFUL GILMAN-CASON-KETONE-SYNTHESIS (BOTTOM).

If this synthesis is pursued further in the future, the subsequent step might involve a Knoevenagel condensation using the generated ketone (Scheme 50). Afterwards, a phenyl cuprate addition might be undertaken since the double bond's electron density and steric bulk has decreased.

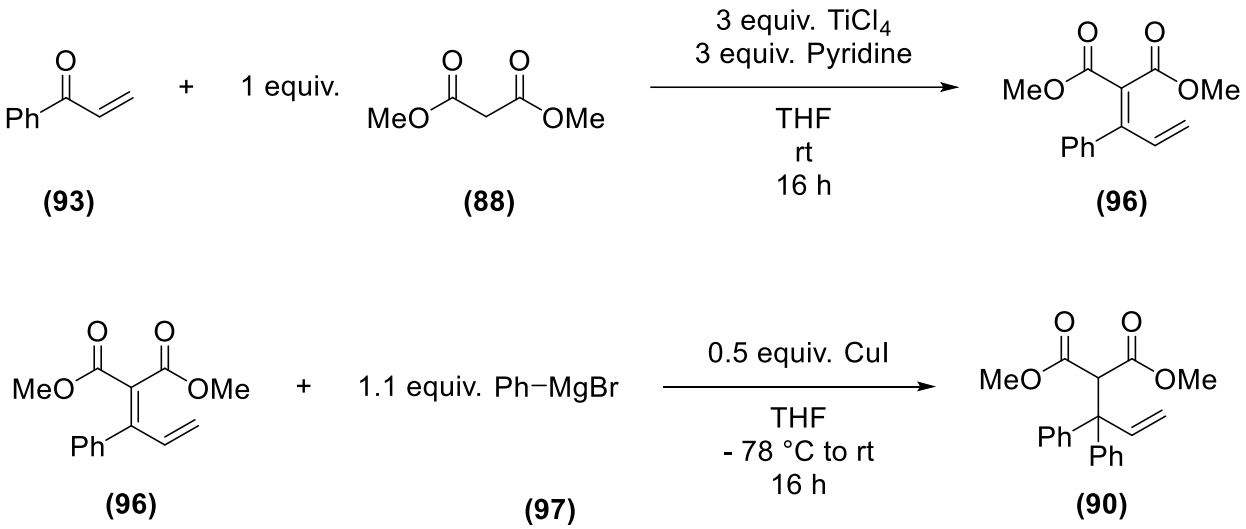

SCHEME 50: KNOEVENAGEL REACTION BETWEEN **93** AND MALONIC ACID DIMETHYL ESTER AND SUBSEQUENT INTRODUCTION OF THE SECOND PHENYL GROUP USING A CUPRATE.

After that, the cyclisation precursor might be created by saponification of the ester groups, a single decarboxylation, subsequent amination of the residual carboxylic acid, and reduction of the resulting amide (Scheme 51). The cyclisation of the obtained precursor can be carried out via both cyclisation methods so that the *N*-butyl-4-diphenyl-3-chloropiperidine (ε) can be obtained.

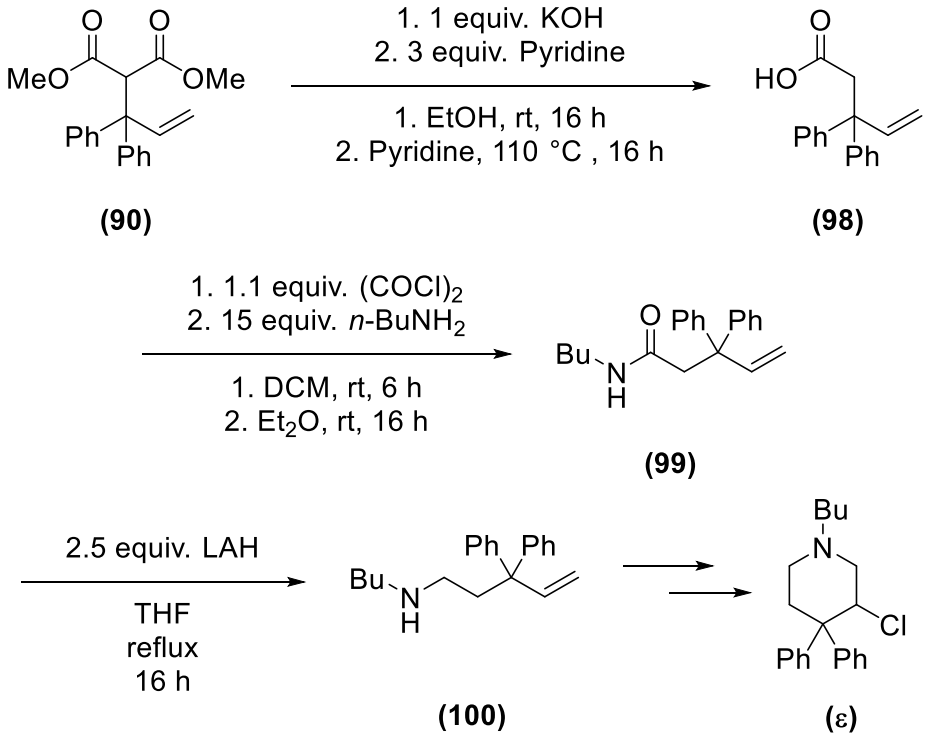

SCHEME 51: DECARBOXYLATION OF **90**, SUBSEQUENT AMINATION, REDUCTION AND LASTLY, CYCLIZATION WITH BOTH PREVIOUSLY USED METHODS.

3.2.5 Synthesis of *N*-butyl-3-chloro-6,6-diphenylpiperidine

The computational calculations have shown that a diphenyl substitution at position six does not significantly change the activation energy. An attempt was conducted to synthesise this derivative and test it using kinetic measurements to verify this prediction. First, the ketimine (**101**) was prepared from benzophenone and *n*-butylamine (Scheme 52, top). With the ketimine produced, the next step was introducing a 1-butene chain utilizing a Grignard reaction analogous to carbonyl compounds (Scheme 52, bottom). However, this did not work.

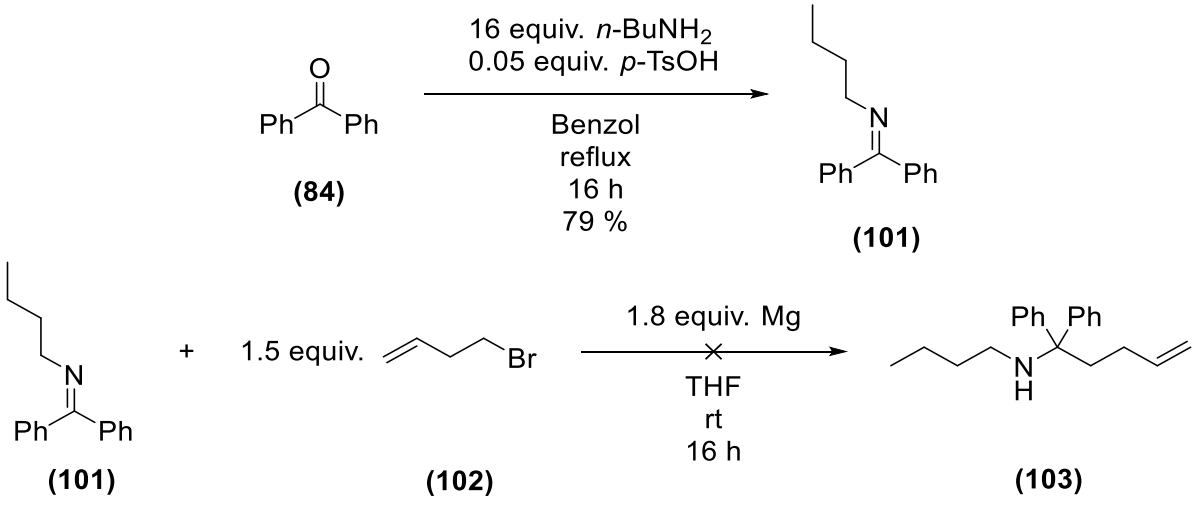

SCHEME 52: SYNTHESIS OF THE KETIMINE FROM BENZOPHENONE AND *N*-BUTYLAMINE AND SUBSEQUENT UNSUCCESSFUL GRIGNARD REACTION AT THE KETIMINE.

Thus, a similar strategy to Scheme 31 was used in the following stage. A halogen-metal exchange was performed on 4-bromo-1-butenes, using *n*-BuLi, at -78 °C (Scheme 53). In addition, the ketimine was activated using $BF_3 \cdot OEt_2$ as a Lewis acid. After the halogen-metal exchange, the lithium species was dropped into the ketimine solution. Nevertheless, once more, no product could be acquired. This approach could be repeated with *sec*- or *tert*-BuLi, as the pk_B values of 1-bromobutene and *n*-BuLi are similar.

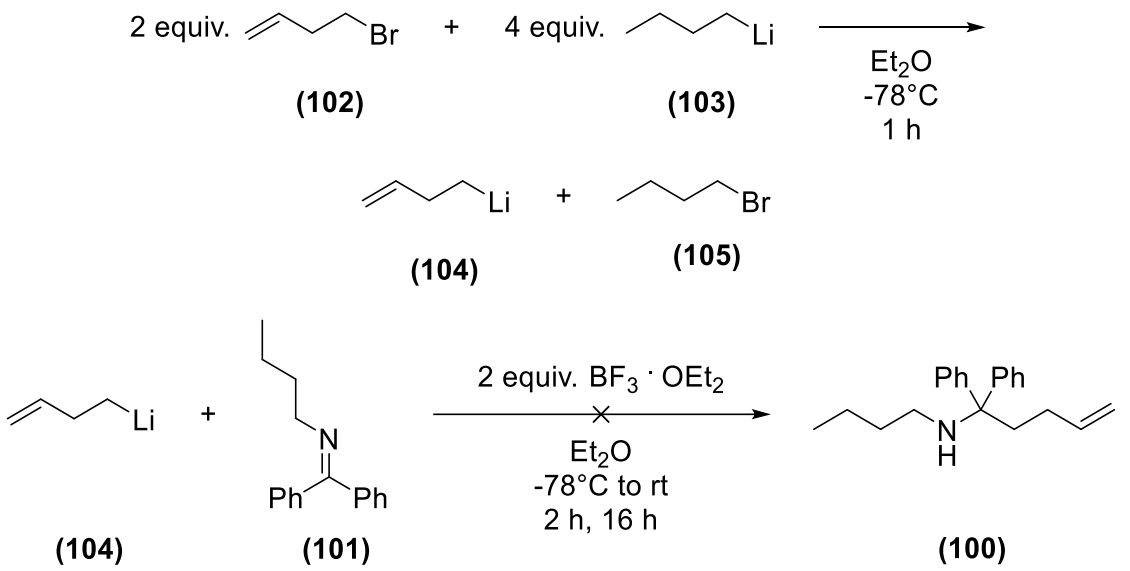

SCHEME 53: LITHIUM-HALOGEN EXCHANGE AND SUBSEQUENT UNSUCCESSFUL ADDITION OF A LITHIUMORGANYL TO THE KETIMINE.

Considering that the ketimine might be too unreactive, another approach was investigated (Scheme 54). The molecule was to be built up starting from the 1-butene chain. For this, 4-pentenoic acid was used as the starting material and was converted to an acid chloride for activation. The activated compound was then added to a phenyl magnesium bromide solution to perform a double Grignard addition. In the process, the product could be obtained.

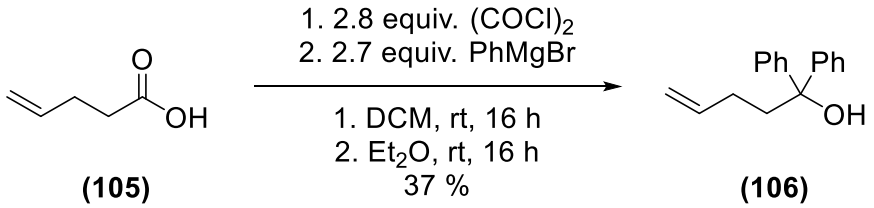

SCHEME 54: DOUBLE ADDITION OF A PHENYL GRIGNARD TO ACTIVATED 1-BUTENOIC ACID.

If the synthesis is pursued in the future, the produced alcohol could be converted into a good leaving group, allowing for the introduction of the butyl chain utilizing an S_N1-reaction (Scheme 55). Lastly, a cyclization might be performed using the previously used techniques to obtain the product *N*-butyl-3-chloro-6-diphenylpiperidine (ϕ).

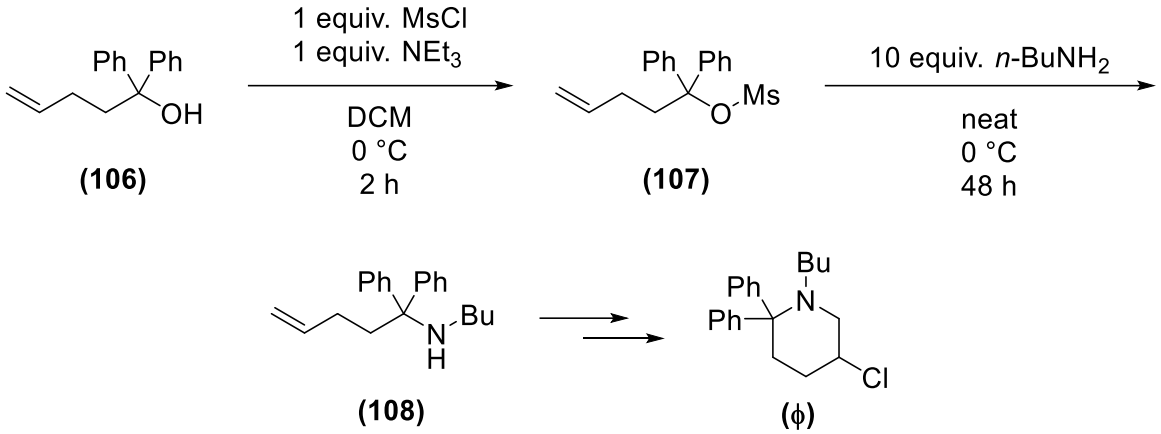

SCHEME 55: CONVERSION OF THE ALCOHOL INTO A GOOD LEAVING GROUP, SUBSEQUENT S_N1-REACTION WITH *N*-BUTYLAMINE AND CYCLISATION OF *N*-BUTYL-3-CHLORO-6,6-DIPHENYLPIPERIDINE (**ϕ**).

3.3 Kinetic study of 3-chloropiperidines

The synthesised 3-chloropiperidine derivatives were heated in methanol-d4 at 50 °C with dibenzyl ether acting as an internal NMR standard to test their reactivity. The reaction speed can be evaluated by contrasting the integral of the same NMR peak across time and subsequent plotting of the obtained integrals against the time. The slope of this plot corresponds to the rate constant. The disubstituted derivatives were first measured (Figure 20). Since this product was unavailable, no analysis of *N*-butyl-3-chloro-2,2-dimethylpiperidine could be done. GC-MS analysis was done for all compounds after completing the kinetic investigation to verify that methanolysis had taken place. The obtained spectra can be viewed electronically in the appendix.

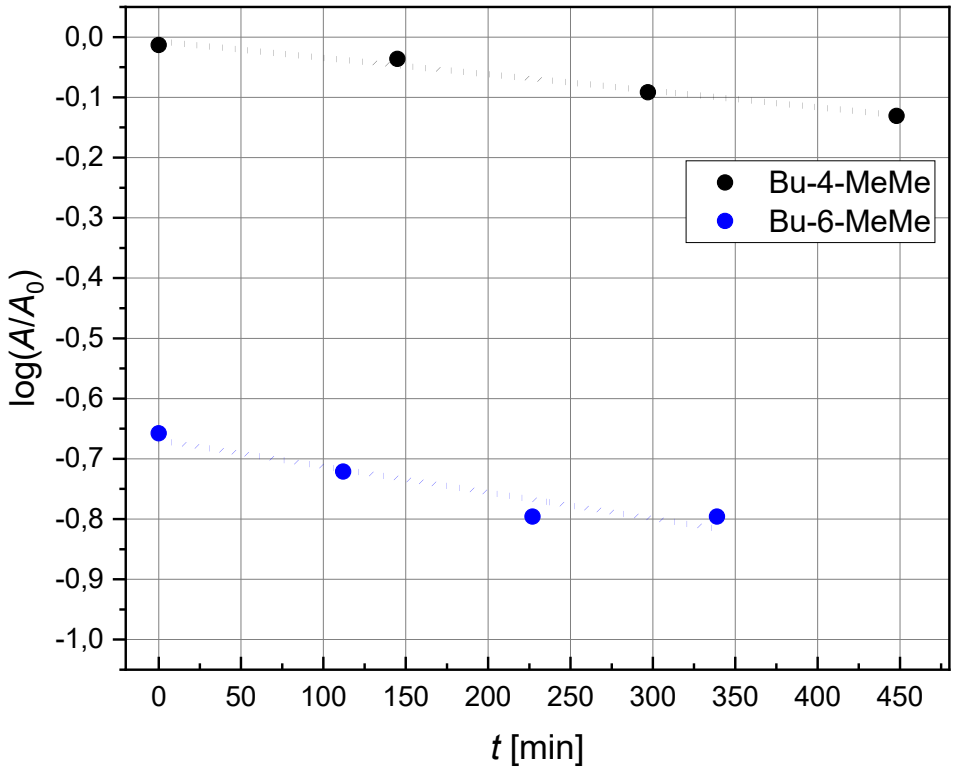

FIGURE 20: KINETIC STUDY OF THE METHANOLYSIS OF *N*-BUTYL-3-CHLOROPIPERIDINE DERIVATIVES WITH DIMETHYL SUBSTITUENTS AT POSITIONS FOUR AND SIX.

The graphical representation shows that the rate constants of the two dimethyl-substituted derivatives are similar. However, when looking closely at the data (Table 7), the derivative with substitution at position four has a lower rate constant than the one with substitution at position six. The reactivities found through computer simulations are comparable with this outcome. Table 7 compares the obtained rate constants to the one of *N*-butyl-3-chloro-5-dimethylpiperidine (Bu-5-MeMe) investigated in previous studies.[8] The data reveals that the derivatives with dimethyl substituents at positions four and six have rate constants that are five to ten times lower.

TABLE 7: COMPARISON OF THE OBTAINED REACTION CONSTANTS WITH THE REACTION CONSTANT OF 5-DIMETHYLPIPERIDINE KNOWN FROM THE LITERATURE.

Compound	**Rate constant / 10^{-3} min^{-1}**
Bu-4-MeMe	0.273 ± 0.04
Bu-5-MeMe	2.97 ± 0.01[8]
Bu-6-MeMe	0.433 ± 0.1

In addition, the substrates with monomethyl substituents at different positions were examined (Figure 21). All derivatives have a similar rate constant except for the derivative with the substitution at position four (Table 8). The rate constant in this instance is only one-third as high as in the others and is comparable to that of the dimethylated substrate in this position.

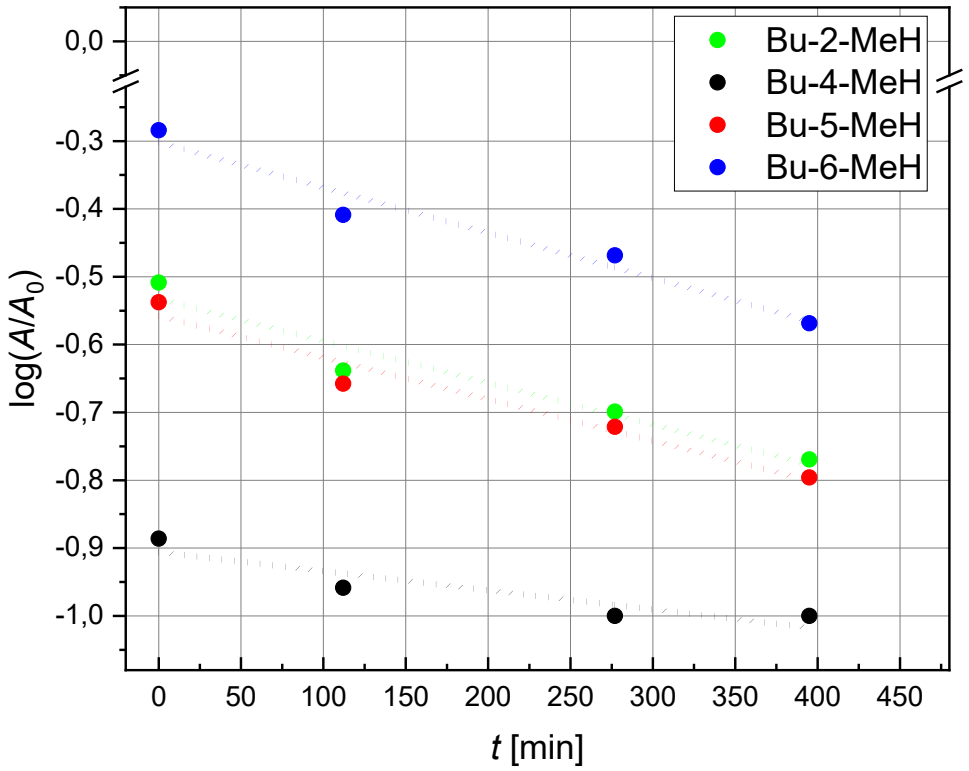

FIGURE 21: KINETIC STUDY OF THE METHANOLYSIS OF 3-CHLOROPIPERIDINE DERIVATIVES WITH MONOMETHYL SUBSTITUENTS AT POSITIONS FOUR AND SIX.

TABLE 8: OBTAINED REACTION CONSTANTS OF 3-CHLOROMETHYLPIPERIDINES.

Compound	Rate constant / 10^{-3} min^{-1}
Bu-2-MeH	0.616 ± 0.1
Bu-4-MeH	0.282 ± 0.09
Bu-5-MeH	0.613 ± 0.09
Bu-6-MeH	0.667 ± 0.1

All obtained reaction constants are compared with each other in Figure 23. The compounds BuHH, Bu-5-MeMe, Bu-5-Cycpropyl and Bu-5-Cycbutyl, which are already known in the literature[8], are also given as a reference (Figure 22).

FIGURE 22: COMPOUNDS KNOWN FROM THE LITERATURE.[8]

It can be observed that dimethyl substitutions at positions four and six significantly decrease the reaction constant (Figure 23). Substitution at position four has a more substantial effect than one at position six. The substitution at position four reduces the rate constant by about 80 %, while the substitution at position six results in a reduction of about 70 %.

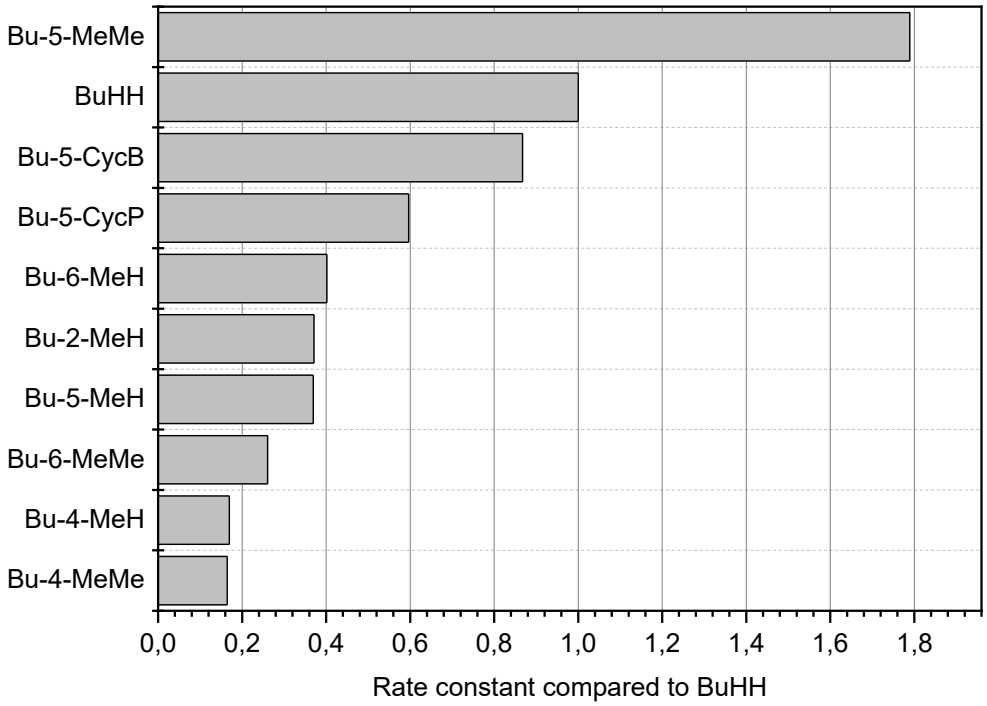

FIGURE 23: COMPARISON OF THE OBTAINED REACTION CONSTANTS WITH THE REACTION CONSTANTS OF BUHH, BU-5-MEME, BU-5-CYCP AND BU-5-CYCB KNOWN FROM PREVIOUS STUDIES.

Additionally, it can be demonstrated that even a single mono substitution lowers the rate constant more than a cyclic substitution at position five. A monosubstitution at all positions leads to a reduction of the rate constant by approximately 60 %. The substitution at position four resulted in the most substantial decrease for monomethylated derivatives, reducing the rate constant by about 80 %. This could be due to other effects that influence the reactivity of the compounds, as mentioned before.

3.4 Comparison of the calculated and measured reactivities

When comparing the obtained rate constants with the calculated activation energies, these agree for the derivative with the dimethyl substitution at position four. In the case of the derivative with dimethyl substitution at position six, however, the calculations should be revised again since this shows a reduced reactivity that was not predicted in the calculations. However, it could also be that other effects play a role in this derivative that were not considered in the calculations.

In the case of derivatives with monomethyl substituents, the calculated activation energies deviate from the reaction rates measured. Therefore, it would be essential to look at the calculations, as there seems to be a severe error. Given that the transition state is extraordinarily energetic, as demonstrated in chapter 3.1.1, this may be the source of the error. Furthermore, the calculated errors must be incorrect, as no reaction should be detected with the calculated activation energies. However, as seen in this chapter, this is not the case.

4 Conclusion and outlook

In the past, 3-chloropiperidines were developed as N-Lost analogues by the *Göttlich* group. These are capable of alkylating DNA, which disrupts cell replication and causes the cell to initiate apoptosis.[4,5] Cell studies show that these compounds' strong reactivity prevents their usage in biological systems.[4] Furthermore, it was found in previous studies that the Thorpe-Ingold effect can influence reactivity.[8] This work investigated to what extent different substitution positions of the piperidine backbone influence the reactivity of 3-chloropiperidines due to the Thorpe-Ingold effect. For this purpose, different structures were investigated computationally, synthesised and the reactivity measured by NMR kinetics.

4.1 Computational investigation of 3-chloropiperidines

Various 3-chloropiperidine derivatives were investigated for their reactivity employing computational calculations. The positions and parameters investigated are shown in Figure 24.

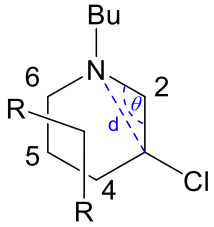

FIGURE 24: INVESTIGATED VALUES OF 3-CHLOROPIPERIDINES.

It was discovered that a substitution at position four brings about a reduction in reactivity, while a substitution at other positions only seems to increase reactivity (Figure 25). However, this influence cannot be explained by the Thorpe-Ingold effect alone since the derivatives with the substitution at position four do not have the most significant angle *θ*.

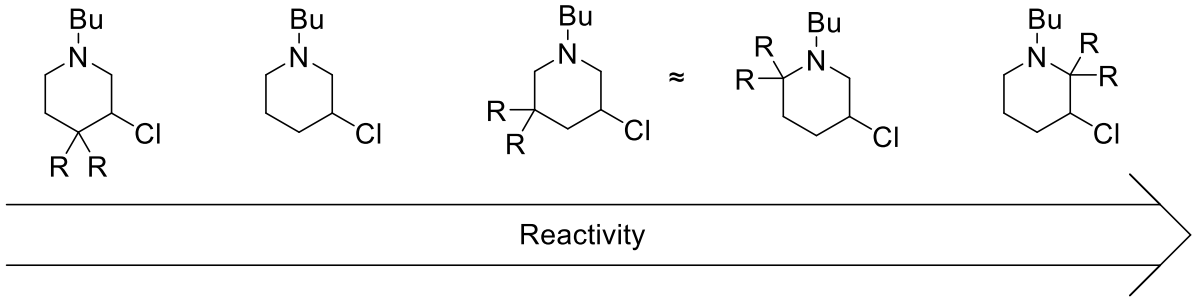

FIGURE 25: REVIEW OF THE IMPACT OF THE SUBSTITUTION POSITION ON THE REACTIVITY OF 3-CHLOROPIPERIDINES WITH R = ME, PH.

Furthermore, it was investigated whether 1,3-diaxial interactions occur with 3-chloropiperidines that influence the reactivity. It was found that with the derivatives with substituents at positions four and six, only a very little interaction occurs; with substituents at position six, a significant interaction occurs, and with substituents at position two, the most potent interaction occurs.

4.2 Synthesis of 3-chloropiperidine derivatives

The synthesis of the derivative with dimethyl substituents at position two proceeded according to a known literature synthesis of prolinol.[4] However, the desired product could not be obtained, as it did not survive the aqueous work-up followed by flash chromatographic purification using DCM/NH_3 in MeOH and subsequent distillation at HV.

The following derivative with dimethyl substituents at position four could be obtained well over four steps. Subsequently, this derivative was converted into a hydrochloride salt to obtain a crystal structure. Therefore, the calculated parameters θ and d could be compared to the experimental data. It was noticed that a dimethyl substitution at position four has a more substantial effect on θ than a cyclopropyl substitution at position five.

Lastly, the derivative with dimethyl substituents at position six was also obtained via four steps. However, the synthesis proved challenging, so it only succeeded in low yields below 25 %. Hence alternative synthesis strategies should be investigated.

Attempts were also made to produce diphenyl derivatives substituted at positions four and six. However, the syntheses were challenging and not completed in this work.

4.3 Kinetic investigation of 3-chloropiperidine derivatives

The prepared 3-chloropiperidines were investigated by NMR kinetics. Dibenzyl ether was added as an internal standard, and the samples were heated at 50 °C in methanol-d4. The rate constant could be obtained by integrating the same NMR peak over time. It was found that substitution on positions four and six and mono substitution leads to a decrease in the reaction rate, compared to the unsubstituted 3-chloropiperidines (Figure 26).

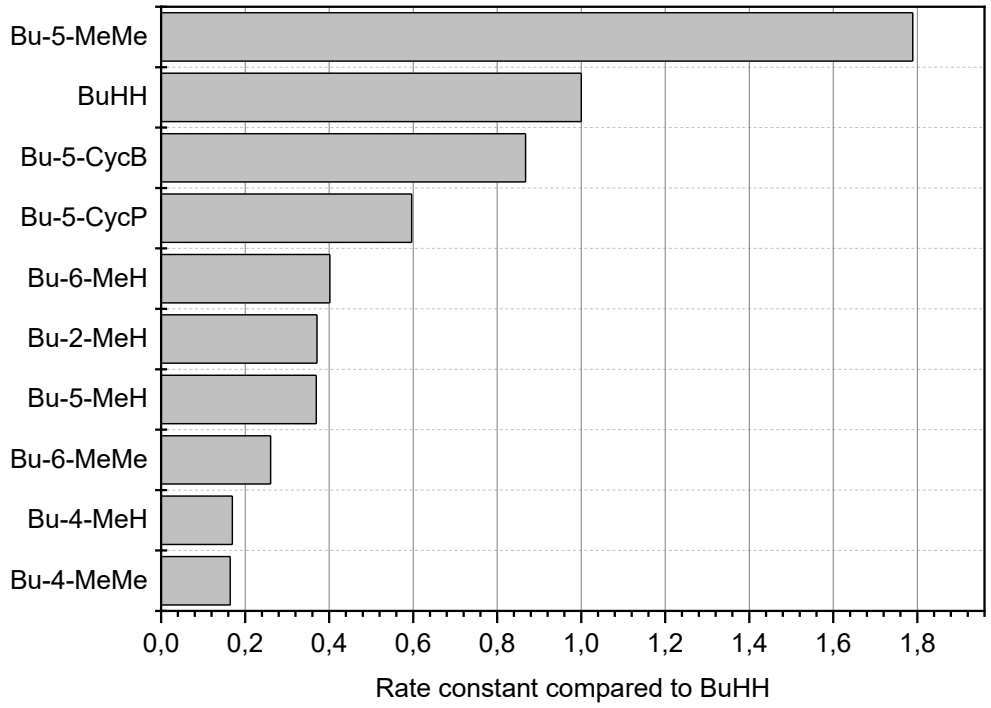

FIGURE 26: COMPARISON OF THE OBTAINED REACTION CONSTANTS WITH THE REACTION CONSTANTS OF BUHH, BU-5-MEME, BU-5-CYCP AND BU-5-CYCB KNOWN FROM PREVIOUS STUDIES.

4.4 Outlook

The computational calculations could be revised in the future as they differ significantly from the values known in the literature.[8] Therefore a more accurate prediction of the reactivities could be conducted in future. Furthermore, the alternative synthesis routes mentioned in chapter 3.2 could be carried out. Thus, other 3-chloropiperidine derivatives could be realised or already obtained compounds could be produced in larger quantities so that a crystal structure analysis or better NMR kinetics could also be carried out from these. Furthermore, the synthesis of 3-chloropiperidine derivatives with additional substituents that have different A-values, such as isopropyl or *tert*-butyl groups, would be interesting to further investigate the influence of the Thorpe-Ingold effect. In addition, the respective diastereomers of the mono-methylated compounds should be separated and kinetically investigated, as they might show different reactivities. Finally, all substances should be investigated in DNA and cell studies to verify the observed reactivity changes.

5 Experimental section

5.1 General working and measuring methods

Unless otherwise stated, all synthesis was carried out in an inert gas atmosphere. For this purpose, the apparatus was heated, dried with an oil pump vacuum, and flooded with nitrogen. Ice water baths were used to cool reactions to 0 °C. Acetone cooling baths were used to cool reactions down to -78 °C.

5.1.1 Solvents and chemicals

The solvents (THF, MeOH, acetonitrile, diethyl ether, chloroform, DCM, hexane, acetone, pentane, TBME) were purified by distillation before use. The absolute (air-, and moisture-free) solvents used (MeOH, THF, DCM, acetonitrile) were purchased from Acros Organics and stored in an AcroSeal® bottle under inert gas. All other chemicals used were applied without further purification.

5.1.2 Chromatography

Silica gel 60 from Merck with a grain size of 40 - 63 µm was used to perform the flash chromatography. The plates used in the thin layer chromatography were coated with silica gel 60 F254 and were purchased from Merck. UV light with a wavelength of 254 and 366 nm was used to visualise the results on the plates. Furthermore, potassium permanganate solution, consisting of potassium permanganate, sodium hydroxide and potassium carbonate in water, and ninhydrin solution, consisting of ninhydrin and acetic acid in ethanol, were used.

5.1.3 NMR-spectroscopy

The nuclear magnetic resonance spectra were measured with Avance II/II devices AV400 from Bruker under standard conditions. The kinetic experiments were measured with Avance II/II devices AV200 from Bruker under standard conditions. For all performed measurements, chloroform-d1, methanol-d4 or DMSO-d6 were used, using the solvent signal as an internal standard. The chemical shifts δ of the solvents are listed in Table 9.

TABLE 9:CHEMICAL SHIFT IN PPM OF SOLVENTS USED IN ^{1}H- AND ^{13}C-NMR.

^{1}H-NMR ($CDCl_3$) δ = 7.26 ppm	**^{13}C-NMR** ($CDCl_3$) δ = 77.16 ppm
^{1}H-NMR (MeOD-d3) δ = 3.31 ppm	**^{13}C-NMR** (MeOD-d3) δ = 49.00 ppm
^{1}H-NMR ($(CD_3)_2SO$) δ = 2.50 ppm	**^{13}C-NMR** ($(CD_3)_2SO$) δ = 39.52 ppm

The spectra were evaluated with the help of the software MestReNova and according to the following scheme:

^{1}H-NMR: Chemical shift δ in ppm (multiplicity, if applicable, coupling constant J in Hertz, integral, assigned protons).

^{13}C-NMR: Chemical shift δ in ppm (assigned carbons).

The following abbreviations of multiplicities were used:
s = singlet, d = duplet, t = triplet, q = quartet, m = multiplet.

5.1.4 Mass spectrometry

All products were characterised by high-resolution electron spray ionisation mass spectrometry (ESI HRMS) using their exact mass. Therefore, a time-of-flight mass spectrometer ESImicroTOF from *Bruker* was used in positive or negative ion mode.

5.1.5 X-ray structural analysis

L. Wagner performed the X-ray structure analysis on a *D8 Venture* device from *Bruker*. The Mercury programme from *CCDC* (*The Cambridge Crystallographic Data Centre*) was used for visualisation. The structures obtained were displayed in the *Oad Ridge Thermal Ellipsoid Plot* (*ORTEP*).

5.1.6 Growing crystals

50 mg of the corresponding hydrochloride was dissolved in 2 mL of solvent, and 1 mL of each was transferred to small screw-cap vials. The small screw-cap jar was then placed in a larger one, with the bottom of the larger one covered with about 5 mL of a non-polar solvent. The outer screw-cap jar is closed, while the inner one is left open (Figure 27).

FIGURE 27: CRYSTALLISATION SETUP.

Crystallisation takes place within one week at room temperature by diffusion. If crystallisation fails to occur during this time, the setup is kept in the refrigerator until crystallisation occurs. The used solvent combinations are listed in Table 10.

TABLE 10: SOLVENT COMBINATIONS USED FOR CYCLIZATION.

Polar solvent	Nonpolar solvent
Acetone/MeOH	Diethyl ether
	Pentane

5.2 Synthesis specification and analytical data

5.2.1 Synthesis of L-Proline methyl ester hydrochloride

5.001 g L-proline (43.44 mmol, 1 equiv.) was dissolved in 45 mL dry MeOH and 3.5 mL (48 mmol, 1.1 equiv.) $SOCl_2$ was added at 0 °C. The reaction was heated for 2.5 h under reflux. Subsequently, the MeOH was removed at the HV and washed with Et_2O until colourless.

$M(C_6H_{12}ClNO_2)$ = 165.617 g/mol

Yield: 7.183 (43.37 mmol), 99 %

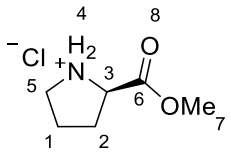

^{1}H-NMR (400 MHz, MeOD-d3):
δ [ppm] = 4.44 (t, J = 7.8 Hz, 1H, H3), 3.85 (s, 3H, H7), 3.46 – 3.35 (m, 2H, H1), 2.48 – 2.37 (m, 1H, H3), 2.20 – 2.02 (m, 3H, H2,3).

Since the data agree with the literature, no further analysis was conducted.

5.2.2 Synthesis of *N*-Butyl-L-proline methyl ester

3.368 g (20.34 mmol, 1 equiv.) L-proline methyl ester hydrochloride and 7.026 g (50.48 mmol, 2.5 equiv.) K_2CO_3 were dissolved in 40 mL dry MeCN. Then 2.2 mL (22 mmol, 1.1 equiv.) of *n*-butyl iodide was added, and the reaction was allowed to stir at 82 °C overnight. The next day the reaction was filtered, concentrated in vacuo, and purified by flash chromatography with DCM/acetone (20:1).

M($C_6H_{12}ClNO_2$) = 165.617 g/mol

Yield: 2.416 (43.37 mmol), 46 %

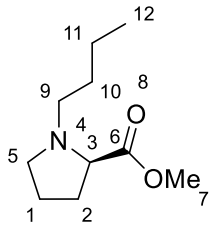

^{1}H-NMR (400 MHz, $CDCl_3$):
δ [ppm] = 3.72 (s, 3H, H7), 3.25 – 3.13 (m, 2H, H3,4), 2.73 – 2.62 (m, 1H, H9), 2.45 – 2.33 (m, 2H, H5,9), 2.20 – 2.08 (m, 1H, H2), 1.99 – 1.88 (m, 2H, H1), 1.87 – 1.77 (m, 1H, H2), 1.54 – 1.44 (m, 2H, H10), 1.37 – 1.23 (m, 2H, H11), 0.90 (t, J = 7.3 Hz, 3H, H12).

^{13}C-NMR (101 MHz, $CDCl_3$):
δ [ppm] = 66.26 (C3), 54.97 (C9), 53.67 (C5), 52.02 (C7), 30.70 (C10), 29.46 (C2), 23.21 (C1), 20.80 (C11), 14.06 (C12).

ESI-HRMS:

m/z(calculated for $C_6H_{12}ClNO_2Na^+$) = 208.1308

m/z(found $C_6H_{12}ClNO_2Na^+$) = 208.1309

5.2.3 Synthesis of (2*R*)-1-butyl-2-(2-methoxypropan-2-yl)pyrrolidine

0.485 g (20.0 mmol, 4 equiv.) Mg turnings and a few beads of I_2 were coated with 10 mL dry Et_2O. Furthermore, 1.06 mL (17.0 mmol, 3.4 equiv.) MeI was diluted in 10 mL dry Et_2O and slowly dropped to the Mg suspension. The reaction was then heated for 1 h under reflux. Then, 0.918 g (4.96 mmol, 1 equiv.) of *N*-butyl-L-proline methyl ester was diluted in 10 mL of dry Et_2O and dropped at 0 °C to the Grignard solution. The reaction was then allowed to stir for 2 h at rt. After this time, the reaction was quenched with 10 mL NH_4Cl solution and 10 mL water. The phases were separated, and the aqueous phase was extracted three times with Et_2O and washed with brine. The solution was then dried over $MgSO_4$, concentrated in vacuo, and purified by flash chromatography with DCM/MeOH/NEt_3 (20:1:0.5 %).

M($C_6H_{12}ClNO_2$) = 185.311 g/mol

Yield: 0.715 (3.86 mmol), 82 %

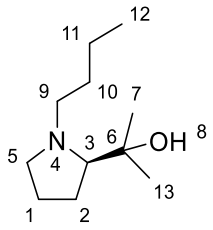

^{1}H-NMR (400 MHz, $CDCl_3$):

δ [ppm] = 3.13 (s, 1H, H3), 2.82 (s, 1H, H5), 2.70 – 2.41 (m, 3H, H5,9), 1.87 – 1.63 (m, 4H, H1,32), 1.55 – 1.26 (m, 4H, H10,11), 1.22 (s, 3H, H7), 1.11 (s, 3H, H13), 0.92 (t, J = 7.3 Hz, 3H, H12).

^{13}C-NMR (101 MHz, $CDCl_3$):

δ [ppm] = 139.16 (C6), 55.26 (C5), 53.56 (C3), 41.77 (C9), 39.66 (C1,2), 28.61 (C10), 26.92 (C7,13), 20.81 (C11), 14.14 (C12).

ESI-HRMS:

m/z(calculated for $C_6H_{13}ClNO_2^+$) = 186.1853

m/z(found $C_6H_{13}ClNO_2^+$) = 186.1851

5.2.4 Synthesis of 5-Hexen-2-one

Before use, acetylacetone and allyl chloride was purified by distillation. Subsequently, 45.80 mL (448.3 mmol, 1.1 equiv.) acetylacetone, 31.19 g (407.6 mmol, 1 equiv.) acetyl chloride, and 63.27 g (457.9 mmol, 1.12 equiv.) anhydrous potassium chloride dissolved in 100 mL ethylene glycol. The flask temperature was raised to 40 °C for 2 h and 80 °C over another 2 h. The flask temperature was then increased to 140 °C, and the product was obtained by fractional distillation.

$M(C_6H_{10}O)$ = 98.145 g/mol

Yield: 17.86 g (182.0 mmol), 41 %

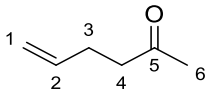

^{1}H-NMR (400 MHz, $CDCl_3$):
δ [ppm] = 5.86 – 5.74 (m, 1H, H2), 5.07 – 4.95 (m, 2H, H1), 2.52 (t, J = 7.4 Hz, 2H, H4), 2.40 – 2.25 (m, 2H, H3), 2.14 (s, 3H, H6).

^{13}C-NMR (101 MHz, $CDCl_3$):
δ [ppm] = 208.57 (C5), 137.46 (C2), 115.69 (C1), 43.18 (C4), 35.62 (C3), 30.39 (C6).

ESI-HRMS:

m/z(calculated for $C_6H_{10}ONa^+$) = 121.0624

m/z(found $C_6H_{10}ONa^+$) = 121.0624

5.2.5 Synthesis of *N*-((2E)-hex-5-en-2-ylidene)butan-1-amine

In 50 mL benzene, 1.562 g (9.071 mmol, 0.05 equiv.) *p*-TosH and 17.860 g (181.98 mmol, 1 equiv.) 5-hexen-2-one were dissolved. After that 310 mL (314 mmol, 17 equiv.) *n*-butylamine was added, and a dean-stark-apparatus was placed on the round bottom flask. The reaction was heated overnight under reflux. The next day, the reaction was concentrated in vacuo, and the residue was taken up in Et_2O. The precipitated solid was filtered off, and the filtrate was concentrated again.

$M(C_{10}H_{19}N)$ = 153.269 g/mol

Yield: 20.041 g (130.76 mmol), 72 %

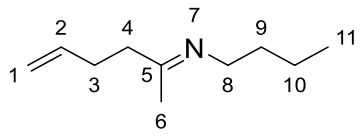

^{1}H-NMR (400 MHz, $CDCl_3$):
δ [ppm] = 5.89 – 5.74 (m, 1H, H2), 5.05 – 4.92 (m, 2H, H1), 3.27 – 3.19 (m, 2H, H8), 2.35 – 2.19 (m, 4H, H3,4), 1.80 (s, 3H, H6), 1.64 – 1.51 (m, 2H, H9), 1.39 – 1.31 (m, 2H, H10), 0.92 (m, 3H, H11).

^{13}C-NMR (101 MHz, $CDCl_3$):
δ [ppm] = 164.48 (C5), 138.08 (C2), 114.90 (C1), 51.25 (C8), 36.91 (C4), 33.08 (C9), 31.00 (C3), 20.85 (C10), 17.33 (C6), 14.12 (C11).

ESI-HRMS:

m/z(calculated for $C_{10}H_{20}N^+$) = 154.1590

m/z(found $C_{10}H_{20}N^+$) = 154.1593

5.2.6 Synthesis of *N*-Butyl-2-methyl-5-hexen-2-amine

In 10 mL dry THF 1.06 mL (8.36 mmol, 1 equiv.) $BF_3 \cdot OEt_2$ and 1.253 g (8.175 mmol, 1 equiv.) *N*-(1-methyl-4-penten-1-ylidene)-1-butanamine were dissolved. Then 6.64 mL (10.6 mmol, 1.3 equiv.) MeLi was diluted with 5 mL dry THF and added to the reaction solution at -78 °C. After 1.5 h the reaction was quenched with 10 mL NH_4Cl solution. A basic pH was adjusted with saturated Na_2CO_3 solution, and the reaction solution was extracted three times with diethyl ether, washed once with brine and dried over Na_2SO_4. The product was purified by flash chromatography with DCM/MeOH/NEt_3 (20:1:0.5 %).

M($C_{11}H_{23}N$) = 169.312 g/mol

Yield: 0.284 (1.68 mmol), 21 %

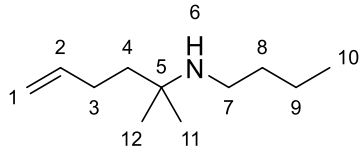

^{1}H-NMR (400 MHz, $CDCl_3$):
δ [ppm] = 5.91 – 5.73 (m, 1H, H2), 5.11 – 4.86 (m, 2H, H1), 2.54 (t, J = 7.4 Hz, 2H, H7), 2.08 – 1.96 (m, 2H, H3), 1.58 – 1.47 (m, 4H, H8,9), 1.41 – 1.30 (m, 2H, H4), 1.11 (s, 6H, H11,12), 0.91 (t, J = 7.3 Hz, 3H, H10).

^{13}C-NMR (101 MHz, $CDCl_3$):
δ [ppm] = 139.13 (C2), 114.36 (C1), 41.76 (C7), 39.54 (C8), 32.66 (C9), 28.60 (C3), 26.76 (C11,12), 20.80 (C4), 14.12 (C10).

ESI-HRMS:

m/z(calculated for $C_{11}H_{24}N^+$) = 170.1903

m/z(found $C_{11}H_{24}N^+$) = 170.1900

5.2.7 Synthesis of *N*-Butyl-3-chloro-6,6-dimethylpiperidine

In 20 mL dry DCM, 0.284 g (1.68 mmol, 1 equiv.) *N*-butyl-2-methyl-5-hexen-2-amine was dissolved. Subsequently, 0.227 g (1.70 mmol, 1 equiv.) NCS was added at 0 °C. The reaction solution was left to stir for 2 h. The reaction was then concentrated in vacuo, and the residue was taken up in 10 mL pentane, filtered and then concentrated again in vacuo. For the subsequent reaction, 0.037 g (0.10 mmol, 0.1 equiv.) of TBAI was dissolved in 20 mL of dry $CHCl_3$, and the solution was heated to 50 °C. At this temperature, the intermediate from the previous reaction was added and allowed to stir overnight. The next day, the reaction was concentrated in vacuo and purified by flash chromatography using pentane/TBME (10:1).

M($C_{11}H_{22}NCl$) = 203.754 g/mol

Yield: 0.030 (0.15 mmol), 11 % over two steps

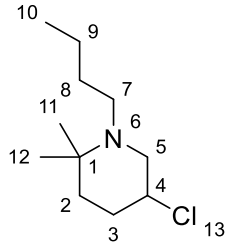

^{1}H-NMR (400 MHz, $CDCl_3$):
δ [ppm] = 4.14 – 3.87 (m, 1H, H4), 3.07 – 2.91 (m, 1H, H5), 2.63 – 2.53 (m, 1H, H5), 2.53 – 2.41 (m, 2H, H7), 2.18 – 1.96 (m, 2H, H3), 1.60 – 1.50 (m, 2H, H2), 1.41 – 1.23 (m, 4H, H8,9), 1.09 (s, 3H, H13), 0.99 (s, 3H, H12), 0.91 (t, J = 7.0 Hz, 3H, H10).

^{13}C-NMR (101 MHz, $CDCl_3$):
δ [ppm] = 92.93 (C1), 57.11 (C4), 54.62 (C5), 48.85 (C7), 39.46 (C2), 31.88 (C3), 31.23 (C8), 27.00 (C12,13), 20.72 (C9), 14.14 (C10).

ESI-HRMS:

m/z(calculated for $C_{11}H_{23}N^+$) = 204.1514

m/z(found $C_{11}H_{23}N^+$) = 204.1517

5.2.8 Synthesis of *N*-Butyl-3-chloro-6,6-dimethylpiperidine

Under atmospheric conditions, 0.065 g (0.38 mmol, 1 equiv.) *N*-butyl-2-methyl-5-hexen-2-amine was dissolved in 50 mL THF and 0.202 g (1.19 mmol, 3 equiv.) $CuCl_2 \cdot 2\ H_2O$ was added. The reaction was allowed to stir at rt for 336 h (14 d). After this time, the reaction was washed with NH_4OH solution until the aqueous phase was no longer blue. The aqueous phase was then extracted four times with DCM, and the combined organic phases were washed four times with water and once with brine. Lastly, the organic phases were dried over $MgSO_4$ and purified by flash chromatography with pentane/TBME (10:1).

M($C_{11}H_{22}NCl$) = 203.754 g/mol

Yield: 0.055 (0.22 mmol), 56 %

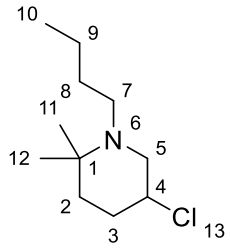

^{1}H-NMR (400 MHz, $CDCl_3$):
δ [ppm] = 4.14 – 3.87 (m, 1H, H4), 3.07 – 2.91 (m, 1H, H5), 2.63 – 2.53 (m, 1H, H5), 2.53 – 2.41 (m, 2H, H7), 2.18 – 1.96 (m, 2H, H3), 1.60 – 1.50 (m, 2H, H2), 1.41 – 1.23 (m, 4H, H8,9), 1.09 (s, 3H, H13), 0.99 (s, 3H, H12), 0.91 (t, J = 7.0 Hz, 3H, H10).

^{13}C-NMR (101 MHz, $CDCl_3$):
δ [ppm] = 92.93 (C1), 57.11 (C4), 54.62 (C5), 48.85 (C7), 39.46 (C2), 31.88 (C3), 31.23 (C8), 27.00 (C12,13), 20.72 (C9), 14.14 (C10).

ESI-HRMS:

m/z(calculated for $C_{11}H_{22}NClNa^+$) = 204.1514

m/z(found $C_{11}H_{22}NClNa^+$) = 204.1517

5.2.9 Synthesis of *N*-Butyl-5-hexen-2-amine

In 30 mL dry methanol 1.901 g (12.66 mmol, 1 equiv.) *N*-(1-methyl-4-penten-1-ylidene)-1-butenamine was dissolved. At 0 °C, 0.866 g (22.8 mmol, 1.8 equiv.) $NaBH_4$ was added, and the reaction was allowed to come to rt overnight. The next day, the reaction solution was concentrated to about 10 mL, and the residue was taken up in 200 mL Et_2O. The solution was then washed three times with 50 mL of water each and twice with each 50 mL of brine. The product was dried over $MgSO_4$ and concentrated.

$M(C_{10}H_{21}N)$ = 155.285 g/mol

Yield: 1.594 (10.27 mmol), 81 %

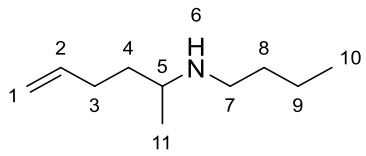

^{1}H-NMR (400 MHz, $CDCl_3$):
δ [ppm] = 5.90 – 5.70 (m, 1H, H2), 5.12 – 4.88 (m, 2H, H1), 2.74 – 2.49 (m, 2H, H7), 2.35 – 1.83 (m, 4H, H4,8), 1.67 – 1.55 (m, 1H, H5), 1.52 – 1.28 (m, 4H, H3,9), 1.21 – 0.96 (m, 3H, H11), 0.95 – 0.88 (m, 3H, H10).

^{13}C-NMR (101 MHz, $CDCl_3$):
δ [ppm] = 138.68 (C2), 114.71 (C1), 52.95 (C5), 46.90 (C7), 35.87 (C4), 32.27 (C8), 30.46 (C3), 20.69 (C9), 19.97 (C11), 14.11 (C10).

ESI-HRMS:

m/z(calculated for $C_{10}H_{22}N^+$) = 156.1747

m/z(found $C_{10}H_{22}N^+$) = 156.1752

5.2.10 Synthesis of *N*-Butyl-3-chloro-6-methylpiperidine

In 20 mL dry DCM 0.698 g (4.50 mmol, 1 equiv.) *N*-butyl-5-hexen-2-amine was dissolved and 0.609 g (4.96 mmol, 1 equiv.) NCS was added at 0 °C. After 2.5 h at 0 °C, the reaction was concentrated in vacuo, the residue taken up in 20 mL pentane and filtered. The filtrate was concentrated again in vacuo. The product obtained was used without further purification. For the next step 0.162 g (0.439 mmol, 0.1 equiv.) TBAI was dissolved in 20 mL dry $CHCl_3$ and heated to 50 °C. Subsequently, 0.799 g (4.21 mmol, 1 equiv.) of the intermediate product was diluted with 5 mL $CHCl_3$ and dropped into the TBAI suspension. The reaction was concentrated in vacuo and purified by flash chromatography with pentane/TBME (10:1).

M($C_{10}H_{20}NCl$) = 189.727 g/mol

Yield: 0.268 (1.41 mmol), 32 % over two steps

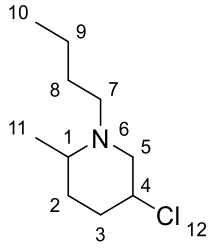

^{1}H-NMR (400 MHz, MeOD-d3):
δ [ppm] = 4.29 – 4.12 (m, 1H, H4), 3.37 – 3.22 (m, 4H, H1,5,7), 3.21 – 3.15 (m, 1H, H5), 2.42 – 2.31 (m, 1H, H3), 2.20 – 2.06 (m, 1H, H3), 1.96 – 1.61 (m, 4H, H2,9), 1.49 – 1.42 (m, 3H, H9), 1.45 – 1.34 (m, 4H, H11), 1.09 – 0.98 (m, 4H, H10).

^{13}C-NMR (101 MHz, MeOD-d3):
δ [ppm] = 60.00 (C5), 57.53 (C1), 54.48 (C4), 51.87 (C7), 34.12 (C3), 32.23 (C2), 26.02 (C8), 20.93 (C9), 17.33 (C11), 13.87 (C10).

ESI-HRMS:

m/z(calculated for $C_{10}H_{21}ClN^+$) = 190.1357

m/z(found $C_{10}H_{21}ClN^+$) = 190.1357

5.2.11 Synthesis of *N*-Butyl-3-chloro-6-methylpiperidine

Under atmospheric conditions, 2.546 g (14.93 mmol, 2.9 equiv.) $CuCl_2 \cdot 2\ H_2O$ was dissolved in 20 mL THF. Subsequently, 0.806 g (5.19 mmol, 1 equiv.) *N*-butyl-5-hexen-2-amine was diluted with 5 mL THF and added to the $CuCl_2$ suspension. The reaction was allowed to stir at rt for 3 h and then refluxed overnight. For purification, concentrated NH_3 solution was added to the reaction until the aqueous phase no longer turned blue. The aqueous phase was then extracted four times with 50 mL DCM each, and the combined organic phases were washed four times with 25 mL H_2O each and once with 25 mL brine. The organic phase was dried with $MgSO_4$ and purified by flash chromatography with pentane/TMBE (10:1).

M($C_{10}H_{20}NCl$) = 189.128 g/mol

Yield: 0.054 (0.29 mmol), 5 %

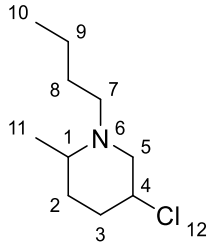

^{1}H-NMR (400 MHz, MeOD-d3):
δ [ppm] = 4.29 – 4.12 (m, 1H, H4), 3.37 – 3.22 (m, 4H, H1,5,7), 3.21 – 3.15 (m, 1H, H5), 2.42 – 2.31 (m, 1H, H3), 2.20 – 2.06 (m, 1H, H3), 1.96 – 1.61 (m, 4H, H2,9), 1.49 – 1.42 (m, 3H, H9), 1.45 – 1.34 (m, 4H, H11), 1.09 – 0.98 (m, 4H, H10).

^{13}C-NMR (101 MHz, MeOD-d3):
δ [ppm] = 60.00 (C5), 57.53 (C1), 54.48 (C4), 51.87 (C7), 34.12 (C3), 32.23 (C2), 26.02 (C8), 20.93 (C9), 17.33 (C11), 13.87 (C10).

ESI-HRMS:

m/z(calculated for $C_{10}H_{21}ClN^+$) = 190.1357

m/z(found $C_{10}H_{21}ClN^+$) = 190.1357

5.2.12 Synthesis of 3,3-Dimethyl-4-pentenoic acid

33.973 g (605.5 mmol, 4 equiv.) KOH was dissolved in 200 mL EtOH, and 24 mL (151 mmol, 1 equiv.) methyl-3,3-dimethylpent-4-enoate was dissolved in 20 mL EtOH. Then the methyl-3,3-dimethylpent-4-enoate solution was dropped into the KOH solution, and the reaction was heated overnight under reflux. The next day the reaction was cooled down to 0 °C and 50 mL conc. HCl was added. The precipitated solid was filtered off, and the solvent was removed in vacuo.

M($C_7H_{12}O_2$) = 128.17 g/mol

Yield: 17.00 g (132.6 mmol), 88 %

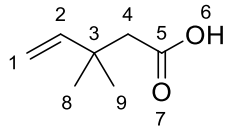

^{1}H-NMR (400 MHz, $CDCl_3$):
δ [ppm] = 10.69 (s, 1H, H6), 5.91 (dd, J = 17.4, 10.7 Hz, 1H, H2), 4.97 (t, 2H, H1), 2.31 (s, 2H, H4), 1.15 (s, 6H, H8, 9).

^{13}C-NMR (101 MHz, $CDCl_3$):
δ [ppm] = 178.02 (C5), 146.86 (C2), 111.11 (C1), 47.00 (C4), 36.14 (C3), 27.05 (C8, 9).

ESI-HRMS:

m/z(calculated for $C_7H_{11}O_2^-$) = 127.0765

m/z(found $C_7H_{11}O_2^-$) = 127.0763

5.2.13 Synthesis of *N*-butyl-3,3-dimethylpent-4-enamide

In 30 mL diethyl ether 3.416 g (24.02 mmol, 1 equiv.) 3,3-dimethyl-4-pentenoic acid was dissolved. To the solution was slowly added 1.94 mL (24.0 mmol, 1 equiv.) of $SOCl_2$ at 0 °C and then allowed to stir at rt. for 3 h. Then 10 mL (101 mmol, 3 equiv.) of *n*-butylamine was diluted with 20 mL of DCM and slowly added to the reaction at 0 °C. After the addition was completed, the reaction was left to stir at rt overnight. The next day the reaction was acidified with HCl and extracted four times with 50 mL DCM each. The combined organic phases were dried over $MgSO_4$. The desiccant was removed, and the solution was concentrated in vacuo. Lastly, the crude product was fractionally distilled in HV over a Vigreux column. The product was obtained at a head temperature of ~107 °C. The product was shaken out with Na_2CO_3 to remove residual reactant.

M($C_{11}H_{21}NO$) = 183.295 g/mol

Yield: 3.927 g (21.43 mmol), 57 %

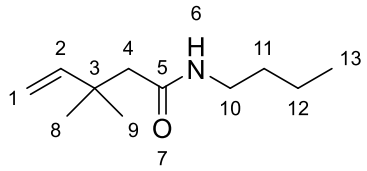

^{1}H-NMR (400 MHz, $CDCl_3$):
δ [ppm] = 5.97 – 5.85 (m, 1H, H2), 5.70 (s, 1H, H6), 5.06 – 4.97 (m, 2H, H1), 3.2 (q, J = 5.5 Hz, 2H, H10), 2.20 (s, 2H, H4), 1.51 – 1.39 (m, 2H, H11), 1.37 – 1.27 (m, 2H, H12), 1.12 (s, 6H, H8,9), 0.91 (t, J = 7.3 Hz, 3H, H13).

^{13}C-NMR (101 MHz, $CDCl_3$):
δ [ppm] = 171.57 (C5), 147.87 (C), 112.02 (C1), 49.89 (C4), 39.67 (C10), 36.77 (C3), 32.11 (C1), 27.39 (C8,9), 20.57 (C12), 14.15 (C13)

ESI-HRMS:

m/z(calculated for $C_{11}H_{21}NONa^+$) = 206.1515

m/z(found $C_{11}H_{21}NONa^+$) = 206.1517

5.2.14 Synthesis of *N*-butyl-3,3-dimethylpent-4-en-1-amine

An LAH suspension was prepared by grinding 0.545 g (13.4 mmol, 2.5 equiv.) LAH and adding 30 mL dry THF. Subsequently, 1.069 g (5.832 mmol, 1 equiv.) of *N*-butyl-3,3-dimethylpent-4-enamide was dissolved in 5 mL of dry THF and dropped into the LAH suspension at 0 °C. After completion of the addition, the reaction was heated overnight under reflux. The next day, the reaction was refluxed with 0.6 mL water, 0.6 mL NaOH (30%), 1.7 mL water, a spatula of $MgSO_4$ was added and stirred at rt for half an hour. The resulting solid was removed by glass frit (4Å), and the filtrate was concentrated in vacuo.

M($C_{11}H_{23}N$) = 169.312 g/mol

Yield: 0.943 g (5.57 mmol), 96 %

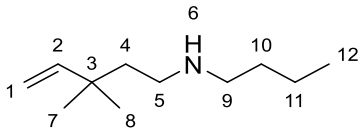

^{1}H-NMR (400 MHz, $CDCl_3$):
δ [ppm] = 5.84 – 5.73 (m, 1H, H2), 4.95 – 4.88 (m, 2H, H1), 2.67 – 2.51 (m, 4H, H5,9), 1.57 – 1.44 (m, 5H, H10,4), 1.40 – 1.28 (m, 2H, H11), 1.00 (s, 6H, H7,8), 0.91 (t, 3H, H12).

^{13}C-NMR (101 MHz, $CDCl_3$):
δ [ppm] = 148.47 (C2), 111.06 (C1), 50.17 (C9), 46.46 (C5), 42.69 (C4), 36.36 (C3), 32.39 (C10), 27.40 (C7,8), 20.97 (C11), 14.44 (C12).

ESI-HRMS:

m/z(calculated for $C_{11}H_{24}N^+$) = 170.1903

m/z(found $C_{11}H_{24}N^+$) = 170.1904

5.2.15 Synthesis of *N*-Butyl-3-chloro-4,4-dimethylpiperidine

In 20 mL dry DCM 0.358 g (2.11 mmol, 1 equiv.) 4-penten-1-amine, *N*-butyl-3,3-dimethyl were dissolved. At 0 °C, 0.283 g (2.12 mmol, 1 equiv.) NCS was added, and the suspension was allowed to stir for 2 h at this temperature. The reaction was then concentrated in vacuo, the residue taken up in pentane, filtered and concentrated again. The product was purified chromatographically with pentane/TBME (50:1). For the next step, 0.079 g (0.22 mmol, 0.1 equiv.) TBAI was dissolved in 20 mL dry $CHCl_3$. Subsequently, 0.430 g (2.11 mmol, 1 equiv.) of the intermediate product, dissolved in 10 mL dry $CHCl_3$, was added. The reaction was heated to 50 °C for 18 h. The reaction was concentrated in vacuo and purified by flash chromatography with pentane/TBME (5:1).

$M(C_{11}H_{22}ClN)$ = 203.754 g/mol

Yield: 0.179 (0.879 mmol), 41 % over two steps

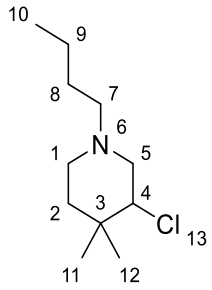

^{1}H-NMR (400 MHz, $CDCl_3$):

δ [ppm] = 4.06 – 3.95 (m, 1H, H4), 3.09 – 3.00 (m, 1H, H5), 2.83 – 2.72 (m, 1H, H5), 2.51 – 2.43 (m, 2H, H1), 2.43 – 2.25 (m, 2H, H7), 1.81 – 1.68 (m, 1H, H2), 1.62 – 1.56 (m, 1H, H2), 1.56 – 1.49 (m, 2H, H8), 1.39 – 1.26 (m, 2H, H9), 1.08 (s, 3H. H12), 0.99 (s, 3H, H11), 0.92 (t, J = 7.3 Hz, 3H, H10).

^{13}C-NMR (101 MHz, $CDCl_3$):

δ [ppm] = 65.84 (C4), 57.93 (C1), 56,38 (C5), 49.22 (C7), 38.45 (C3), 34.82 (C2), 29.22 (C12), 28.57 (C8), 20.75 (C11), 18.91 (C9), 14.06 (C10)

ESI-HRMS:

m/z(calculated for $C_{11}H_{23}ClN^+$) = 204.1514

m/z(found $C_{11}H_{23}ClN^+$) = 204.1514

5.2.16 Synthesis of *N*-Butyl-3-chloro-4,4-dimethylpiperidine

Under ambient conditions, 1.480 g (8.521 mmol, 3 equiv.) $CuCl_2 \cdot 2\ H_2O$ dissolved in 50 mL THF, 0.441 g (2.48 mmol, 1 equiv.) *N*-butyl-3,3-dimethylpent-4-en-1-amine diluted with 10 mL THF and added to the $CuCl_2$ solution. The reaction was allowed to stir for 10 d at rt. The reaction was then washed with NH_4OH solution until the aqueous phase no longer turned blue. The aqueous phase was then extracted four times with DCM, washed once with brine, dried over $MgSO_4$, and purified by flash chromatography with pentane/TBME (10:1).

M($C_{11}H_{22}ClN$) = 203.754 g/mol

Yield: 0.292 (1.43 mmol), 50 %

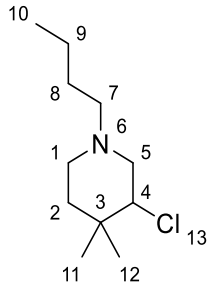

^{1}H-NMR (400 MHz, $CDCl_3$):

δ [ppm] = 4.06 – 3.95 (m, 1H, H4), 3.09 – 3.00 (m, 1H, H5), 2.83 – 2.72 (m, 1H, H5), 2.51 – 2.43 (m, 2H, H1), 2.43 – 2.25 (m, 2H, H7), 1.81 – 1.68 (m, 1H, H2), 1.62 – 1.56 (m, 1H, H2), 1.56 – 1.49 (m, 2H, H8), 1.39 – 1.26 (m, 2H, H9), 1.08 (s, 3H. H12), 0.99 (s, 3H, H11), 0.92 (t, J = 7.3 Hz, 3H, H10).

^{13}C-NMR (101 MHz, $CDCl_3$):

δ [ppm] = 65.84 (C4), 57.93 (C1), 56,38 (C5), 49.22 (C7), 38.45 (C3), 34.82 (C2), 29.22 (C12), 28.57 (C8), 20.75 (C11), 18.91 (C9), 14.06 (C10)

ESI-HRMS:

m/z(calculated for $C_{11}H_{23}ClN^+$) = 204.1514

m/z(found $C_{11}H_{23}ClN^+$) = 204.1514

5.2.17 Synthesis of 1,3-dimethyl-2-(diphenylmethylidene)propanedioate

In 50 mL of dry THF, 1.946 g (10.954 mmol, 1 equiv.) of benzophenone, 1.25 mL (10.9 mmol, 1 equiv.) of dimethyl malonate and 2.65 mL (32.8 mmol, 3 equiv.) of pyridine were dissolved, and 3.6 mL (33 mmol, 3 equiv.) of $TiCl_4$ was added at 0 °C. The reaction was then allowed to stir overnight at rt. The next day the reaction was equilibrated with 50 mL water and extracted three times with EtOAc. The combined organic phases were washed once with brine and dried over Na_2SO_4. Lastly, purification was carried out by flash chromatography with a gradient pentane/EtOAc (100:1 → 50:1).

$M(C_{18}H_{16}O_4)$ = 296.322 g/mol

Yield: 0.361 (1.22 mmol), 11 %

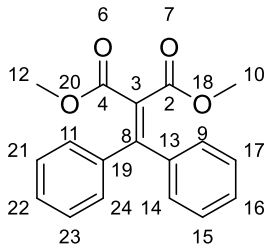

^{1}H-NMR (400 MHz, $CDCl_3$):
δ [ppm] = 7.37 – 7.30 (m, 6H, H15-17, H21-23), 7.20 – 7.16 (m, 4H, H9, H11, H14, H24), 3.61 (s, 6H, H10, H12).

^{13}C-NMR (101 MHz, $CDCl_3$):
δ [ppm] =

ESI-HRMS:

m/z(calculated for $C_{18}H_{16}O_4Na^+$) = 319.0941

m/z(found $C_{18}H_{16}O_4Na^+$) = 319.0940

5.2.18 Synthesis of *N*-(diphenylmethylene)-1-butanamine

In 50 mL of benzene, 2.019 g (11.08 mmol, 1 equiv.) of benzophenone and 0.094 g (0.55 mmol, 0.05 equiv.) of *p*-TsOH were dissolved. Then 12.5 mL (177 mmol, 16 equiv.) of *n*-butylamine was added, and the reaction was refluxed overnight using a Dean-Stark apparatus. The next day, the reaction was concentrated in vacuo, and the residue was taken up in Et_2O, filtered and purified by flash chromatography with pentane/EtOAc (50:1).

M($C_{17}H_{19}N$) = 237.346 g/mol

Yield: 2.074 (8.738 mmol), 79 %

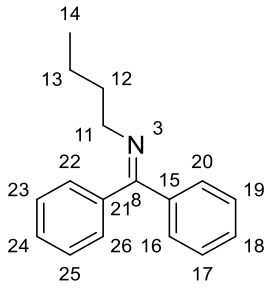

^{1}H-NMR (400 MHz, $CDCl_3$):
δ [ppm] = 7.53 – 7.49 (m, 4H, H16,20,22,26), 7.44 – 7.41 (m, 6H, H17-19,23-25), 3.34 (t, *J* = 7.1 Hz, 2H, H11), 1.68 – 1.59 (m, 2H, H12), 1.34 – 1.22 (m, 2H, H13), 0.80 (t, *J* = 7.4 Hz, 3H, H14).

^{13}C-NMR (101 MHz, $CDCl_3$):
δ [ppm] = 196.92 (C8), 137.76 (C21), 132.56 (C15), 130.21 (C18,24), 128.42 (C16,20,22,26), 128.06 (C17,19,23,25), 53.42 (C11), 33.35 (C12), 20.71 (C13), 14.05 (C14).

ESI-HRMS:

m/z(calculated for $C_{17}H_{20}N^+$) = 238.1590

m/z(found $C_{17}H_{20}N^+$) = 238.1588

5.2.19 Synthesis of 1,1-diphenylpent-4-en-1-ol

With 20 mL of dry THF, 0.947 g (40.9 mmol, 4.2 equiv.) of Mg-turnings and three beads of I_2 were coated. Subsequently, 4.1 mL (39 mmol, 4 equiv.) of benzyl bromide was diluted with 10 mL of THF, dropped into the Mg-suspension, and the reaction was heated for 1.5 h under reflux and allowed to stir overnight at rt. Simultaneously, 1 mL (10 mmol, 1 equiv.) pentenoic acid was diluted with 20 mL DCM and five drops of DMF, as well as 0.92 mL (11 mmol, 1.1 equiv.) oxalyl chloride was added. This reaction was allowed to stir overnight at rt. The next day, the reaction was concentrated in vacuo, the residue taken up in 20 mL THF, dropped into the Grignard-reaction and left to stir overnight at rt. The reaction was then quenched with NH_4Cl solution, extracted three times with Et_2O, washed with brine, dried over $MgSO_4$, and purified by flash chromatography with pentane/EtOAc (20:1).

M($C_{17}H_{18}O$) = 238.330 g/mol

Yield: 0.860 (3.61 mmol), 37 %

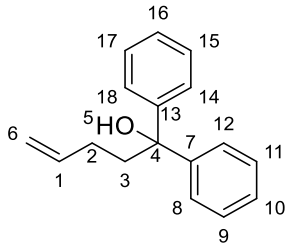

^{1}H-NMR (400 MHz, $CDCl_3$):

δ [ppm] = 7.42 – 7.34 (m, 4H, H8,12,14,18), 7.31 – 7.24 (m, 4H, H9,11,15,17), 7.21 – 7.14 (m, 2H, H10,16), 5.90 – 5.72 (m, 1H, H1), 5.03 – 4.84 (m, 2H, H6), 2.37 – 2.27 (m, 2H, H3), 2.12 (s, 1H, H5), 2.06 – 1.94 (m, 2H, H2).

^{13}C-NMR (101 MHz, $CDCl_3$):

δ [ppm] = 147.01 (C3,7), 138.83 (C1), 128.33 (C9,11,15,17), 127.01 (C10,16), 126.16 (C8,12,14,18), 114.87 (C6), 78.41 (C4), 41.11 (C3), 28.46 (C2).

ESI-HRMS:

m/z(calculated for $C_{17}H_{18}ONa^+$) = 261.1250

m/z(found $C_{17}H_{18}ONa^+$) = 261.1253

5.2.20 Synthesis of methyl 2-amino-2-methylpropanoate hydrochloride

In 25 mL of dry MeOH, 5.013 g (48.61 mmol, 1 equiv.) of 2-methyl alanine was dissolved, and 7 mL (97 mmol, 2 equiv.) of $SOCl_2$ was added at 0 °C. The reaction was then refluxed for 3 h and allowed to stir overnight at rt. The solvent was removed the next day at the HV, and the product was titruated with Et_2O until a colourless solid was obtained. The product was dried in vacuo.

$M(C_5H_{12}ClNO_2)$ = 153.606 g/mol

Yield: 5.345 (34.80 mmol), 72 %

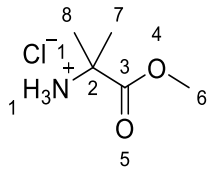

^{1}H-NMR (400 MHz, MeOD-d3):
δ [ppm] = 3.85 (s, 3H, H6), 1.58 (s, 6H, H7,8).

^{13}C-NMR (101 MHz, MeOD-d3):
δ [ppm] = 173.18 (C3), 57.83 (C2), 54.01 (C6), 24.00 (C7,8).

ESI-HRMS:

m/z(calculated for $C_5H_{12}ClNO_2^+$) = 118.0863

m/z(found $C_5H_{12}ClNO_2^+$) = 118.0863

5.2.21 Synthesis of 2-((tert-butoxycarbonyl)amino)-2-methylpropanoic acid

In 40 mL of water and 40 mL of 1,4-dioxane, 1.016 g (9.853 mmol, 1 equiv.) of 2-methyl alanine was dissolved, and 20 mL of 1M NaOH was added. Then, 2.370 g (10.864 mmol, 1.1 equiv.) of Boc_2O was added at 0 °C, and the reaction was allowed to stir overnight at rt. The next day, the dioxane was removed in vacuo, and the remaining solution was adjusted to a pH of ≈ 2 with saturated $KHSO_4$ solution and extracted three times with EtOAc. The combined organic solutions were washed with brine and dried over $MgSO_4$.

$M(C_9H_{17}NO_4)$ = 203.238 g/mol

Yield: 0.971 (4.78 mmol), 44 %

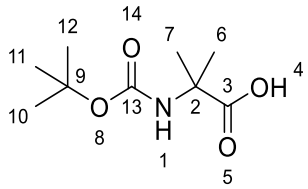

^{1}H-NMR (400 MHz, DMSO-d6):
δ [ppm] = 12.16 (s, 1H, H4), 7.02 (s, 1H, H1), 1.36 (s, 9H, H10-12), 1.29 (s, 6H, H6,7).

^{13}C-NMR (101 MHz, DMSO-d6):
δ [ppm] = 176.15 (C3), 154.55 (C13), 77.73 (C9), 54.87 (C2), 28.23 (C10-12), 25.17 (C6,7).

ESI-HRMS:

m/z(calculated for $C_9H_{17}NO_4Na^+$) = 226.1050

m/z(found $C_9H_{17}NO_4Na^+$) = 226.1046

5.2.22 Synthesis of methyl 2-(butylamino)-2-methylpropanoate

In 100 mL dry DCM, 2.516 g (16.38 mmol, 1 equiv.) α-aminoisobutyric acid methyl ester hydrochloride and 1.353 g (16.45 mmol, 1 equiv.) NaOAc was dissolved and allowed to stir for 10 min at rt. Subsequently, 1.73 mL (19.7 mmol, 1.2 equiv.) butanal was added at 0 °C and allowed to stir for 10 min. Lastly, 4.211 g (19.66 mmol, 1.2 equiv.) $NaBH(OAc)_3$ was added, and the reaction was allowed to stir at RT overnight. The next day, the reaction was mixed with sat. $NaHCO_3$ solution and left to stir for half an hour. Then a pH of ≈ 10 was adjusted using Na_2CO_3, the phases were separated, the aqueous phase was extracted three times with DCM, and the combined organic phases were washed twice with brine. The solution was then dried over $MgSO_4$ and purified by flash chromatography with pentane/TBME (10:1 → 1:1).

$M(C_9H_{19}NO_2)$ = 173.256 g/mol

Yield: 1.111 (6.412 mmol), 39 %

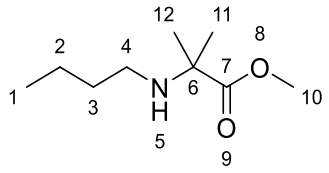

^{1}H-NMR (400 MHz, $CDCl_3$):
δ [ppm] = 3.70 (s, 3H, H10), 2.43 (t, J = 7.2 Hz, 2H, H4), 1.80 – 1.66 (m, 1H, H5), 1.50 – 1.38 (m, 2H, H2), 1.41 – 1.30 (m, 2H, H3), 1.30 (s, 6H, H11,12), 0.90 (t, J = 7.2 Hz, 3H, H1).

^{13}C-NMR (101 MHz, $CDCl_3$):
δ [ppm] = 177.77 (C7), 59.21 (C6), 52.00 (C10), 44.32 (C4), 32.83 (C2), 25.46 (C11,12), 20.57 (C3), 14.07 (C1).

ESI-HRMS:

m/z(calculated for $C_9H_{19}NO_2Na^+$) = 196.1308

m/z(found $C_9H_{19}NO_2Na^+$) = 196.1304

5.2.23 Synthesis of 2-(butylamino)-2-methylpropan-1-ol

An LAH suspension was prepared by grinding 0.662 g (18.0 mmol, 2.7 equiv.) LAH and adding 30 mL dry THF. Subsequently, 1.111 g (6.412 mmol, 1 equiv.) of *N*-Butyl-2-methylalanine methyl ester was dissolved in 5 mL of dry THF and dropped into the LAH suspension at 0 °C. After completion of the addition, the reaction was heated for 1.5 h under reflux. The next day 0.7 mL water, 0.7 mL NaOH (30%), 2.1 mL water and a spatula of $MgSO_4$ was added and allowed to be stirred at rt for half an hour. The resulting solid was removed by glass frit (4Å), and the filtrate was concentrated in vacuo.

M($C_9H_{21}NO$) = 145.147 g/mol

Yield: 1.009 (6.949 mmol), quantitative

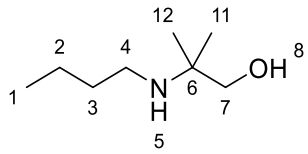

^{1}H-NMR (400 MHz, $CDCl_3$):
δ [ppm] = 3.27 (s, 2H, H7), 2.49 (t, J = 6.9 Hz, 2H, H4), 1.48 – 1.31 (m, 4H, H2,3), 1.06 (s, 6H, H11,12), 0.91 (t, J = 7.2 Hz, 3H, H1).

^{13}C-NMR (101 MHz, $CDCl_3$):
δ [ppm] = 68.36 (C7), 53.68 (C6), 41.49 (C4), 33.24 (C3), 24.25 (C9,10), 20.66 (C2), 14.12 (C1).

ESI-HRMS:

m/z(calculated for $C_9H_{22}NO^+$) = 146.1450

m/z(found $C_9H_{22}NO^+$) = 146.1538

5.2.24 Synthesis of 5-Nitro-1-pentene

In 20 mL dry DMSO 0.508 g (8.46 mmol, 2 equiv.) urea and 0.856 g (7.61 mmol, 1.8 equiv.) $NaNO_2$ were dissolved. Furthermore, 0.5 mL (4 mmol, 1 equiv.) 5-Bromo-1-pentene was dissolved in 5 mL of DMSO and dropped at 0 °C to the previously prepared solution. The reaction was allowed to come to rt overnight, diluted with 80 mL water the next day and extracted five times with EtOAc. Lastly, the solution was dried over Na_2SO_4 and purified by flash chromatography with pentane/$CHCl_3$ (10:1).

$M(C_5H_9NO_2)$ = 115.063 g/mol

Yield: 0.378 (3.28 mmol), 78 %

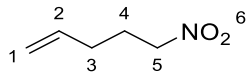

^{1}H-NMR (400 MHz, $CDCl_3$):
δ [ppm] = 5.84 – 5.69 (m, 1H, H2), 5.14 – 5.03 (m, 2H, H1), 4.39 (t, *J* = 6.7 Hz, 2H, H5), 2.37 – 2.07 (m, 4H, H3,4).

^{13}C-NMR (101 MHz, $CDCl_3$):
δ [ppm] = 135.88 (C2), 116.99 (C1), 74.90 (C5), 30.31 (C4), 26.48 (C3).

ESI-HRMS:

m/z(calculated for $C_5H_9NO_2Na^+$) = 138.0524

m/z(found $C_5H_9NO_2Na^+$) = 138.0525

5.2.25 Synthesis of 1-Phenyl-2-propen-1-ol

In 20 mL dry THF, 1.021 g (9.620 mmol, 1 equiv.) freshly distilled benzaldehyde was dissolved, and 10.58 mL (10.58 mmol, 1 mmol/mL, 1.1 equiv.) vinyl magnesium bromide solution was slowly added at 0 °C. The reaction was allowed to come to rt overnight, quenched the next day with saturated NH_4Cl solution and extracted three times with 50 mL Et_2O each. The combined organic phases were washed with brine and dried over $MgSO_4$.

M($C_9H_{10}O$) = 134.178 g/mol

Yield: 0.792 (5.90 mmol), 61 %

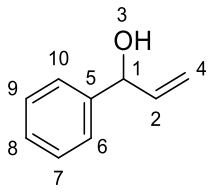

^{1}H-NMR (400 MHz, $CDCl_3$):
δ [ppm] = 7.26 – 7.13 (m, 5H, H6-10), 6.01 – 5.88 (m, 1H, H2), 5.29 – 5.18 (m, 1H, H1), 5.14 – 5.05 (m, 2H, H4), 4.58 (s, 1H, H3).

^{13}C-NMR (101 MHz, $CDCl_3$):
δ [ppm] = 142.72 (C5), 140.36 (C2), 128.71 (C7,9), 127.91 (C8), 126.46 (C6,10), 115.27 (C4), 75.50 (C1).

ESI-HRMS:

m/z(calculated for $C_9H_{10}ONa^+$) = 157.0624

m/z(found $C_9H_{10}ONa^+$) = 157.0629

5.2.26 Synthesis of 1-Phenyl-2-propen-1-on

In 20 mL dry THF, 1.16 mL (10.1 mmol, 1 equiv.) benzoyl chloride and 0.095 g (0.52 mmol, 0.05 equiv.) CuI were dissolved. At -78 °C, 10 mL (10 mmol, 1 mmol/mL, 1 equiv.) of a vinyl magnesium bromide solution was added, and the reaction was allowed to stir for 1.5 h at this temperature. After that, the reaction was allowed to come to rt overnight. The next day, the THF was removed in vacuo, and the residue was taken up in DCM, acidified with 1 M HCl and extracted three times with DCM. The combined organic phases were washed with $NaHCO_3$ solution and brine, dried over $MgSO_4$, and purified by flash chromatography with pentane/EtOAc (20:1).

$M(C_9H_8O)$ = 132.162 g/mol

Yield: 0.364 (2.75 mmol), 27%

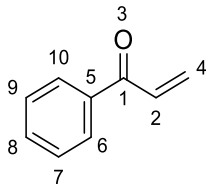

^{1}H-NMR (400 MHz, $CDCl_3$):
δ [ppm] = 7.92 – 7.81 (m, 2H, H6,10), 7.54 – 7.45 (m, 1H, H8), 7.42 – 7.34 (m, 2H, H7,9), 5.89 – 5.75 (m, 1H, H2), 5.09 – 4.91 (m, 2H, H4).

^{13}C-NMR (101 MHz, $CDCl_3$):
δ [ppm] = 195.66 (C1), 136.13 (C5), 135.23 (C8), 133.69 (C2), 129.04 (C6,10), 128.74 (C7,9), 117.38 (C4).

ESI-HRMS:

m/z(calculated for $C_9H_8ONa^+$) = 155.0467

m/z(found $C_9H_{10}ONa^+$) = /

5.2.27 Synthesis of 3,3-diphenylprop-2-enenitrile

In 20 mL dry MeCN, 1.560 g (27.91 mmol, 1.02 equiv.) KOH was dissolved, and the reaction was heated to 84 °C. Meanwhile, 5.001 g (27.44 mmol, 1 equiv.) of benzophenone was dissolved in 10 mL of MeCN and added to the KOH solution at 84 °C. The reaction was then left to stir at temperature overnight. The next day, the hot reaction solution was poured onto 85 g ice, the phases were separated, and the aqueous phase was extracted three times with DCM. The combined organic phases were washed once with water, dried over $MgSO_4$, and purified by flash chromatography with pentane/Et_2O (5:1).

M($C_{15}H_{11}N$) = 205.260 g/mol

Yield: 3.803 (18.53 mmol), 68 %

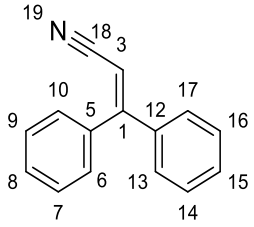

^{1}H-NMR (400 MHz, DMSO-d6):

δ [ppm] = 7.57 – 7.30 (m, 10H, H6-10, 13-17), 6.34 (s, 1H, H3).

^{13}C-NMR (101 MHz, DMSO-d6):

δ [ppm] = 161.81 (C1), 137.94 (C5), 137.12 (C12), 130.52 (C10,13), 129.75 (C6,17), 129.07 (C14,16), 128.76 (C8), 128.67 (C15), 128.20 (C7,9), 118.12 (C18), 96.12 (C3).

ESI-HRMS:

m/z(calculated for $C_{15}H_{11}Na^+$) = 228.0783

m/z(found $C_{15}H_{11}Na^+$) = 228.0786

6 Bibliography

[1] Zentrum für Krebsregisterdaten im Robert Koch-Institut (Ed.) *Bericht zum Krebsgeschehen in Deutschland 2016*, Berlin, **2016**.

[2] B. A. Chabner, T. G. Roberts, *Nature reviews. Cancer* **2005**, *5*, 65.

[3] R. K. Singh, S. Kumar, D. N. Prasad, T. R. Bhardwaj, *European journal of medicinal chemistry* **2018**, *151*, 401.

[4] C. Carraro, A. Francke, A. Sosic, F. Kohl, T. Helbing, M. de Franco, D. Fabris, R. Göttlich, B. Gatto, *ACS medicinal chemistry letters* **2019**, *10*, 552.

[5] I. Zuravka, R. Roesmann, A. Sosic, W. Wende, A. Pingoud, B. Gatto, R. Göttlich, *ChemMedChem* **2014**, *9*, 2178.

[6] T. Helbing, M. Georg, F. Stöhr, C. Carraro, J. Becker, B. Gatto, R. Göttlich, *Eur. J. Org. Chem.* **2021**, *2021*, 5905.

[7] a) K. D. Tew, *Cancer research* **1994**, *54*, 4313; b) K. Ghabili, P. S. Agutter, M. Ghanei, K. Ansarin, Y. Panahi, M. M. Shoja, *Critical reviews in toxicology* **2011**, *41*, 384.

[8] T. Helbing, M. Kirchner, J. Becker, R. Göttlich, *Eur. J. Org. Chem.* **2022**.

[9] R. Brown, N. van Gulick, *J. Org. Chem.* **1956**, *21*, 1046.

[10] K. Ward, *J. Am. Chem. Soc.* **1935**, *57*, 914.

[11] A. Gilman, F. S. Philips, *Science (New York, N.Y.)* **1946**, *103*, 409.

[12] G. A. R. KON, W. C. J. ROSS, *Nature* **1948**, *162*, 824.

[13] a) F. Bergel, J. A. Stock, *Br. Emp. Cancer Campaign. A* **1953**, *31*, 6; b) D. T. Vistica, *Biochimica et Biophysica Acta (BBA) - Biomembranes* **1979**, *550*, 309.

[14] V. Ravery, K. Fizazi, S. Oudard, L. Drouet, J.-C. Eymard, S. Culine, G. Gravis, C. Hennequin, M. Zerbib, *BJU international* **2011**, *108*, 1782.

[15] D. M. Noll, T. M. Mason, P. S. Miller, *Chemical reviews* **2006**, *106*, 277.

[16] J. W. Shay, Y. Zou, E. Hiyama, W. E. Wright, *Human molecular genetics* **2001**, *10*, 677.

[17] L. H. Hurley, *Nature reviews. Cancer* **2002**, *2*, 188.

[18] K. W. Kohn, J. A. Hartley, W. B. Mattes, *Nucleic acids research* **1987**, *15*, 10531.

[19] A. Gilman, *The American Journal of Surgery* **1963**, *105*, 574.

[20] M. J. Waring, *Nature* **1968**, *219*, 1320.

[21] E. Cavalieri, M. Saeed, M. Zahid, D. Cassada, D. Snow, M. Miljkovic, E. Rogan, *IUBMB life* **2012**, *64*, 169.

[22] J. Lhomme, J.-F. Constant, M. Demeunynck, *Biopolymers* **1999**, *52*, 65.

[23] J. Piette, *Journal of Photochemistry and Photobiology B: Biology* **1991**, *11*, 241.

[24] Y. Kuchino, F. Mori, H. Kasai, H. Inoue, S. Iwai, K. Miura, E. Ohtsuka, S. Nishimura, *Nature* **1987**, *327*, 77.

[25] a) S. Y. Wang, A. J. Varghese, *Biochemical and Biophysical Research Communications* **1967**, *29*, 543; b) A. J. Varghese, S. Y. Wang, *Science (New York, N.Y.)* **1967**, *156*, 955.

[26] A. K. Basu, *International journal of molecular sciences* **2018**, *19*.

[27] C. O. Gitterman, E. L. Rickes, D. E. Wolf, J. Madas, S. B. Zimmerman, T. H. Stoudt, T. C. Demny, *The Journal of antibiotics* **1970**, *23*, 305.

[28] T. Fukuyama, R. K. Frank, C. F. Jewell, *J. Am. Chem. Soc.* **1980**, *102*, 2122.

[29] Michael Kirchner, *Masterthesis*, Justus-Liebig-Universität Gießen, Gießen, **2021**.

[30] M. E. Jung, G. Piizzi, *Chemical reviews* **2005**, *105*, 1735.

[31] L. Eberson, H. Welinder, *J. Am. Chem. Soc.* **1971**, *93*, 5821.

[32] R. M. Beesley, C. K. Ingold, J. F. Thorpe, *J. Chem. Soc., Trans.* **1915**, *107*, 1080.

[33] A. J. Kirby, G. J. Lloyd, *J. Chem. Soc., Perkin Trans. 2* **1976**, 1753.

[34] T. C. Bruice, U. K. Pandit, *J. Am. Chem. Soc.* **1960**, *82*, 5858.

[35] A. L. Parrill, D. P. Dolata, *Tetrahedron Letters* **1994**, *35*, 7319.

[36] N. L. ALLINGER, V. ZALKOW, *J. Org. Chem.* **1960**, *25*, 701.

[37] A. L. Parrill, D. P. Dolata, *Journal of Molecular Structure: THEOCHEM* **1996**, *370*, 187.

[38] K. C. Brannock, *J. Am. Chem. Soc.* **1959**, *81*, 3379.

[39] R.-L. Li, G.-Q. Liu, W. Li, Y.-M. Wang, L. Li, L. Duan, Y.-M. Li, *Tetrahedron* **2013**, *69*, 5867.

[40] M. Noack, R. Göttlich, *Eur. J. Org. Chem.* **2002**, *2002*, 3171.

[41] F. Neese, F. Wennmohs, U. Becker, C. Riplinger, *The Journal of chemical physics* **2020**, *152*, 224108.

[42] S. Grimme, J. G. Brandenburg, C. Bannwarth, A. Hansen, *The Journal of chemical physics* **2015**, *143*, 54107.

[43] K. Fukui, *Acc. Chem. Res.* **1981**, *14*, 363.

[44] P. Pracht, F. Bohle, S. Grimme, *Physical chemistry chemical physics : PCCP* **2020**, *22*, 7169.

[45] J. P. Perdew, M. Ernzerhof, K. Burke, *The Journal of chemical physics* **1996**, *105*, 9982.

[46] F. Weigend, R. Ahlrichs, *Physical chemistry chemical physics : PCCP* **2005**, *7*, 3297.

[47] V. Barone, M. Cossi, *J. Phys. Chem. A* **1998**, *102*, 1995.

[48] G. Santra, N. Sylvetsky, J. M. L. Martin, *The journal of physical chemistry. A* **2019**, *123*, 5129.

[49] P. Hohenberg, W. Kohn, *Phys. Rev.* **1964**, *136*, B864-B871.

[50] W. Kohn, *Rev. Mod. Phys.* **1999**, *71*, 1253.

[51] W. Kohn, L. J. Sham, *Phys. Rev.* **1965**, *140*, A1133-A1138.

[52] P. A. M. Dirac, *Math. Proc. Camb. Phil. Soc.* **1930**, *26*, 376.

[53] D. M. Ceperley, B. J. Alder, *Phys. Rev. Lett.* **1980**, *45*, 566.

[54] S. H. Vosko, L. Wilk, M. Nusair, *Can. J. Phys.* **1980**, *58*, 1200.

[55] Perdew, Wang, *Physical review. B, Condensed matter* **1992**, *45*, 13244.

[56] A. J. Cohen, P. Mori-Sánchez, W. Yang, *Chemical reviews* **2012**, *112*, 289.

[57] Becke, *Physical review. A, General physics* **1988**, *38*, 3098.

[58] Perdew, Burke, Ernzerhof, *Phys. Rev. Lett.* **1996**, *77*, 3865.

[59] Lee, Yang, Parr, *Physical review. B, Condensed matter* **1988**, *37*, 785.

[60] A. D. Becke, *The Journal of chemical physics* **1993**, *98*, 1372.

[61] L. Goerigk, S. Grimme, *WIREs Comput Mol Sci* **2014**, *4*, 576.

[62] S. Grimme, J. Antony, S. Ehrlich, H. Krieg, *The Journal of chemical physics* **2010**, *132*, 154104.

[63] a) A. D. Becke, E. R. Johnson, *The Journal of chemical physics* **2005**, *123*, 154101; b) E. R. Johnson, A. D. Becke, *The Journal of chemical physics* **2006**, *124*, 174104.

[64] H. Kruse, S. Grimme, *The Journal of chemical physics* **2012**, *136*, 154101.

[65] C. Adamo, V. Barone, *The Journal of chemical physics* **1999**, *110*, 6158.

[66] S. Kozuch, J. M. L. Martin, *Physical chemistry chemical physics : PCCP* **2011**, *13*, 20104.

[67] a) T. A. Halgren, *J. Comput. Chem.* **1996**, *17*, 490; b) T. A. Halgren, *J. Comput. Chem.* **1996**, *17*, 520; c) T. A. Halgren, *J. Comput. Chem.* **1996**, *17*, 553; d) T. A. Halgren, *J. Comput. Chem.* **1996**, *17*, 616; e) T. A. Halgren, R. B. Nachbar, *J. Comput. Chem.* **1996**, *17*, 587.

[68] J. A. Hirsch, *Topics in stereochemistry* **1967**, *1*, 199.

[69] J. Clayden, N. Greeves, S. G. Warren, *Organic chemistry*, Oxford University Press, Oxford, New York, Auckland, **2012**.

[70] J. D. ALBRIGHT, L. GOLDMAN, *J. Org. Chem.* **1965**, *30*, 1107.

[71] H. Stetter, *Angew. Chem.* **1976**, *88*, 695.

[72] G. Vassilikogiannakis, N. Chronakis, M. Orfanopoulos, *J. Am. Chem. Soc.* **1998**, *120*, 9911.

[73] Y. Xu, Z. Yin, X. Lin, Z. Gan, Y. He, L. Gao, Z. Song, *Organic letters* **2015**, *17*, 1846.

[74] M. Hatano, S. Suzuki, K. Ishihara, *Synlett* **2010**, *2010*, 321.

[75] R. G. Pearson, *J. Am. Chem. Soc.* **1963**, *85*, 3533.

[76] J. H. Babler, M. J. Coghlan, *Synthetic Communications* **1976**, *6*, 469.

[77] a) J. CASON, *Chemical reviews* **1947**, *40*, 15; b) H. Gilman, J. F. Nelson, *Recl. Trav. Chim. Pays-Bas* **1936**, *55*, 518; c) S. Nicolai, J. Waser, *Organic letters* **2011**, *13*, 6324.

7 Appendix

The appendix can be viewed electronically.